CHAPTER - 2

Synthesis and study of pyrrolo[5]helicenes :

From stereodynamic to configurationally stable molecules

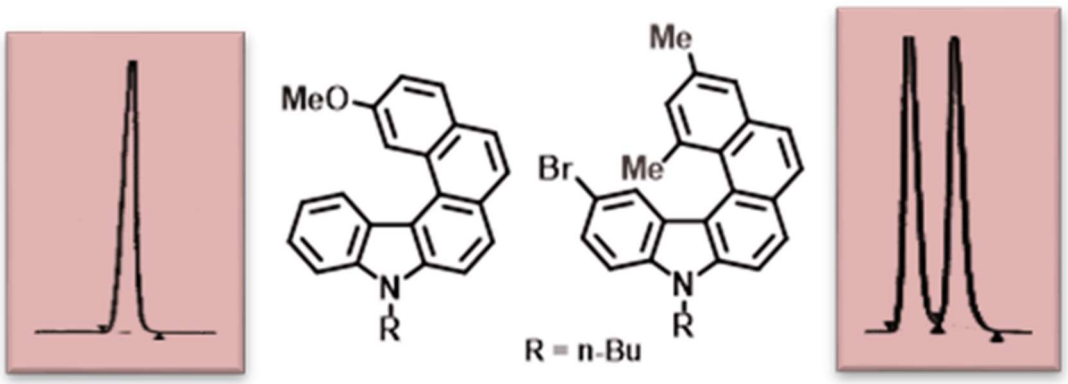

Table of Contents

2.1 Introduction

The first two helicenes synthesized were five-membered azahelicenes in 1903 by Meisenheimer and Witte when they studied the reduction of 2-nitronaphthalene[1] (Figure 2.1). The next landmark synthesis of carbo[5]helicene was reported in 1918 by Klingler and group[2] using Pschorr reaction followed by double decarboxylation as shown in Scheme 2.1. However, the yield was low due to a competitive formation of linear isomer which made the purification process difficult.

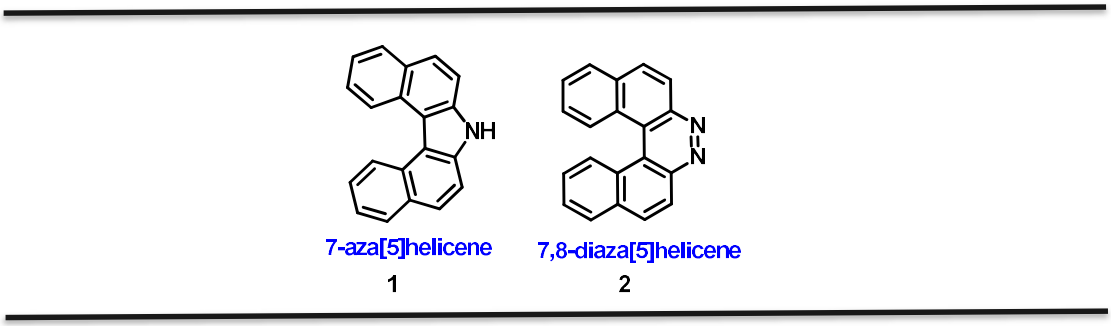

Figure 2.1: The first helicenes

However, it was much later that the photocyclization approach was used for the synthesis of helicene. The oxidative photocyclization approach for the synthesis of helicenes can be generalized in two steps: a) the syntheses of stilbene precursors by Wittig reaction between aldehyde and P-ylides or Heck type coupling reaction between aryl halides and aryl olefin and b) irradiation of the stilbene derivatives in the presence of an oxidant. Since the first reports, oxidative photocyclization strategy was widely used in the synthesis of smaller helicenes as well as larger helicene([16]helicene).

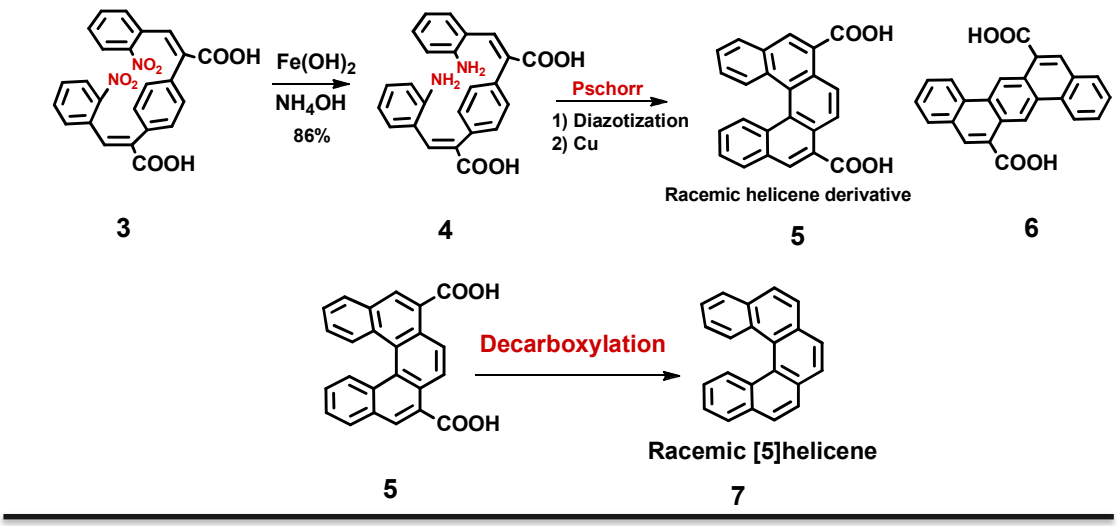

Scheme 2.1: First synthesis of carbo[5]helicene in 1918 by Pschorr reaction

The first photochemical synthesis of a carbohelicene was carried out by Scholz *et al* in 1967 in which they reported the synthesis of [4]helicene. However using the same strategy when cyclization of 1,2-di(naphtahalen-2-yl)ethane **8** and 3-styrylphenanthrene was carried out, instead of [5]helicene, 1,12-benzoperylene **10** was formed by a rearrangement of [5]helicene as shown in Scheme 2.2**.** Similar observation was reported by other groups in which the [5]helicene scaffold quickly transformed into the benzoperylene core as [5]helicene was found to be easily oxidized than its stilbene precursor.[3]

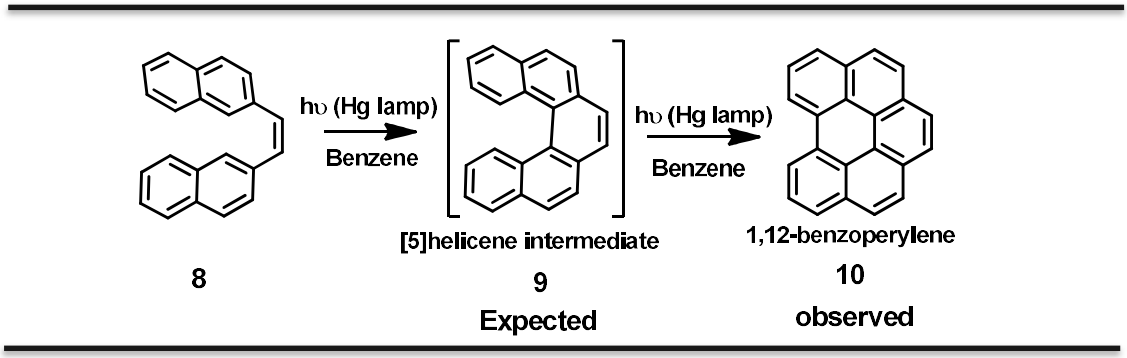

***Scheme 2.2**: Over-annellation leading to Benzoperylene formation*

Yet another rearrangement was reported by Mallory and group in 1982[4] while working on the oxidative photocyclization of 1-fluoro[5]helicenes. The formation of 8-fluorobenzo[*ghi*]perylenes was observed in this case through an unprecedented inter-ring fluorine atom migration and a competitive formation of benzo[*ghi*]perylenes was also detected by photoelimination of HF. They revealed that the relative yields of the rearrangement product and the elimination product depend on the reaction conditions. The rearrangement product was predominantly formed when the irradiation was carried out at 0°C in air saturated benzene solution containing 10^{-3} M iodine while the presence of solid potassium carbonate in the reaction mixture or at higher temperatures the predominance of the elimination product was observed.

In 2015, Usui and group studied the synthesis of [5]helicenes with functional groups on the sterically hindered 1-position (**12,13**) and/or 2-position (**11**) of the helix.[5] The racemic [5]helicenyl acetates **12** were then subjected to lipase catalysed kinetic resolution. It was found that the position of the acetate group on the helicene directs the reactivity towards enzymatic hydrolysis. The two enantiomers of 1-[5]helicenol **13b** were separated using (1*S*)-10-camphorsulfonyl chloride as the chiral resolving agent.(Scheme 2.3). A new helically chiral cyano-functionalized pentacyclic system **21** was synthesized by Raouafi and group in 2017 using Knoevenagel reaction to develop phenanthrene system **18a** which was then coupled with bromostyrene **19** using the Heck reaction to afford the corresponding

stilbene derivative which when subjected to photocyclization rendered the methoxypentahelicene **21** with a cyano functionality.[6] (**Scheme 2.4**)

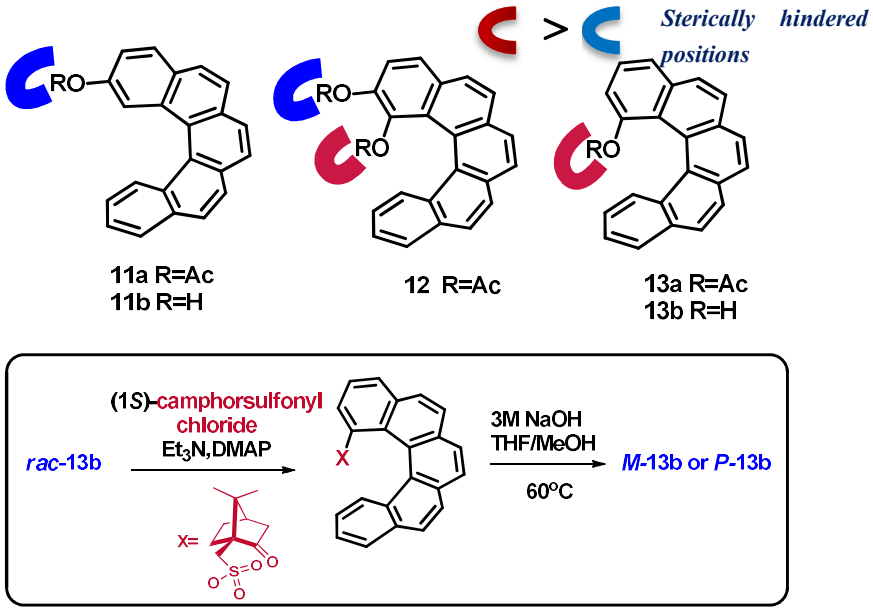

(A) ***Enantiomeric resolution using a chiral resolving agent***

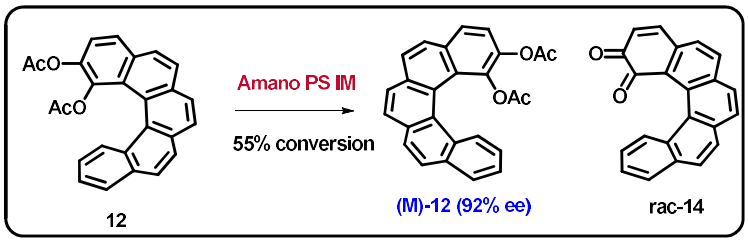

(B) ***Lipase catalyzed kinetic resolution***

Scheme 2.3*: *[5]helicenyl acetates synthesized and resolved by Usui and group

For building azahelicenes by photocyclization, the main approach was based on the stilbene precursors with two aryl groups bearing heteroaromatic ring with *N*-atom. In 2005, Caronna *et al*. synthesized monoaza and diaza[5]helicenes **25** using the classical oxidative photocyclization of stilbene derivatives **23**.[7] They synthesized the stilbene precursors using Wittig reaction between the corresponding aldehydes **22** and phosphonium salts followed by photocyclization using visible light. The photocyclization proceeds with *trans* to *cis* isomerization of the precursor followed by formation of a dihydroproduct **24** with a *trans* configuration which was then oxidized to the fully aromatic system in open air as shown in **Scheme 2.5**

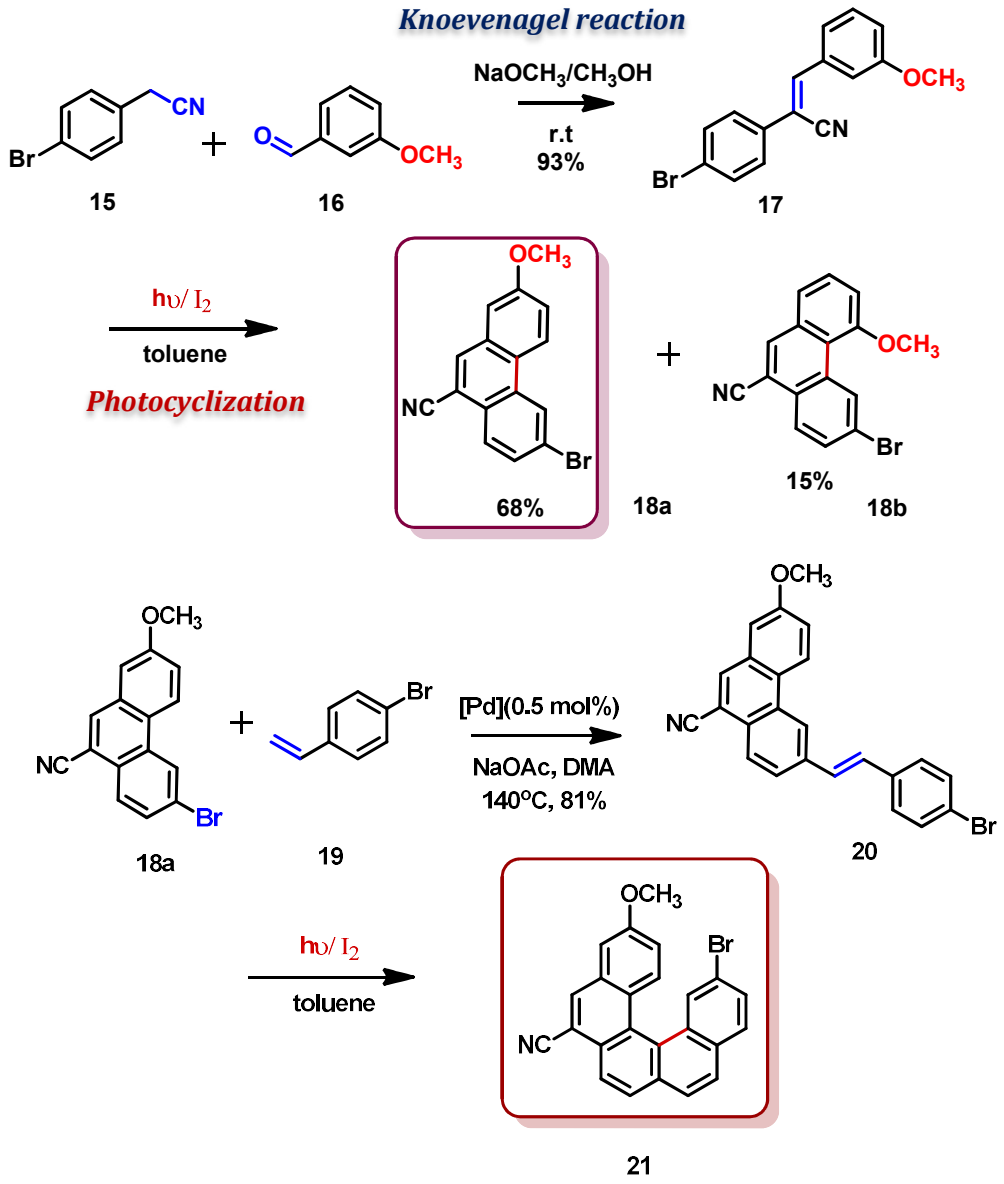

Scheme 2.4: Cyano-functionalized pentahelicene by Raoufi and group

A pyrrole based aza[5]helicene **29** was synthesized by Ben Braiek[8] utilizing the carbazole moiety. They accomplished the synthesis in a three-step sequence involving Heck-coupling reaction and oxidative photocyclization in moderate yields. The nitrogen atom could serve as a hydrogen acceptor as well as a metal-chelating agent for chiral recognition. The thermal and optical properties of this bromo-substituted pentahelicene were also investigated.

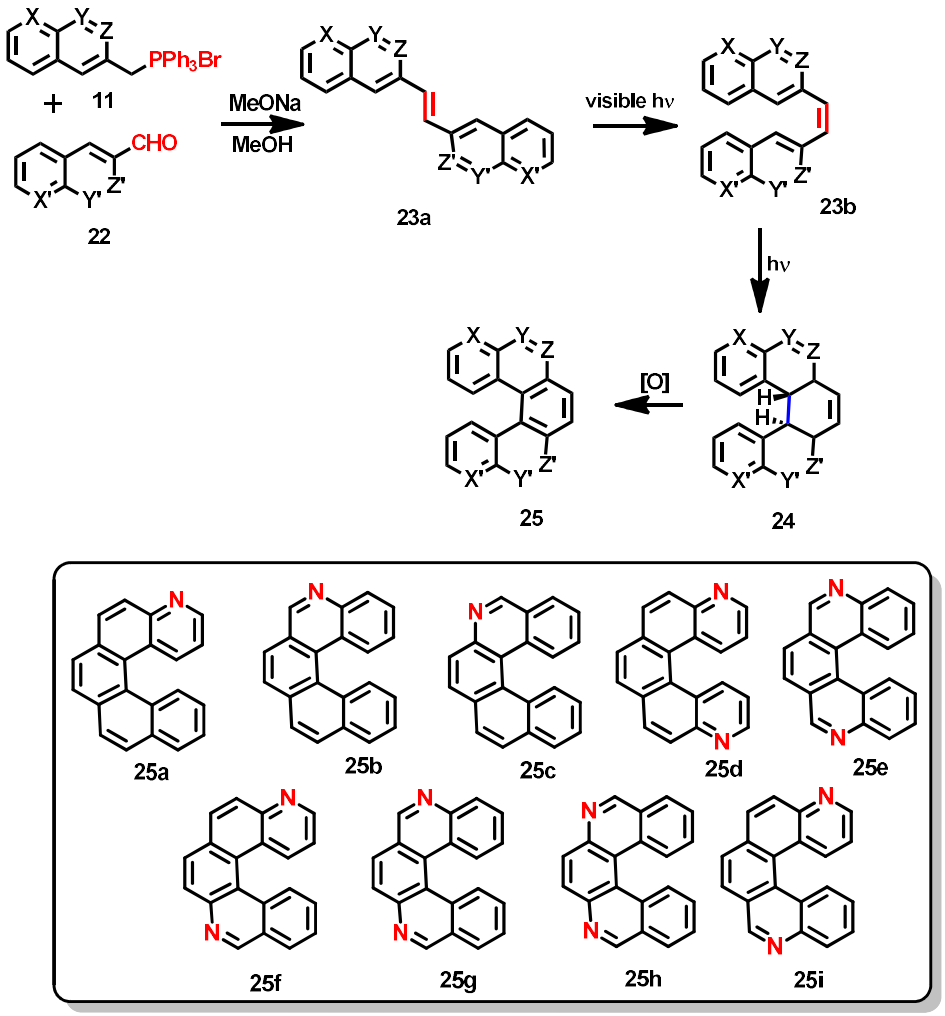

Scheme 2.5: *Mono and diaza[5helicene screened by Caronna and group*

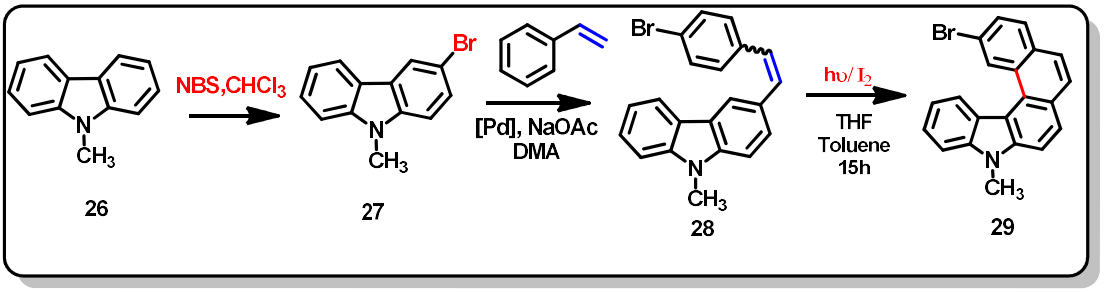

Scheme 2.6: *Pentahelicene synthesized using carbazole moiety*

Next, considering the application part, it is important to note that majority of the helicene-based research for catalytic applications focuses on [6]helicene and substituted [5]helicene-based systems This is because any substitution at the terminal ring is more geometrically accessible thus enabling better co-ordination with the reactive partners unlike in [7] or higher helicene where the functional groups are more apart and face opposite directions.

Dreher and group[9] designed and synthesized a bis[5]helicenediol ligand([5]HELOL) **32** for asymmetric catalysis. The ligand was synthesized considering the ease of preparation on a large scale and its stability against decomposition and racemization under the conditions for catalytic transformation. This dimeric helicene was more effective than its monomeric unit because it can surround a metal with a chiral pocket. The ligand was investigated for its catalytic activity in the addition of diethylzinc to aryl aldehydes **30**. The ligand rendered the nonracemic alcohols in high yield with enantiomeric excesses as high as 81%. The stereoselectivities and yields are much greater than when the catalyzing diol is BINOL. The proposed intermediate structure had one zinc atom bound to [5]HELOL and the Oxygen atom on the substrate, and the chiral groove rendered the attack of the ethyl unit from the Si-face.

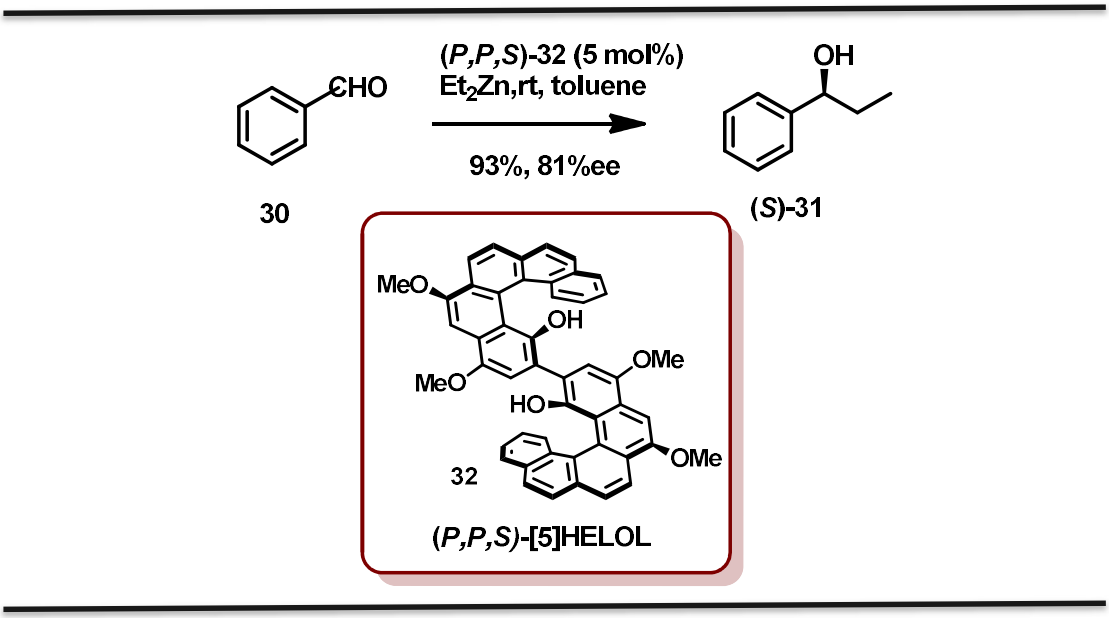

***Scheme 2.7**: Addition reaction between aldehyde and diethylzinc catalysed by 32*

In 2016, Yamamoto and group[10] rationally designed the synthesis of [5]helicene derived phosphine ligands (**L1**, with a 7,8-dihydro[5]helicene core structure- and **L2**, with a fully aromatic [5]helicene core structure) and studied their application in Pd-catalyzed asymmetric reactions (Scheme 2.8). The [5]helicene was successfully resolved using spiro-TADDOL. Inspite of having structural similarities, **L1** and **L2** exhibit particularly different characteristics in their use as chiral ligands. **L1** was highly effective in the asymmetric allylation of indoles **36** with 1,3-diphenylallyl acetate (up to 99% ee), and in the etherification of alcohols **38** (up to 96% ee), whereas **L2** was highly effective in the

stereocontrol of helical chirality in Suzuki–Miyaura coupling (SMC) reaction (up to 99% ee).

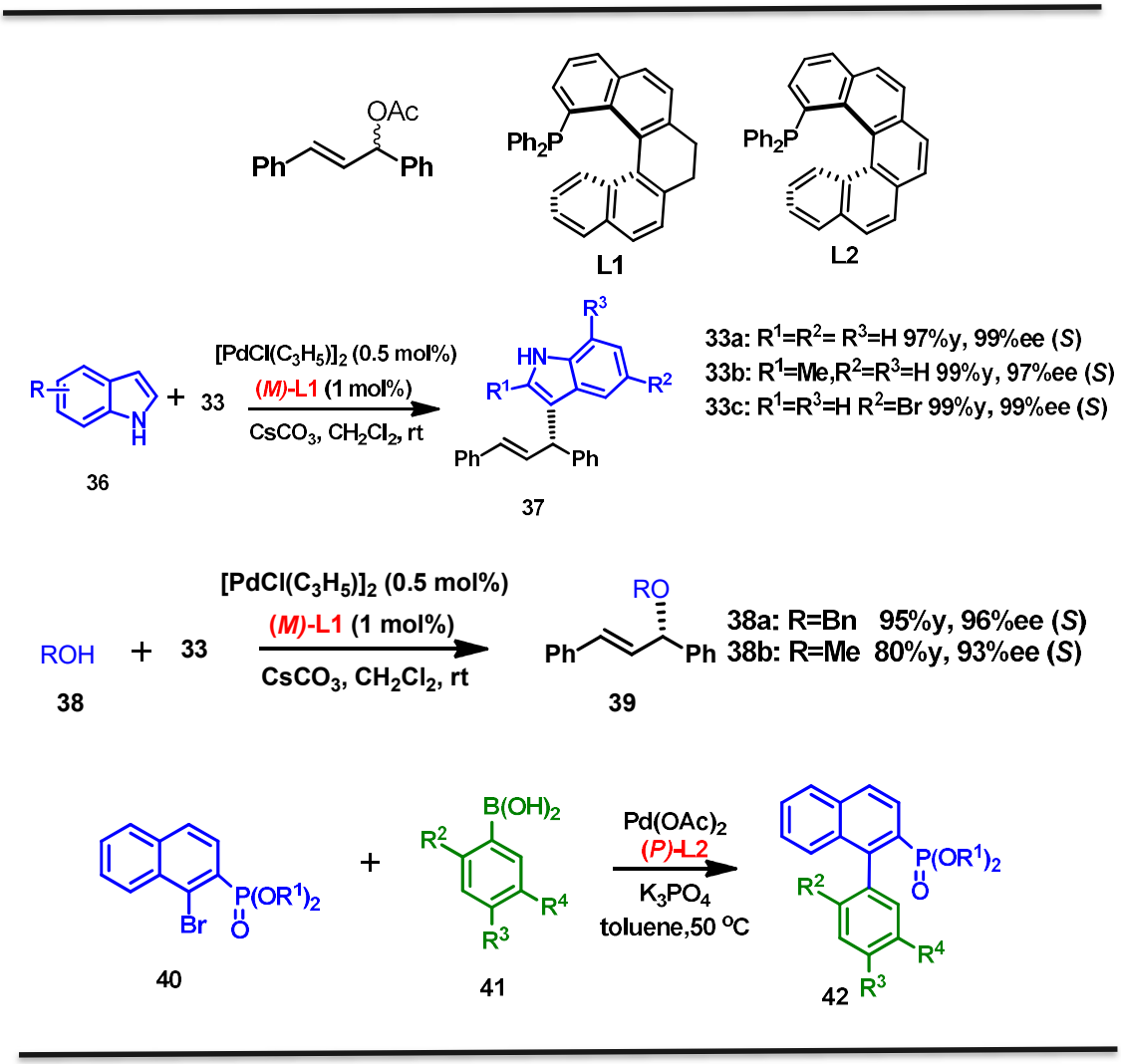

***Scheme 2.8**: Pentahelicene based phosphine ligands in allylic substitution and SMC reaction*

Nakazaki group described the synthesis of helicene crown ethers as early as 1983. The host **43** was prepared by photochemical cyclization of stilbene-type precursors to build helicene moiety, followed by the construction of crown ether rings, and examined for their chiral recognition toward racemic amine salts **44-46**.[11] As depicted in Fig. 2.2, the host was resolved in the organic layer ($CHCl_3$), and the amine salt was resolved in outer part of the aqueous phase, which was separated by the tube. With stirring, the host transports the amine salt to the aqueous phase in the tube. And the selectivity could be calculated by analysis of inner aqueous solution. It was found that (1) the selectivity of the (*R*)-/(*S*)-enantiomer was totally reversed for the crown ethers with the same helicity; (2) the enantioselectivity of **44** was much better than that of **45**, which meant that the complementarity between the hosts and the guests was important.

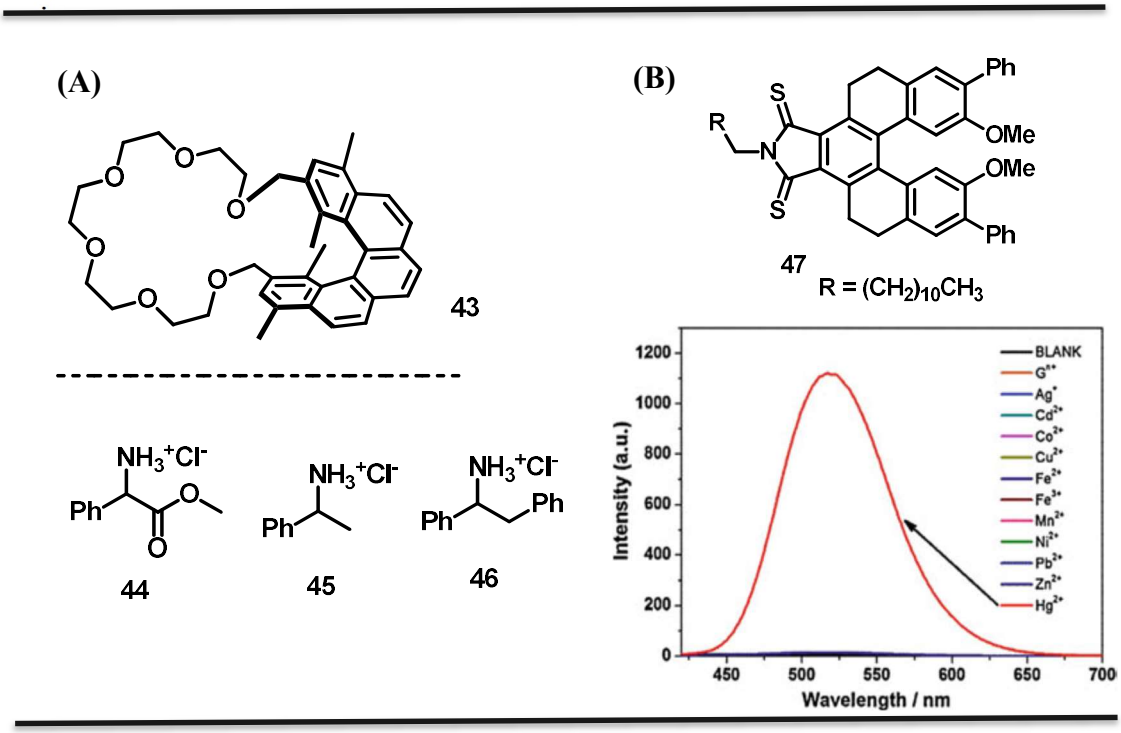

Figure 2.2: *(A) Helicene derived chiral crown ethers and guest molecules (B) Structure of chemodosimeter (top) and fluorescence spectra(bottom) of 47 with the addition of 20 eq of metal ions.* λ_{ex}*=385 nm*

Chen, Lu, and co-workers[12] synthesized a tetrahydro[5]helicene thioimide-based chemodosimeter **47** for highly selective and sensitive detection of Hg^{2+}. The solution of **47** in CH_3CN/water was investigated with the addition of different metal ions. There was a considerable increase in the emission intensity with the addition of Hg^{2+}. The enhancement was estimated to be 200-fold, and the detection limit of **47** for Hg^{2+} was about 5.0 x10−7 M.

A novel sultam-based hetero[5]helicene[13] **48** was synthesized by Wong *et al* in 2016 which displays deep-blue emission in solution and in solid state. Interestingly the PL efficiency enhanced two-fold upon crystallization. This helicene fluorophore is a promising candidate for the design and synthesis of pure blue emitters for organic optoelectronic and sensing applications.

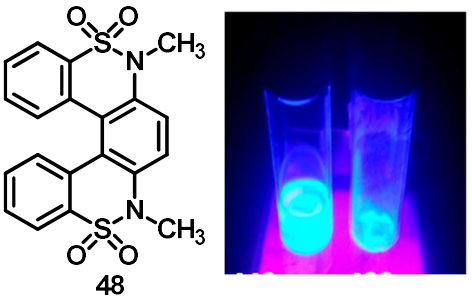

Figure 2.3: *sultam based fluorophore*

2.2 Results and Discussion

2.2.1. C-2 substituted pyrrolo[5]helicene

2.2.1.1 Synthesis of methoxy substituted pyrrolo[5]helicene

Five-membered azahelicenes, being good models for illustrating many parameters like regioselectivity, side reactions, configurational stability etc. we decided to synthesize some substituted pentahelicenes and study their properties. The synthetic route to the target helicene **55** began with *N*-alkylation of carbazole as shown in scheme 2.9. Here *N*-butyl chain was preferred owing to good solubility in the reaction conditions specified. The butylated carbazole was then subjected to iodination in the presence of potassium iodide-iodate mixture yielding mono-iodo-*N*-butyl carbazole **51**. The olefin precursor was obtained in good yield by a Pd-catalysed one-pot Wittig-Heck reaction sequence with the iodo-carbazole, *p*-anisaldehyde and methyltriphenylphosphonium iodide where the aldehyde **52** and the wittig salt **53** will in-situ generate the 4-methoxystyrene in Wittig reaction and the styrene will react with carbazole derivative **51** in Heck reaction. This was followed by photocyclization of the styryl derivative in toluene under 125W high pressure mercury vapour lamp in the presence of iodine as the oxidizing agent and THF as the scavenger of hydrogen iodide formed during the course of the reaction. Careful analysis of the reaction mixture revealed consumption of the starting material and formation of a major product, which was isolated by column chromatography over silica gel.

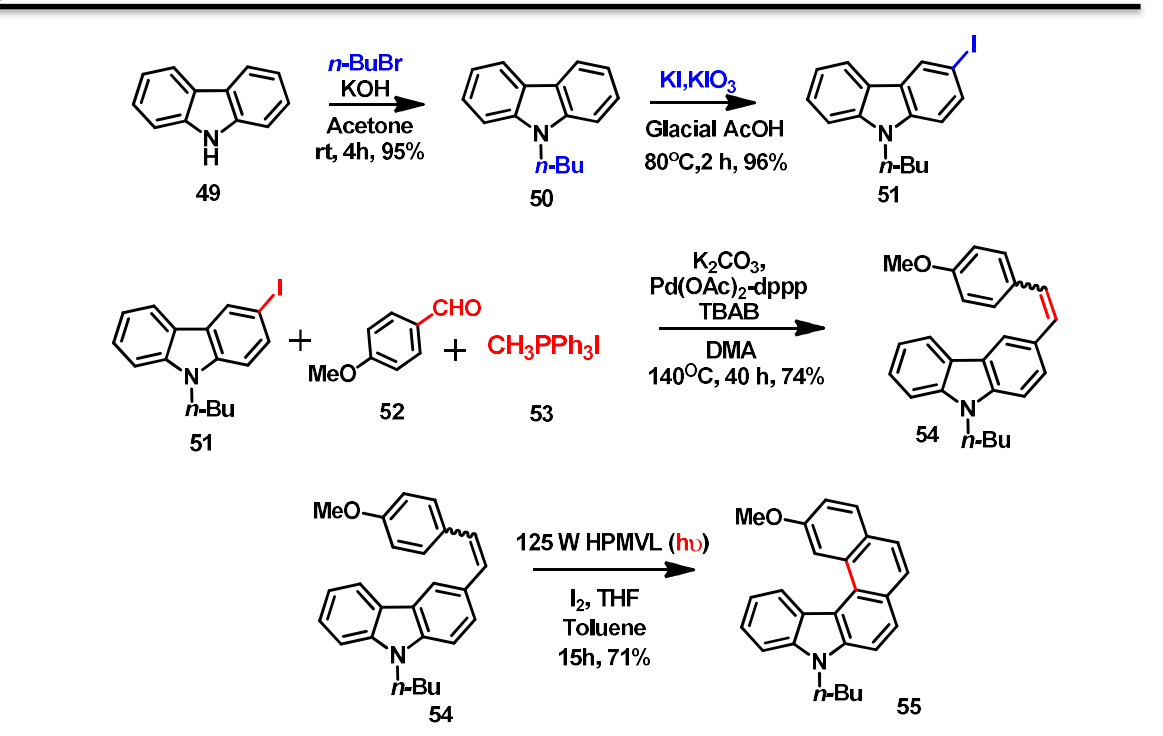

***Scheme 2.9**: Synthesis of methoxy-substituted pyrrolo[5]helicene 55*

2.2.1.2 Regioselectivity of photocyclization

The photocyclization of compound **54** proceeded with the formation of exclusively the angular regiomer of pentahelicene. This was confirmed from the ^{1}H NMR analysis of the crude reaction mixture after completion of the reaction. As shown in Figure 2.4, the absence of singlet signals clearly indicates the absence of linear product. The hydrogen attached to C1 of **55** appeared at 8.7 as a doublet with a coupling constant value of 2.4 MHz. The most downfield signal which appeared as a doublet corresponds to C13.

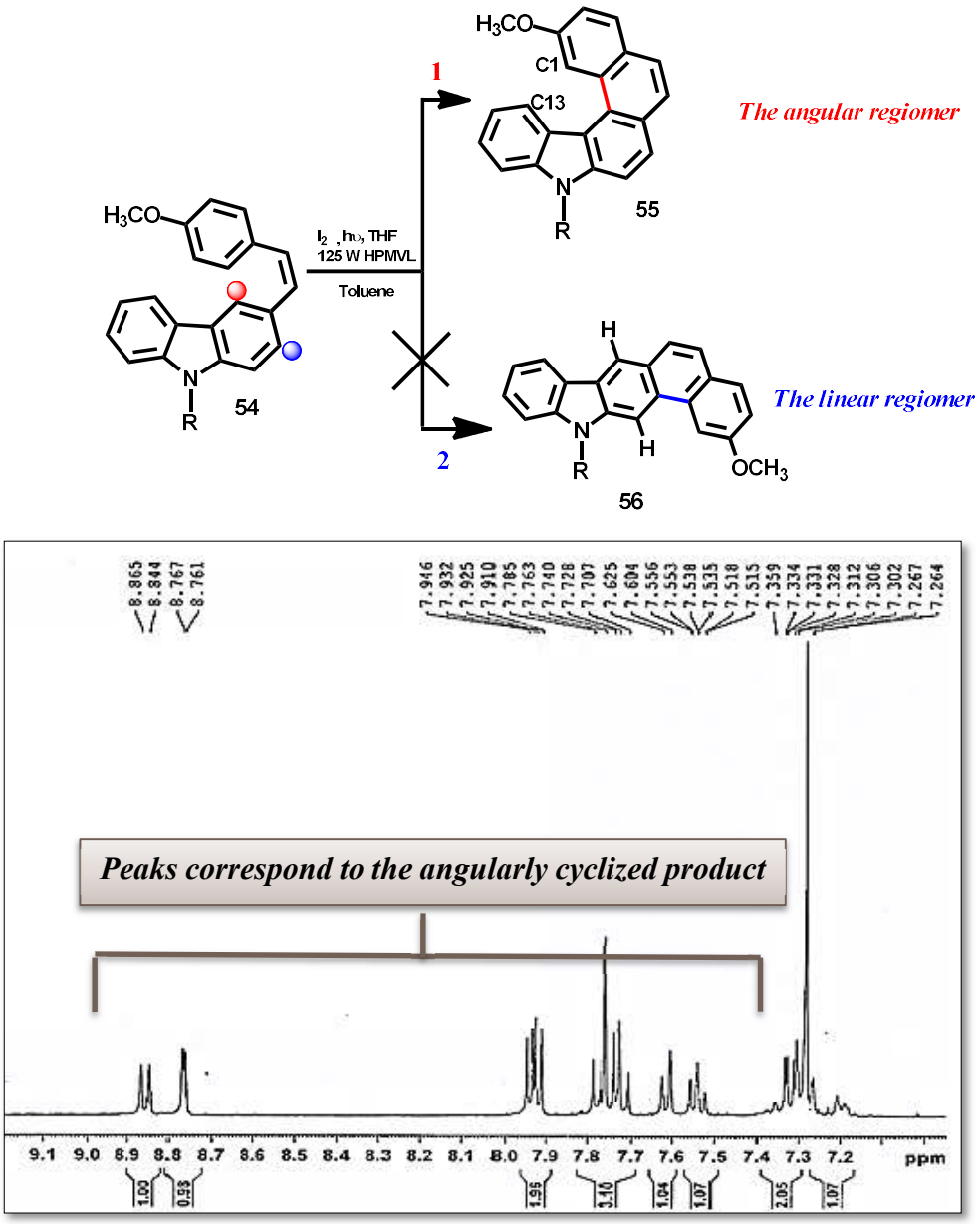

Figure 2.4: Aromatic region of the ^{1}H-NMR spectra of compound 55

2.2.1.3 Solid- state structure analysis of compound 55

Single crystal of compound **55** which was obtained by slow evaporation of dichloromethane at room temperature was subjected to X-ray analysis. The compound belongs to the *P*na2$_1$ space group. The outer bonds C(5)–C(6), C(8)–C(9), C(11)–C(12) were shortened to 1.34 Å with respect to the average bond length in benzene (1.39 Å), whereas the inner bond distances C(1)–C(17), C(16)–C(17), C(15)–C(16), C(14)–C(15) were lengthened to 1.40–1.45 Å. The torsion angles along the inner helical rim (φ1 = C14–C15–C16–C17; φ2 = C15–C16–C17–C1; φ3 = C16–C17–C1–C21), which varied from 7.51° to 24.37°, were also a convenient measure of the helicity (Table 2.1).The terminal inner helical torsion angles (C14–C15–C16–C17 and C16–C17–C1–C21) were not equal and were relatively small angles of 17.28° and 7.51°, respectively. The distortion of the molecular structure (49.16°) is defined by the sum of the three torsion angles (C14–C15–C16–C17, C15–C16–C17–C1and C16–C17–C1–C21). The repulsion of the facing terminal benzene rings leads to an interplanar angle of 41.61° between the terminal benzene rings.

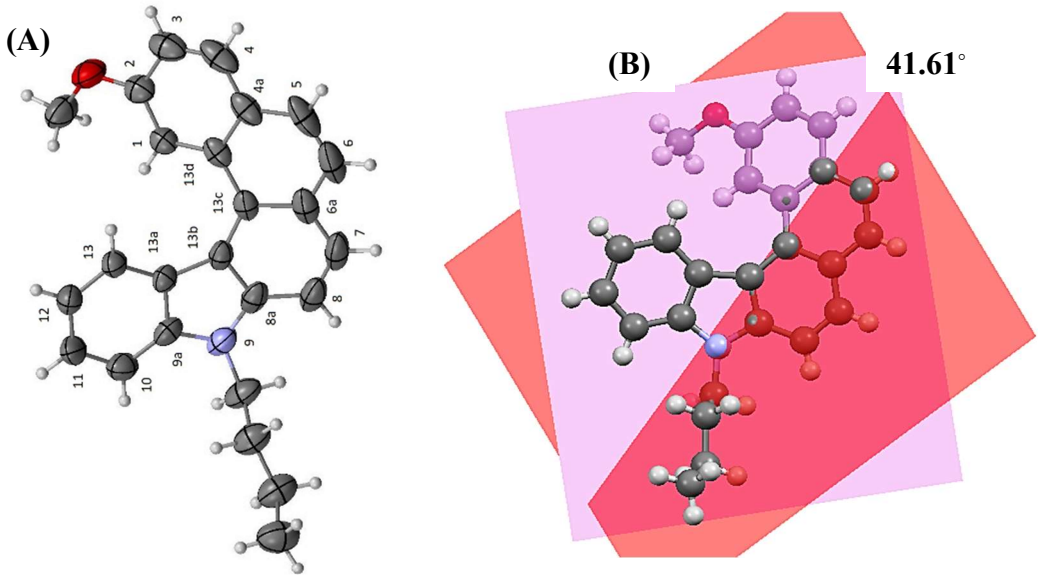

***Figure 1.5**: (A) ORTEP plot of compound 55 CCDC 1062828 (B) figure showing the interplanar angle*

Torsion Angle (°)	Distortion of the Molecular Structure (°)	Dihedral Angle θ(°)
φ1 =17.28 φ2 =24.37 φ3 =7.51	φ1+φ2+φ3 = 49.16	41.61

***Table 1**: Crystallographic properties of compound 55*

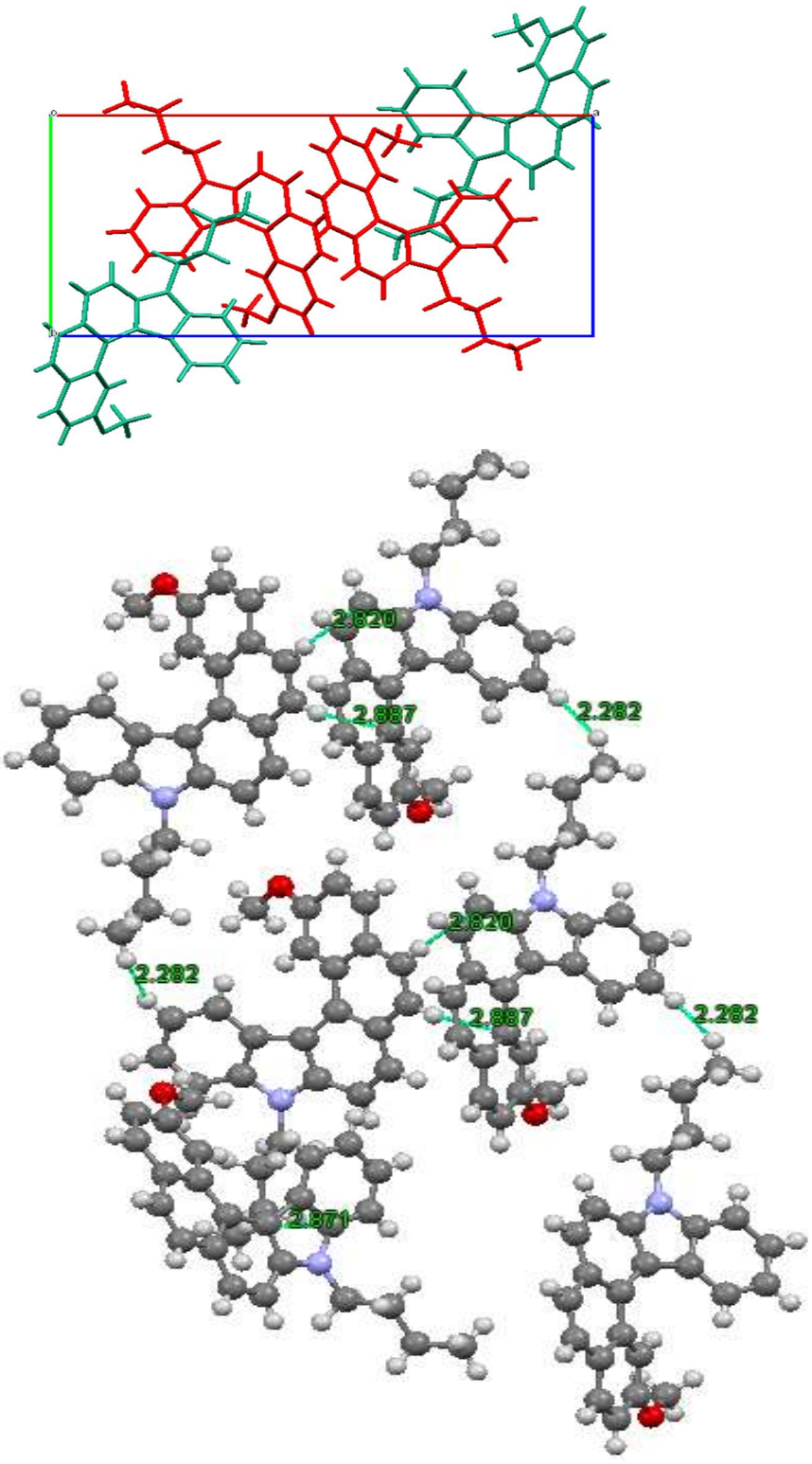

***Figure 2.6**: Crystal packing structure along the a axis (top) and short contacts in the crystal (bottom)*

2.2.1.4 *Functionalization of compound 55*

Functionalization of helical molecules is important to explore various applications. The most common among the transformations is that of bromohelicenes and hydroxyl helicenes. Bromine atom can be easily incorporated by bromination of the substrates whereas hydroxyl group is generally introduced in the scaffold via methoxy group. The methoxy substituted pentahelicene **55,** was converted into bromo **57** and iodo derivatives **58** using *N*-bromosuccinimide and potassium iodide-iodate respectively. Demethylation was also carried out using Boron tribromide to yield hydroxy pentahelicene derivative **56**. Earlier work from our group involves the synthesis of chiral helical 1,3-oxazines from hydroxyl derivatives.[14a] Inspired from this work we thought constructing oxazine units using the hydroxyl pentahelicene. However, we did not observe the formation of oxazine even after repeated experiments with modified conditions probably due to the already over-crowded helical system which makes it sterically unfavourable for these reactions.

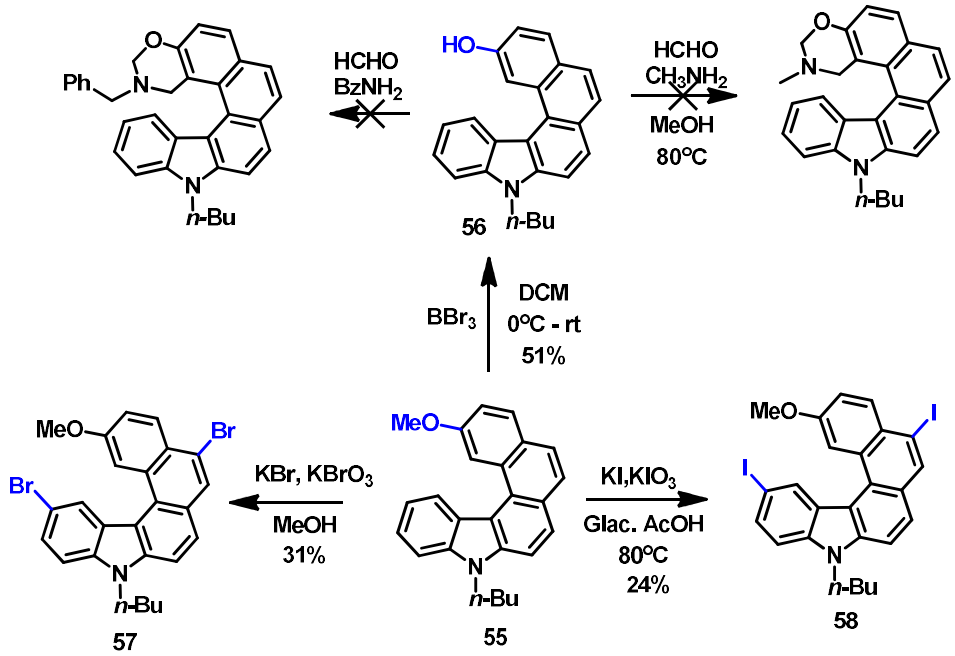

Scheme 2.10: Functionalization of compound 55

2.2.1.5 *Stereodynamic behaviour of compound 55*

In order to check the stereodynamicity of this pentahelicene, we carried out HPLC analysis in Hexane-Isopropanol solvent system (97.5:2.5) with IC Chiralpak column. The resulting chromatogram showed a single peak indicating the instability of the isomers at room temperature as shown in figure 2.7.

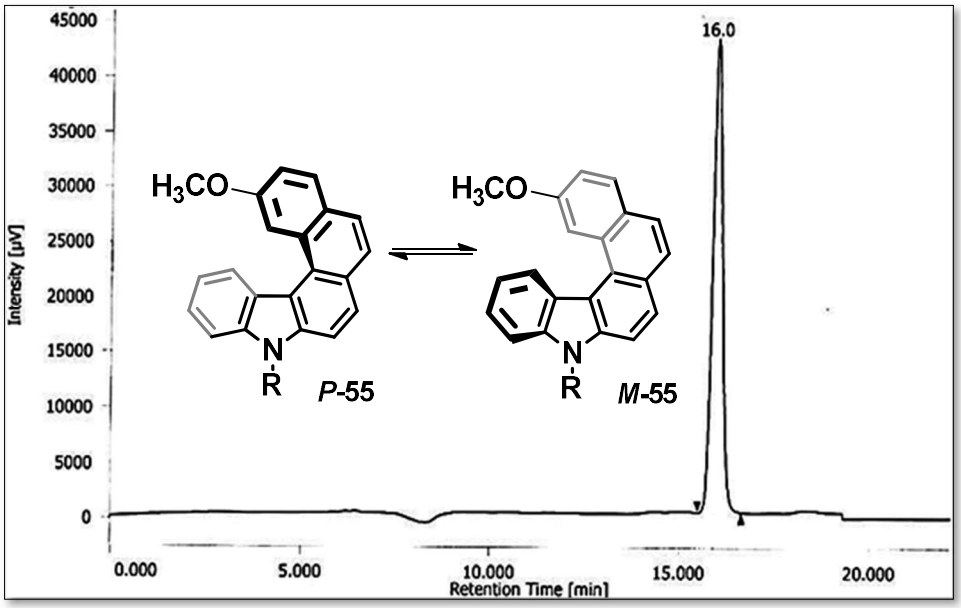

***Figure 2.7**: HPLC Chromatogram of compound 55*

This result is not unusual considering the structural characteristics of small order helicenes. Lack of sufficient steric bulk leads to rapid interconversion of the isomers at room temperature. A similar observation was reported by Dehaen group. A racemic chloro-substituted diaza[5]helicene derivative was synthesized by Dehaen *et al.*[14c] using oxidative photocyclization of stilbenic system. It was then converted into diastereomeric mixture by Buchwald-Hartwig coupling with (*S*)-α–methylbenzylamine. However, when they tried to separate the diastereomers by column chromatography, they found that these compounds were not configurationally stable with half-life times ($t_{1/2}$) of 26 min at 25°C. This result also ascertains that helicenes incorporating 1*N* or 2*N* atoms racemize more readily than their carbo[5]helicene counterparts Hence, our next target was to synthesize configurationally stable five-membered azahelicene. So, it is important to revisit the literature of small order helicenes and their stability.

2.2.2. Spatial diversity of helicenes

The helical skeleton is not as rigid as it is shown albeit composed of aromatic rings. So before delving further into the chemistry of five-membered helicenes, it is important to understand the spatial diversity of helicene. Based on stereochemistry, helicenes can be categorized into: 1) Achiral 2) Chiral 3) Meso and 4) Stereodynamically labile helicene. Let us comprehend each of these in detail.

1. **Achiral helicenes**: This type is limited to smaller helicenes like [4]helicene or [5]helicene without any substitution. Although the rings are *ortho*-fused, the molecule does not intrinsically adapt the helical topology due to lack of overlap of the terminal rings. Thus, these molecules have flat structures. Nonetheless, they can be studied for their application in material science due to good optical properties and enhanced conjugation.

2. **Chiral or configurationally stable helicenes**: A chiral helicene is a result of the inherent helicity adopted by the molecule to avoid the steric hindrance between the terminal rings. As already discussed in section 1.1, right-handed helixes are assigned as *P*-enantiomer and left-handed helixes as *M*-enantiomer. Both the enantiomers are thermodynamically stable and have a highly strained transition state. These molecules are suitable to be explored for chiral auxiliary and various chirogenic processes due to their chiroptical properties.

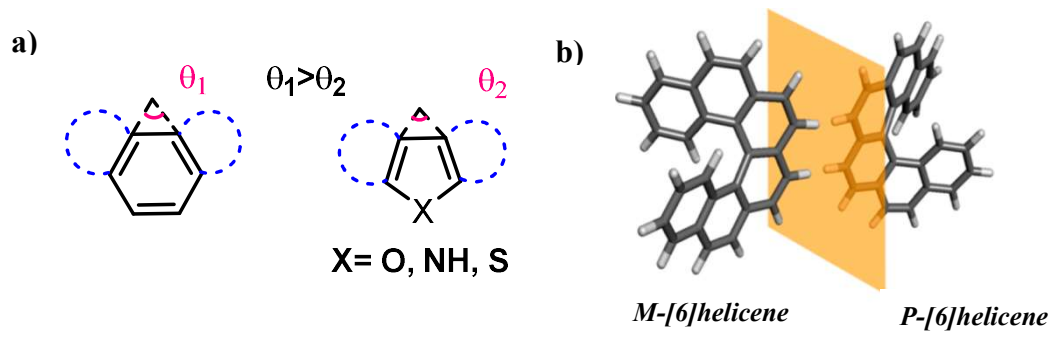

Figure 2.8: Schematic representation of (a) in-plane turn angle and (b)Enantiomers of [6]helicene.

3. **Meso helicenes**: They are achiral helicene but differ in the sense that meso helicenes are symmetrical molecules having two equivalent helical part with opposite helicity.

As both the helical moieties are chemically equivalent, it is difficult to selectively desymmetrize any one. An example of a meso double helicene is shown in figure 2.9

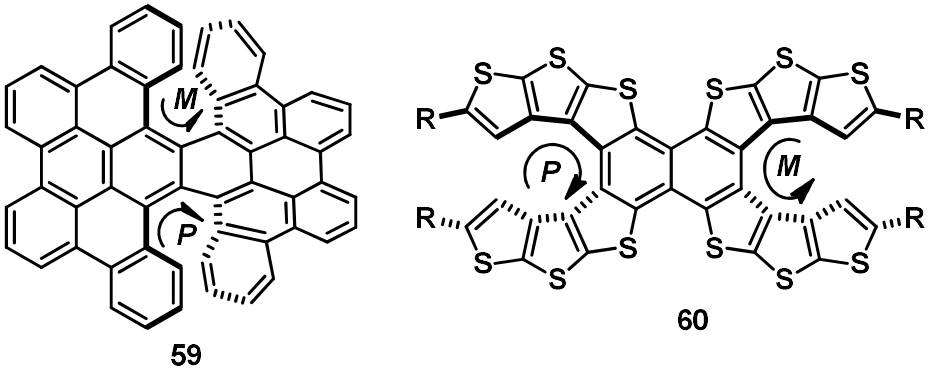

***Figure 2.9**: Examples of meso double helicene*

4. **Stereodynamic helicenes**: Stereodynamic helicenes are intermediate between chiral and achiral helicenes. They are as such non-resolvable in solution owing to the low (*P*)-(*M*) interconversion energy barrier. The six-membered aromatic rings have an in-plane turn angle of 60° but in the case of five-membered heteroaromatic systems, the value is considerably less for eg. in case of thiophene it is at 45°, for pyrrole it is 35°, and 32° for furan. Therefore, to exhibit intrinsic chirality a helical system with a five-membered heteroaromatic ring needs to have n>6, whereas for carbohelicenes n=6 suffices this tendency. However, it is known that introduction of bulky substituents which additionally increase the steric hindrance can improve the configurational stability of lower homologues of helicene.

The five-membered azahelicenes are good models to study the stereodynamicity of a helicene as it shows partial configurational stability. As already discussed, these helicenes are stereodynamically labile owing to the low (*P*)-(*M*) interconversion energy barrier. This interconversion is called as enantiomerization. Here it is important to understand the terms enantiomerization and racemization. Enantiomerization is a microscopic and molecular process of reversible conversion of *P*-*M* or *M*-*P* while the macroscopic process which yields 1:1 mixture of these enantiomers is called racemization.

In 1956, partial racemization was observed by Newman and Lednicer for the first time in [6]helicene during its melting point determination.[14b] Later the kinetics of racemization of a series of [*n*]helicenes (n=6-9) was studied by Martin and Marchant wherin they calculated

the activation energy barriers as 35 kcal/mol for hexahelicene and approximately 41 kcal/mol for other helicenes.[15] Lindner proposed a planar C_{2v} transition state (TS) for [5]helicene, however due to excessive steric hindrance a planar TS is impossible for higher helicenes so a non-planar and non-chiral C_s TS was suggested by the author. Grimme and Peyerimhoff, in 1994, computed the racemization of [*n*]helicenes (*n* = 4-8) using a B3LYP/SV+d+p level. The theoretical values for the racemization barriers are in line with the experimental values, showing an increase until *n* = 6. This increase can be attributed to the enhanced intramolecular interactions between the terminal rings in the TS up to *n* = 6.[16] The C_s TS has been adopted most often in the reported computational calculations for pentahelicene. Hence the structure of unsubstituted pentahelicene in the ground state first twists into the non-planar and non-chiral C_s TS and subsequently transforms into either of the enantiomers with equal probability releasing the torsional strain and repulsion and thus results in racemization.

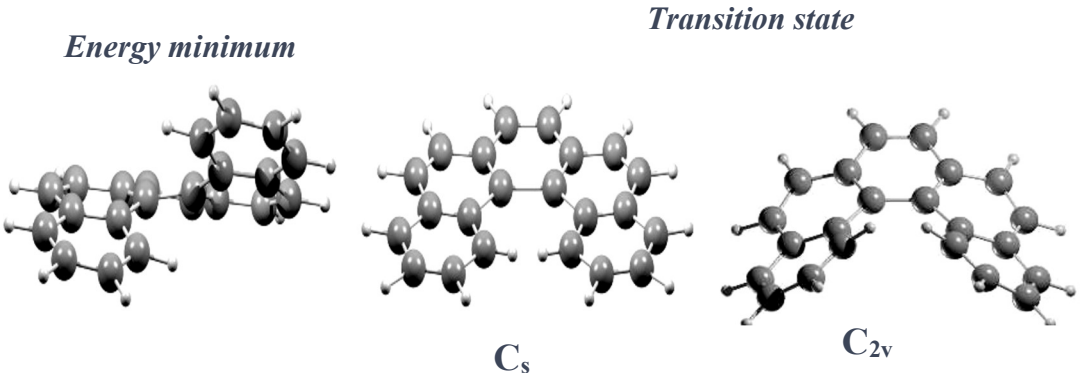

***Figure 2.10:** Transition structure of [5]helicene along with the corresponding minimum as suggested by Lindner and Grimme*

Further, Caronna et al. carried out a combined experimental and computational study on the stereodynamics of monoaza[5]helicenes.[17] The activation parameters of [5]helicene and seven monoaza analogs were determinied for the first time by enantioselective dynamic HPLC (DHPLC) in normal phase mode using n-hexane/2-propanol as the eluent. The enantiomers were separated on coated and immobilized derivatized polysaccharide stationary phases at temperatures below 10°C. It was established from this study that the position of nitrogen atom has a considerable effect on the activation parameters. The activation energy is lowered when a CH-group is substituted by a nitrogen atom in [5]helicene which leads to significantly faster enantiomerization kinetics. Thus, in the case of aza[5]helicenes, the presence and the position of the heteroatom can modify helicity parameters, such as dihedral angles and bond lengths which in turn affects the configurational stability and the enantiomerization barrier.

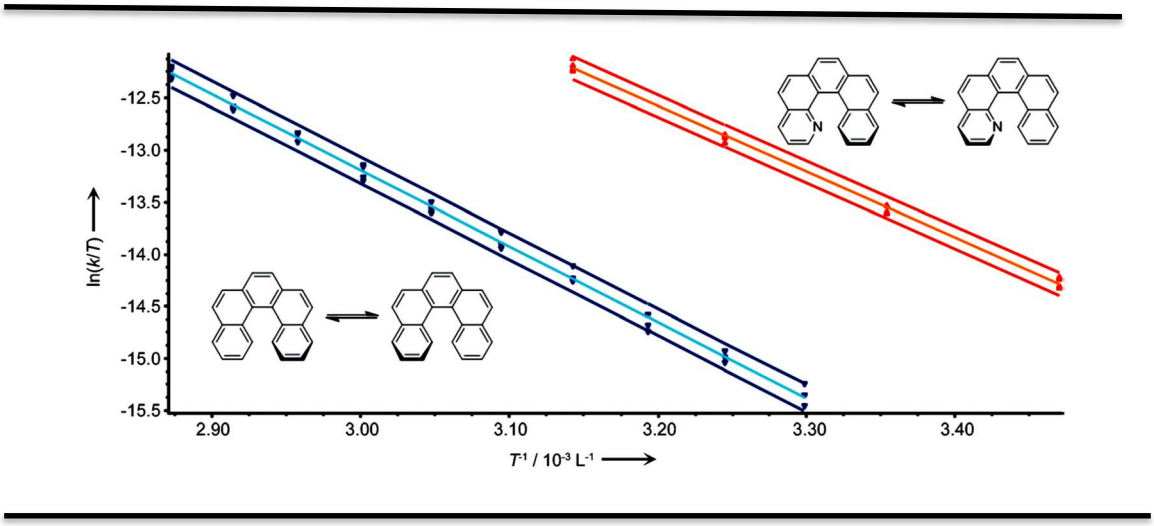

***Figure 2.11**: Eyring plot to determine activation parameters ΔH and ΔS of the enantiomerization barriers of [5]helicene (left) and 1-aza-[5]helicene (right).*

Usui *et al* reported the synthesis of [5]helicenes **66** with a substituent exclusively on the bay region of the helix by metal-catalysed cycloisomerization. The separation of enantiomers of 1-functionalized [5]helicenes was achieved by HPLC on a chiral column and, accordingly, the racemization barriers were determined.[18]

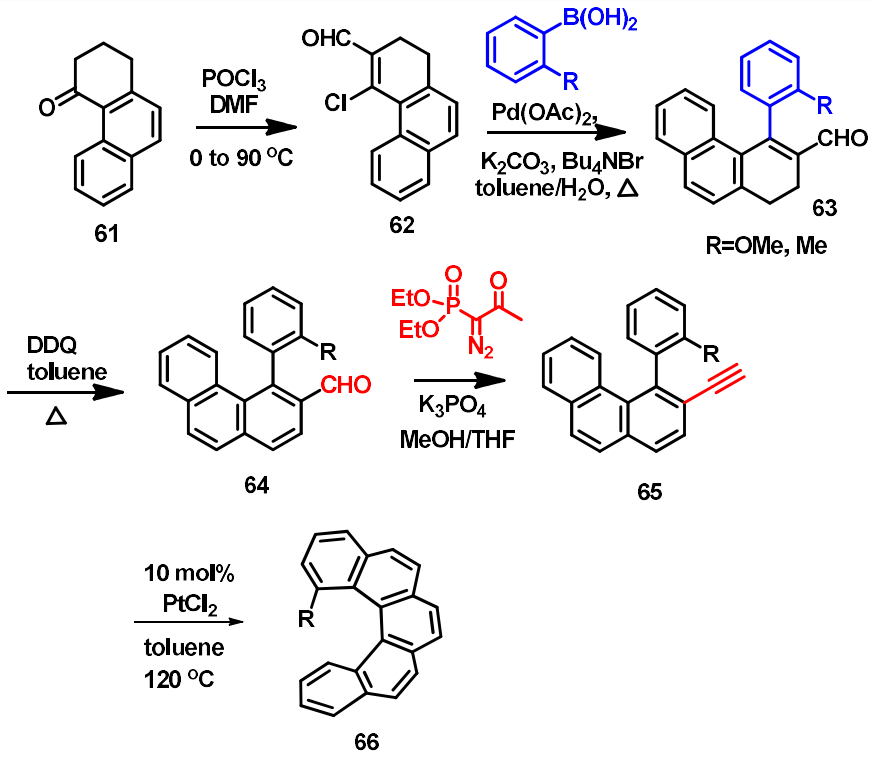

***Scheme 2.11**: [5]helicene with a substituent exclusively in the bay region*

Dehaen *et al* reported a facile method for the synthesis of several bay functionalized thiaaza[5]helicene[19] **68** and the implication of the substituents on the structural and spectroscopic properties. These thiaza[5]helicenes with different substituents were prepared in a straightforward manner through indole- and benzo[b]thiophene synthesis, palladium-catalyzed Suzuki coupling, oxidative cyclization, and functional group interconversion reactions. They concluded that a single substituent in the bay area of a thia[5]helicene was not enough to prevent enantiomerization at room temperature.

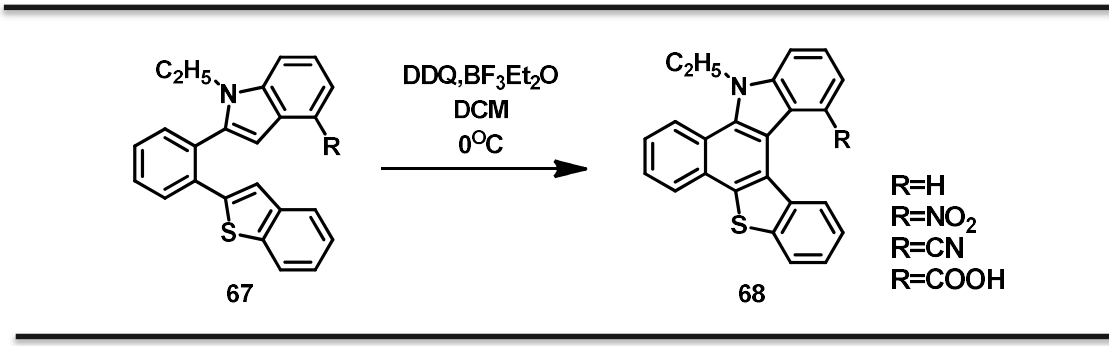

***Scheme 2.12**: Series of thiaza[5]helicene with different substituents*

Recently Michal Juricek *et al* carried out a detailed study of fjord funtionalized [5]helicenes and their configurational stability. They synthesized a series of [5]helicenes difunctionalized in the fjord region with either fluoro, methoxy, or methyl groups via photochemical and benzylic coupling route and carried out their resolution Gibbs activation energies of enantiomerization ($\Delta G^{\ddagger}(T)$) was also determined and compared with those of their monofunctionalized analogues and the parent [5]helicene. From the experimental and theoretical data it was established that the dimethyl derivative exhibits one of the highest configurational stabilities among [n]helicenes reported to date, comparable to that of [9]helicene.[20]

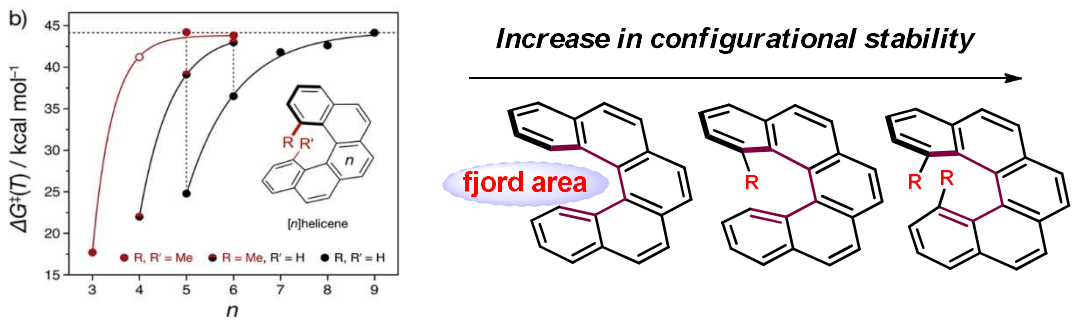

***Figure 2.12**: Configurational stability of [5]helicenes*

2.2.3. C-1 substituted pyrrolo[5]helicene

2.2.3.1 *Synthesis of 1,3-dimethyl-9-butyl-9H-aza[5]helicene*

It is important to synthesize helical molecules which do not racemize under the ambient conditions in order to explore its application as chiral auxiliaries or catalysts. With this background about racemization, we undertook the synthesis of a fjord substituted pentahelicene. The retrosynthetic scheme to synthesize five-membered aza-helicene with a substituent in the fjord region is shown in scheme 2.13. We thought of installing a methyl substituent in the bay area, as a single methyl substituent itself enhances the barrier of racemization to a considerable extent. As shown in scheme 2.13, for this transformation, 3-methyl benzyl triphenyl phosphonium salt would be necessary for the Wittig reaction. However, the cyclization can take place at C-2 or C-6 of the Wittig salt. Considering the steric parameters it is more probable that cyclization may take place at C-6 of the salt rendering the [5]helicene with a C-3 substituted methyl group which will serve the purpose of our study. Hence it was necessary to block this position. So, we thought of using 3,5-dimethylbenzylphosphonium salt which in either case will exclusively yield the C-1 methyl substituted pentahelicene.

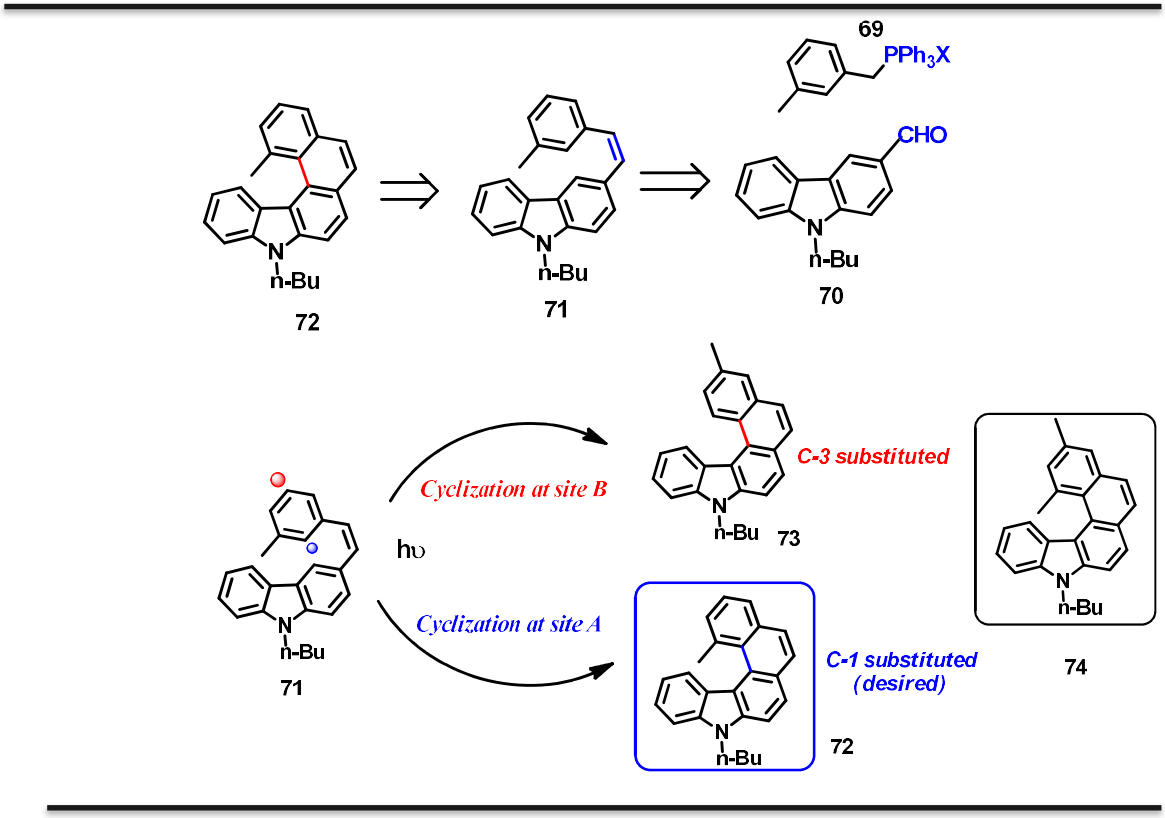

Scheme 2.13 : Retrosynthetic scheme for C-1 methyl substituted pyrrolo[5]helicene

As seen in the literature reviews, for a carbohelicene, a methyl substituent in the fjord region would be sufficient to accomplish the objective to synthesize conformationally stable pentahelicenes at room temperature. However, our target was to synthesize azahelicenes. So, to check if this theory can be extended to azahelicenes, we carried out computational study of the structural parameters of the C-2 methoxy substituted pentahelicene **55** and compared it with the 3,5-dimethylpentahelicene **74**. The calculations were carried out at the B3LYP/6-31G level of theory to get the optimized geometry of the aforementioned molecules. Torsional angle being a good measure to understand the extent of distortion, we compared this value for both the molecules. It was observed that, there was an increase of about 9° in the distortion of the molecule (sum of torsion angles), when a methyl group was installed in the fjord region. This further supported the theory and enthused us to proceed with the synthesis.

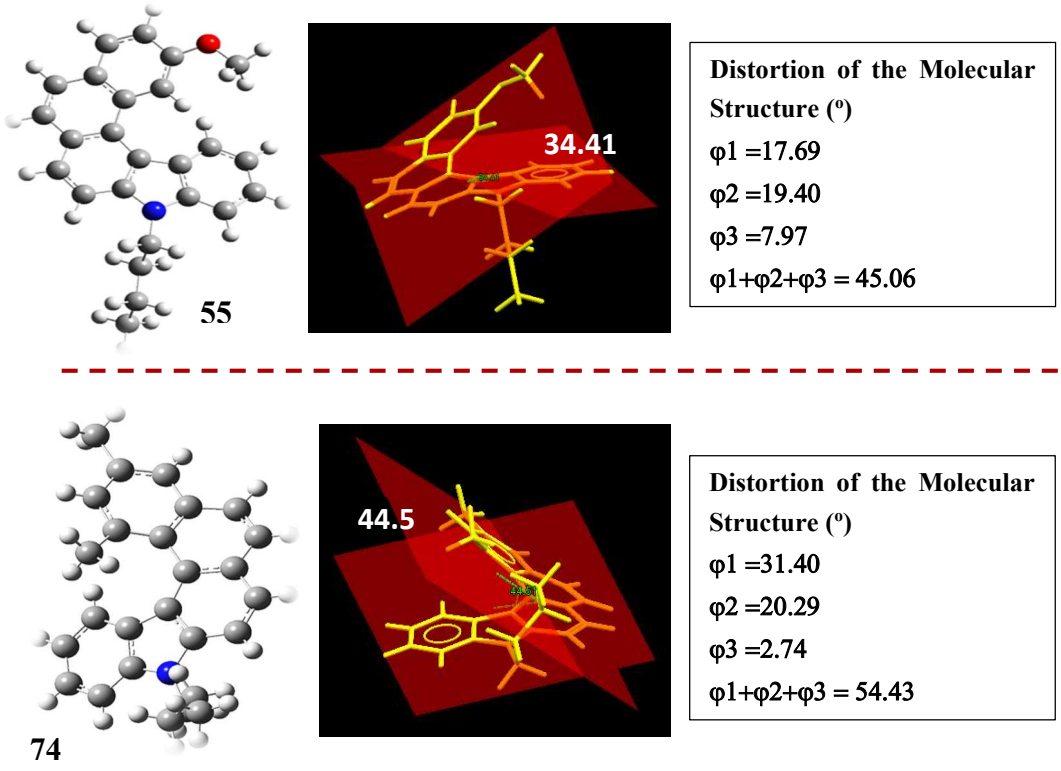

***Figure 2.13:** computational analysis of the structural parameters of compound 55 and 74*

So to synthesize the target helicene **74**, we started with Vilsmeier-Haack formylation reaction of the butylated carbazole, in the presence of *N,N*-Dimethyl formamide and Phosphorous oxychloride yielding mono-formyl-*N*-butyl carbazole **70**. The olefin precursor was obtained in good yield by Wittig reaction with 3,5-dimethyl benzyl triphenylphosphonium bromide. This was followed by photocyclization of the styryl

derivative in toluene under 250 W high pressure mercury vapour lamp in the presence of Iodine as the oxidizing agent and THF as the scavenger of hydrogen iodide formed during the course of the reaction.

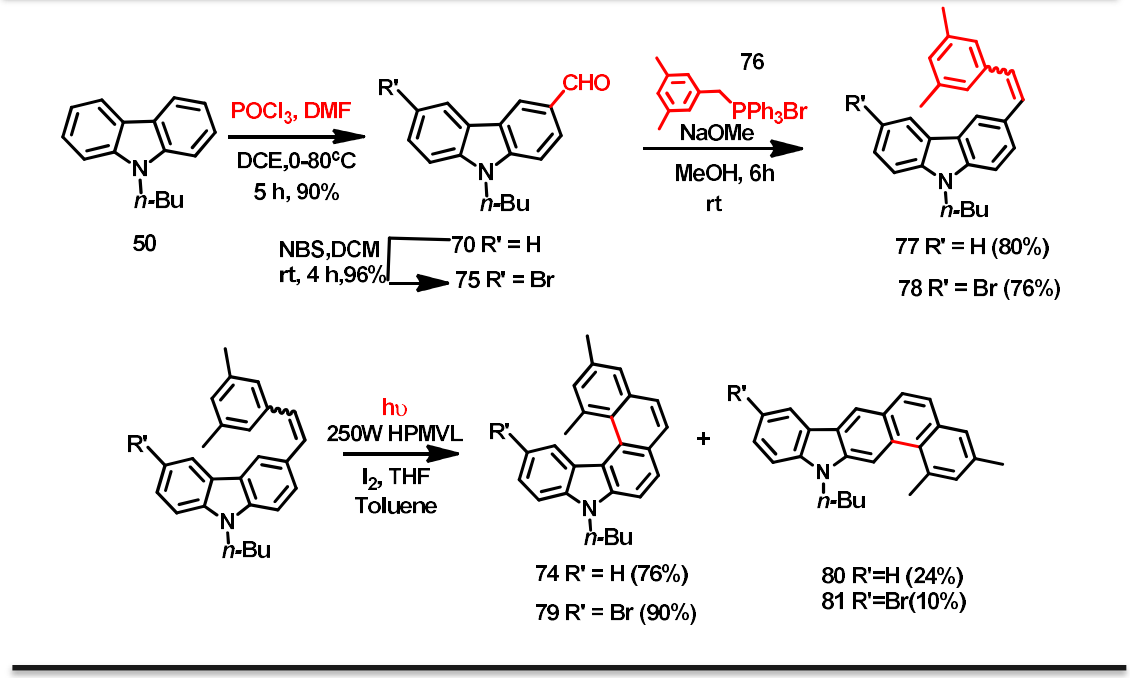

***Scheme 2.14**: Synthesis of 3,5-dimethyl pyrrolo[5]helicene*

However, the ^{1}H-NMR analysis of the product of photoreaction of the dimethyl stilbene derivative, showed a mixture of angular and linear isomers as shown in figure 2.14 (A). We attempted to separate the linear isomer from the angular one by repeated column chromatography, but our efforts were in vain. In a previous study by our group, the effect of concentration on the regioselectivity of photocyclization was studied. It was observed that at higher dilutions, the desired angular regiomer was more favourable.[21] Hence, we also tried to repeat the photoreaction in very low concentration but still could not obtain the angular regiomer exclusively. Next, we tried to grow the crystals of the same expecting some separation or enrichment during crystallization, but it did not work by this method also. Hence, we thought of introducing a bromo substituent on the carbazole ring and repeat the entire synthesis with the thought that probably a bromo group will improve the quality of the crystals of the helicene which may aid in separation of the regiomers. In this way we synthesized the 12-bromo derivative of the pyrrolo[5]helicene. By repeated crystallization and column chromatography of the bromohelicene, we were able to separate the angular and the linear regiomers. This was confirmed from the ^{1}H-NMR analysis of compound **79**.

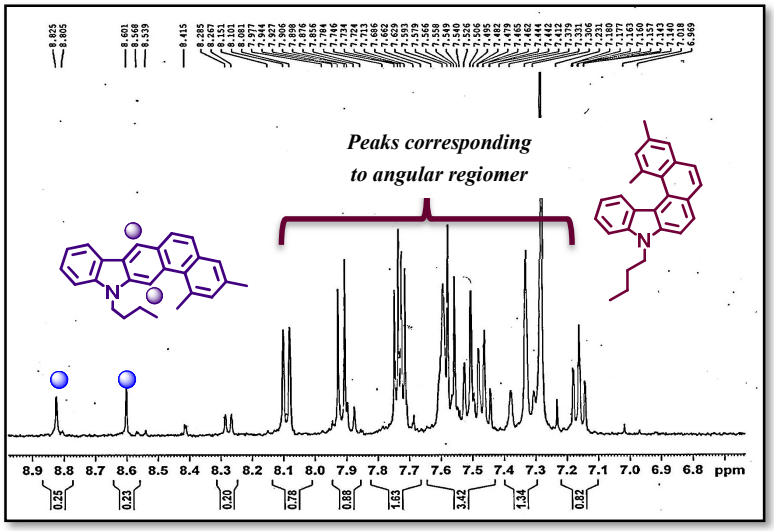

Figure 2.14: Separation of angular and linear regiomers

2.2.3.2 *Stereodynamic behaviour of compound 79*

The separated and purified angular isomer of the pentahelicene with a methyl fjord substituent and a bromo group was then subjected to HPLC analysis on IC Chiralpak column to check the stereodynamic stability of this compound at room temperature. The analysis was carried out in 99:1 Hexane-Isopropanol solvent system. As preferred, the resulting chromatogram showed two peaks corresponding to the *P* and *M* isomers, indicating the stability of the isomers at room temperature as shown in figure 2.15.

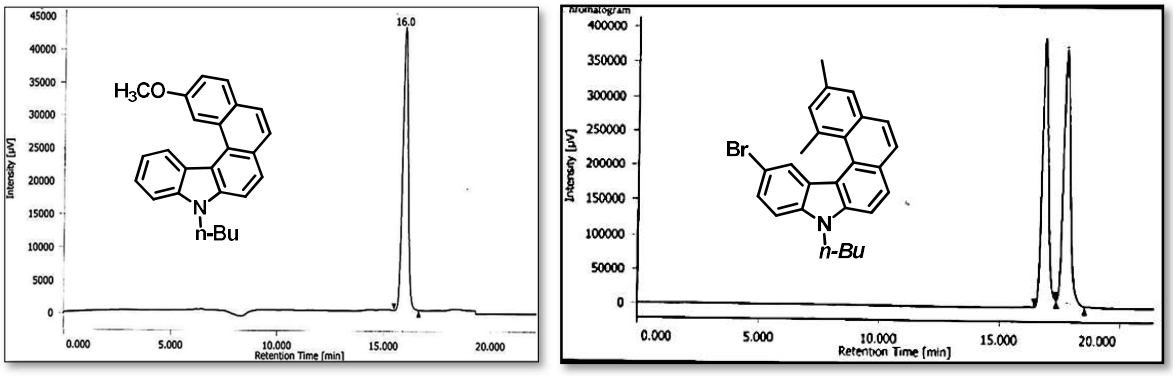

Figure 2.15: HPLC Chromatogram of compounds 55(left) and 79(right)

2.2.3.3 *Functionalization of compound 79*

Compound **79** was subjected to side chain bromination reaction of Ar-CH_3 in the presence of *N*-bromosuccinimide under irradiation. However, the product obtained was a result of electrophilic aromatic bromination as due to the presence of the carbazole moiety, the scaffold was more activated towards aromatic bromination. This was also confirmed from the H-NMR analysis.

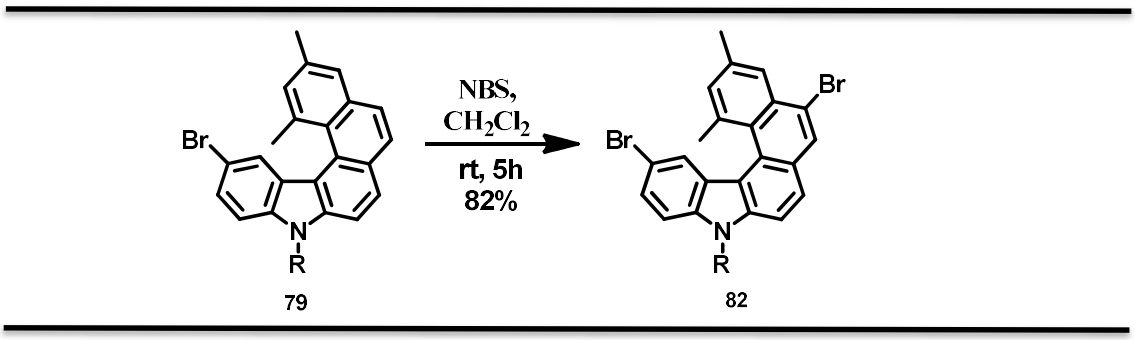

Scheme 2.15: Bromination of compound 79

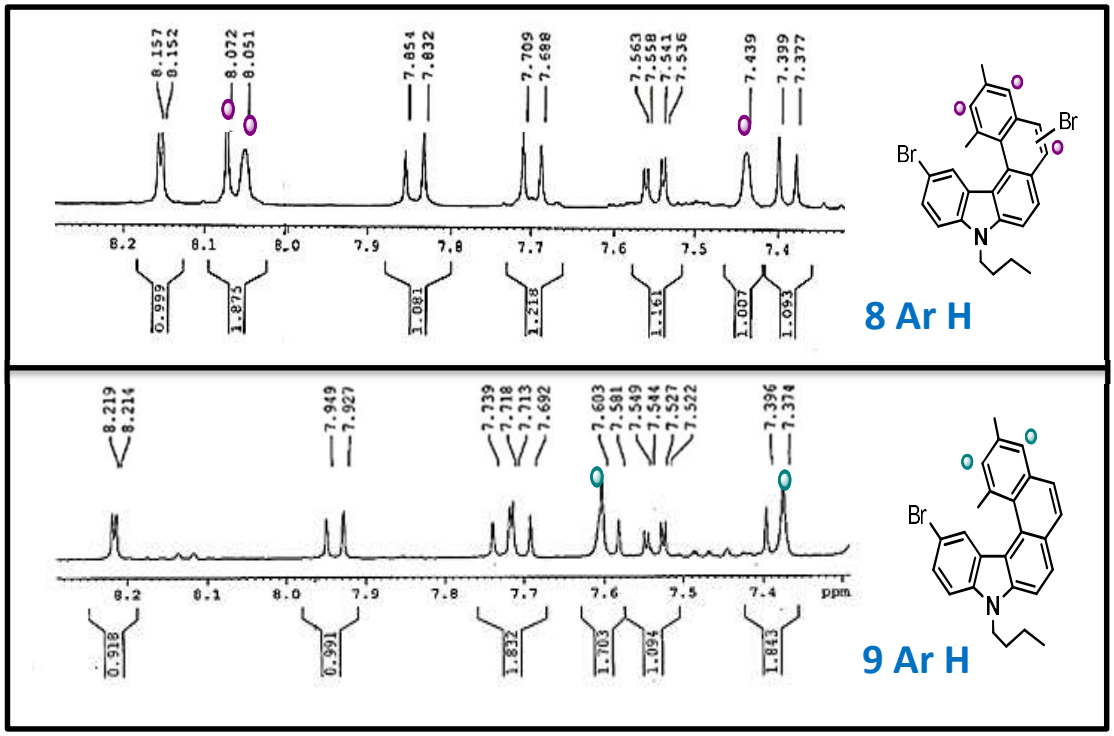

Figure 2.16: ^{1}H-NMR spectra of 79 and 80

As shown in figure 2.16, the dibromo-derivative shows three singlet peaks in the aromatic region which corresponds to the proton next to the methyl-substituted carbons and the proton next to the carbon with the bromo substitution which in the monoderivative appears as a doublet signal. Moreover, there is no change in the peaks corresponding to the aliphatic groups in the spectrum which indicates the absence of any side-chain substitution to have taken place. This confirms the product to be 5,12-dibromo-1,3-dimethylpyrrolo[5]helicene. We had also attempted Buchwald-Hartwig amination reaction under several conditions but in no case the formation of the desired product was observed.

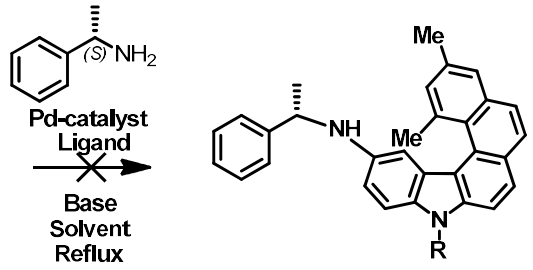

Sr. No.	Solvent	Pd-catalyst	ligand	Base
1.	Toluene	$Pd(OAc)_2$	Xantphos	Cs_2CO_3
2.	Toluene	$Pd(OAc)_2$	BINAP	Cs_2CO_3
3.	Toluene	$Pd_2(dba)_3$	Xantphos	Cs_2CO_3
4.	Dioxane	$Pd_2dba)_3$	Xantphos	Cs_2CO_3
5.	Dioxane	Pd_2 $(dba)_3$	BINAP	K_3PO_4

Scheme 2.16: Attempted Buchwald-Hartwig reaction and condtions

2.2.3.4 Solid- state structure analysis of compound 82

The linear regiomer of the mono-bromo-dimethyl compound **81** crystallized out in dichloromethane solvent but even after several attempts we were not able to get good quality single crystals of the angular regiomer. To our delight the dibromo compound **82**, crystallized out in fine quality by slow evaporation of acetonitrile at room temperature and it was subjected

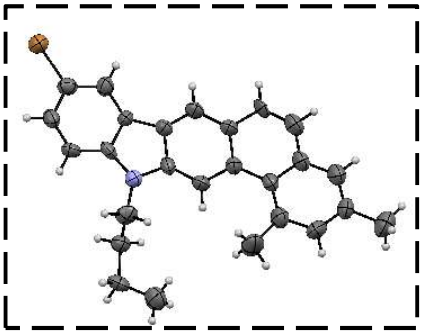

Figure 2.17: ORTEP plot of the linear regiomer (81)

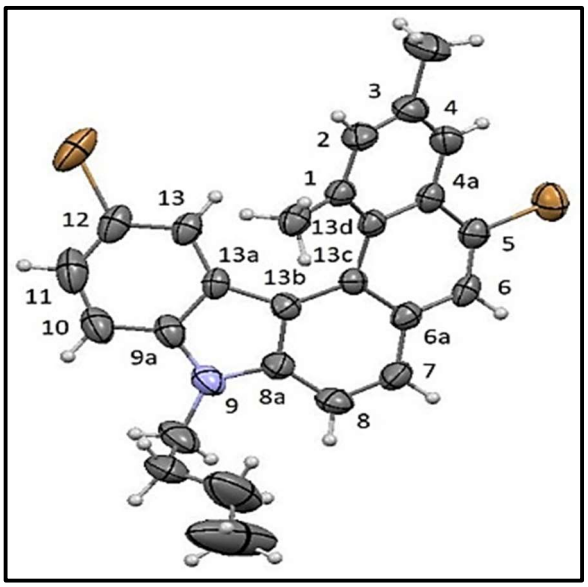

Figure 2.18: ORTEP plot of compound 82

to X-ray analysis. The crystal belonged to the chiral space group $P2_12_12_1$. As observed for a helical framework, the outer bonds C(5)–C(6), C(7)–C(8), C(3)–C(4) were shortened to 1.36 Å while the inner bond distances C(1)–C(13d), C(13d)–C(13c), C(13c)–C(13b), C(13b)–C(13a) were lengthened to 1.40–1.45 Å as seen in the previous case. The torsion angles along the inner helical rim (φ1 = C-13, C-13a, C-13b, C-13c; φ2 = C-13a, C-13b, C-13c, C-13d; φ3 = C-13b, C-13c, C-13d, C-1) varied from 1.46° to 33.64° (Table 1). The distortion of the molecular structure which is the sum of the three torsion angles (C-13, C-13a, C-13b, C-13c, C-13a, C-13b, C-13c, C-13d and C-13b, C-13c, C-13d, C-1) was found to be 56.95°. The dihedral angle or the interplanar angle was found to be 50.60°.

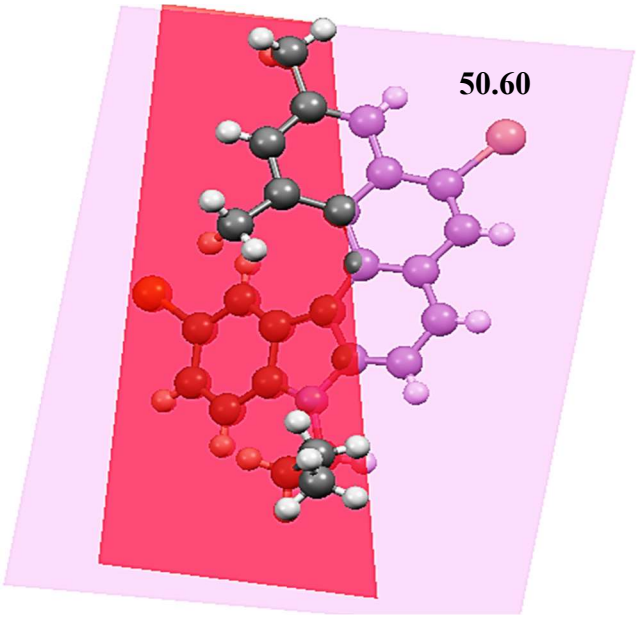

Figure 2.19: Figure showing the interplanar angle

Torsion Angle (º)	Distortion Of The Molecular Structure (º)	Dihedral Angle θ(º)
φ1 =1.46 φ2 =21.85 φ3 =33.64	φ1+φ2+φ3 = 56.95	50.60

Table 2: crystallographic properties of compound 82

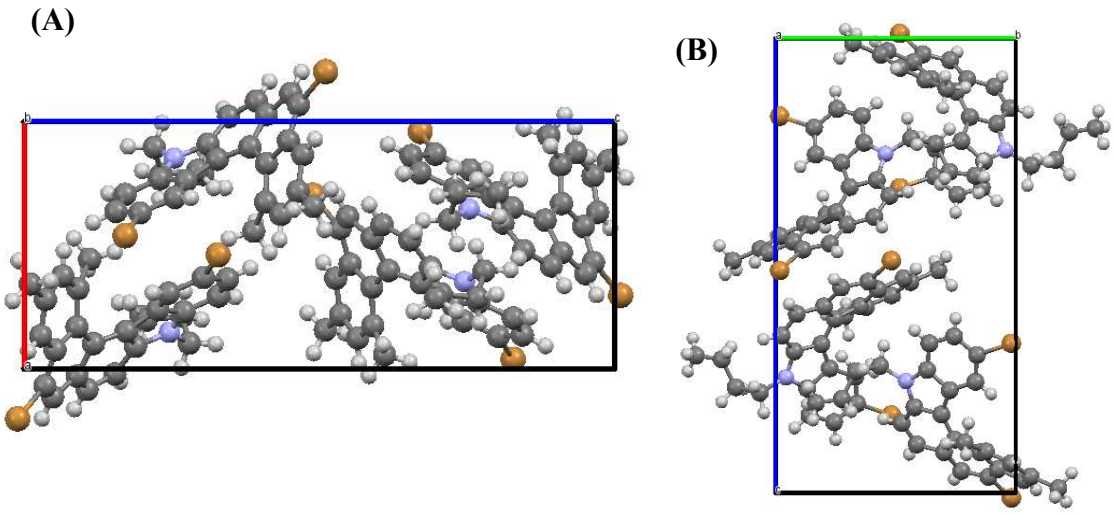

Figure 2.20: (A) Crystal packing along the b axis and (B) a axis

2.2.4. C-1 substituted pyrrolo[5]helicene with an auxiliary group

As seen in the previous section, albeit achieving success in constructing small order heterohelicenes with a scaffold stable against racemization at room temperature, a major drawback in the scheme was the presence of the linear regiomer which had to be separated tediously and the decline in the yield in this process of separation. It was therefore necessary to address this issue and find an appropriate solution. A detailed probe into the literature takes us to the work of Katz and group[21] wherein they had developed an efficient bromine-directed photocyclization method in which helicenes can be regioselectively synthesized in good yield. (Scheme 2.17).

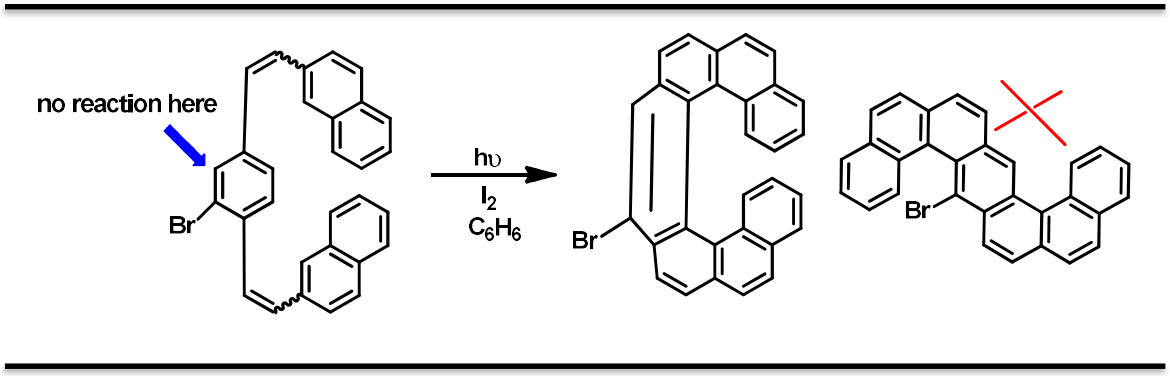

Scheme 2.17: Bromine auxiliary for controlling regioselectivity in photocyclization

As shown in scheme 2.17, the bromine atom acts as a blocking group to prevent cyclization at its ortho-position. So, in this way the unwanted formation of the other regiomer can be thwarted. Using the same strategy, we thought to introduce a cyano functional group on the C-1 substituted pentahelicene which will act as an auxiliary group to prevent linear mode of cyclization to avert steric repulsion. So, the formyl derivative of *N*-butyl carbazole was subjected to Knoevenagel condensation reaction with 3,5-dimethylbenzylcyanide to yield the cyano-substituted olefin precursor in excellent yield. This precursor was then irradiated under 125W HPMVL and constantly monitored. To our surprise in just four hours, the starting material was completely consumed, and a new spot was observed in TLC. Further, the compound was analysed by ^{1}H-NMR spectroscopy to confirm the formation of the product. It was evident from the spectrum that the photocyclization proceeded in the angular mode and the linear regiomer was almost negligible (6.27%). Hence the strategy to install an auxiliary group to improve yield as well as control regioselectivity worked in this case.

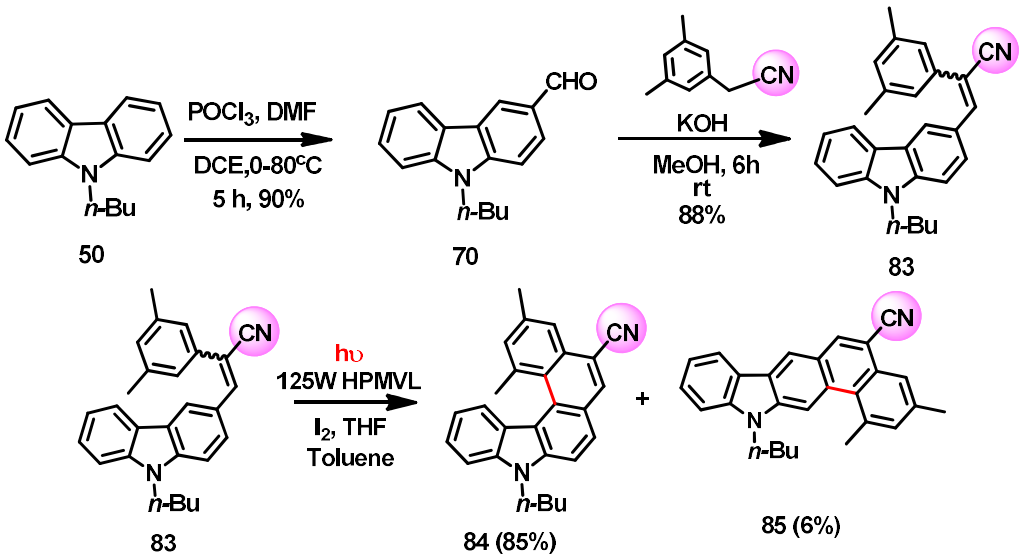

Scheme 2.18: Synthetic scheme for cyano-substituted pyrrolo[5]helicene

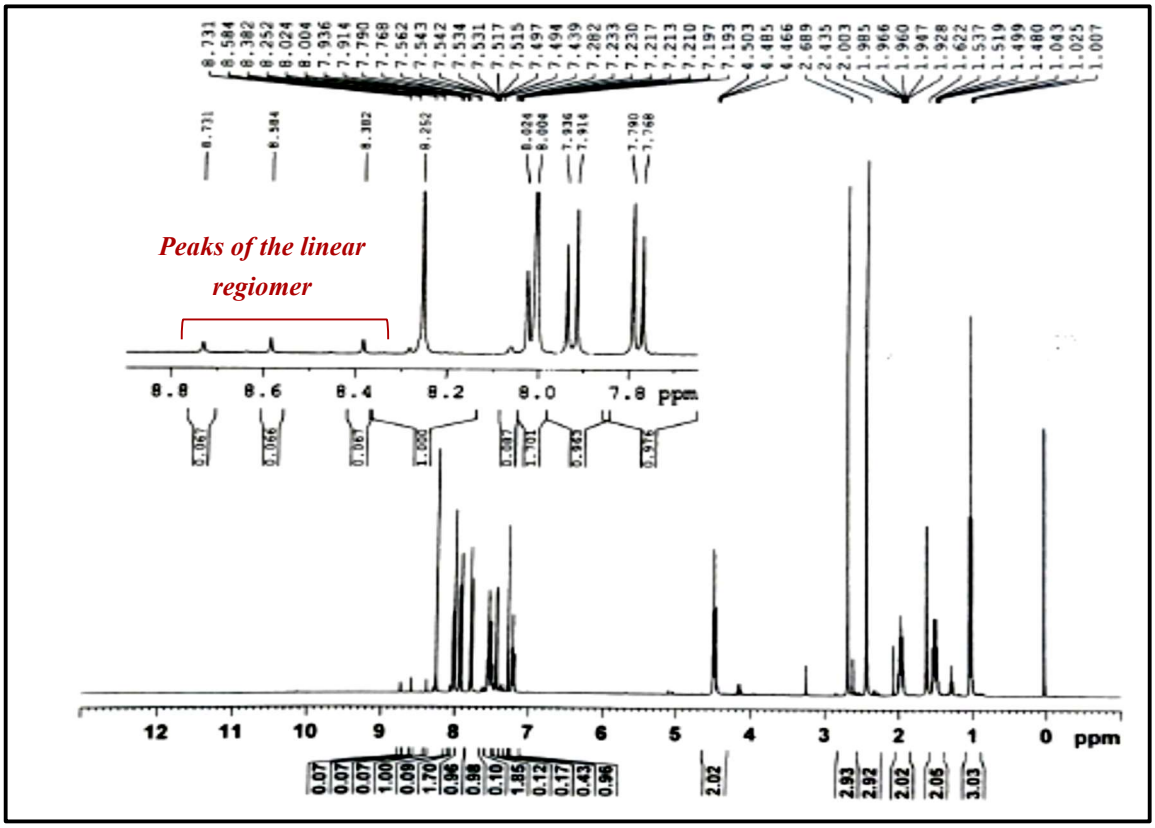

Figure 2.20: H-NMR spectra of cyano-substituted aza[5]helicene

In a previous study from our group, the role of -CN as a synthon for the process of spontaneous resolution was studied.[23] The self-assembly was based on supramolecular interactions like CN….HC(Ar)hydrogen bonding and dipolar CN…CN interaction. Moreover, crystallization being the most convenient method to access enantiopure compounds, we thought of utilizing the compound **84** and carry out crystallization experiments for conglomerate formation. We attempted crystallization in dichloromethane, acetone-hexane, 1,2-dichloroethane, toluene, THF, ethyl acetate, chloroform etc. but we could isolate only racemic crystals which was confirmed by HPLC analysis in hexane-IPA solvent system (90:10).

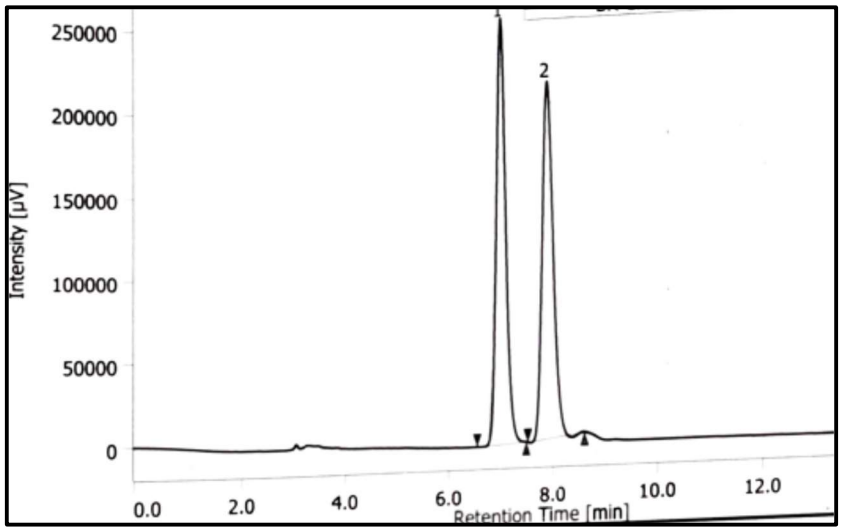

***Figure 2.21**: HPLC Chromatogram of compound 84*

2.2.5. Photophysical properties of 55 and 82

Photophysical properties of aza[5]helicenes **55** and **82** were investigated by UV-Vis absorption and fluorescence spectroscopy (Table 2 and Figure 2.22). These compounds showed an absorption maximum around 300-320 nm along with a shoulder peak in the region 380-400 nm in dichloromethane. For similar pentacyclic helicene, comparable spectra were reported wherein the helical system exhibited strong absorption in the region of 300-400 nm corresponding to π–π* and n-π* electronic transitions.[8d] Blue luminescence was also observed for compounds **55** and **82** upon excitation at 320 and 305 nm respectively.

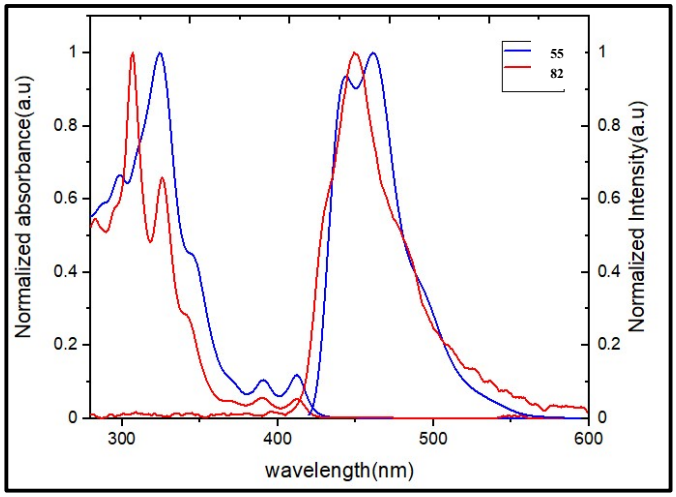

Compound	Absorption λ_{max} (nm)	Fluorescence λ_{emiss} (nm)	Stokes Shift (nm)
55	320	457	137
82	305	406	101

***Figure 2.22:** Optical properties of compound 55 and 82*

2.3 Conclusion

Thus in this chapter we present synthesis and study of few derivatives of aza[5]helicenes. The presence of methyl group in the fjord region offers sufficient steric bulk to prevent the flipping of conformational isomers which are detected by HPLC analysis at ambient conditions. The structural parameters were investigated by single crystal X-ray diffraction study and computational analysis. The compounds were further analyzed for their photophysical properties.

2.4 Experimental Data

All reactions were carried out in oven-dried glassware with magnetic stirring. Purification of reaction products was carried out by column chromatography using silica gel (60-120 mesh). Thin layer chromatography was performed on TLC Silica Gel 60 F254 (Merck). The spots were visualized under UV light or with iodine vapour. 1H-NMR spectra were recorded on Bruker Avance II 400 NMR spectrometer (400 MHz) and were run in CDCl3 unless otherwise stated. Mass spectra were recorded on Thermo-Fischer DSQ II GCMS instrument; IR spectra were recorded on Perkin-Elmer FTIR RXI spectrometer as KBr pallets. UV-Visible absorption of all the compounds was measured as a solution in THF at room temperature on Perkin-Elmer Lambda 35 spectrometer and fluorescence was measured on Jasco FP-6300 spectro fluorometer. Melting points were recorded in Thiele's tube using paraffin oil and are uncorrected. Solvents were dried and purified by distillation under reduced pressure and stored on molecular sieves. All chemicals were purchased from Sigma-Aldrich Chemicals Limited, SD Fine, Sisco, Qualigens, Avara Chemicals Limited etc., and used without further purification

Synthetic procedures and analytical data

9-Butyl-9*H*-carbazole (50)

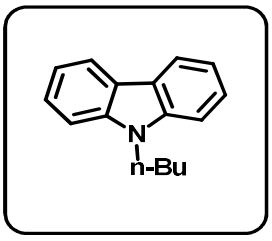

Molecular formula: $C_{16}H_{17}N$
Molecular weight: 223.31
Physical state: white crystalline solid
R_f =0.5 (1:99 EtOAc/petroleum ether).
M.p = 58°C

In a dry round bottom flask, carbazole (5.0g, 29.9 mmol) was dissolved in acetone (25mL). To this homogenous solution, KOH (6.7g, 119.4 mmol) was added and the solution was allowed to stir at room temperature for 30 minutes. To this solution, 1-bromobutane (5.325g, 4.2mL, 38.9 mmol) was added. The mixture was allowed to stir for 4-5 hours at room temperature. After the completion of reaction (which is monitored by TLC), the reaction mixture was poured on ice cold water (50mL) and extracted using ethyl acetate (3 x 50 mL). Combined organic layer was washed with water (50mL) and dried over anhydrous sodium sulfate and concentrated at reduced pressure. Compound was purified by performing column chromatography over silica gel using pet ether as eluent. White solid of N-butyl carbazole was obtained **Yield:** 6.54g (97.47%)

^{1}H NMR (400 MHz, $CDCl_3$): δ 8.15 (d, *J*=8.0 Hz, 2H), 8.52-7.48 (m, 2H), 7.45 (d, *J*=8.0 Hz, 2H), 7.29-7.25 (m, 2H), 4.36-4.32 (t, *J*=7.2 Hz, 2H), 1.93-1.86 (m, 2H), 1.0-0.96 (t, *J*=7.2 Hz, 3H)

9-Butyl-3-iodo-9*H*-carbazole (51):

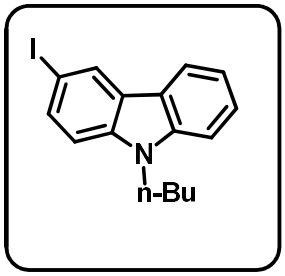

Molecular formula: $C_{16}H_{16}IN$
Molecular weight: 349.21
Physical state: brown viscous liquid
R_f = 0.2 (1:99 EtOAc/petroleum ether).
M.p = 45°C

In a round bottom flask KIO_3 (0.632 g, 2.95 mmol) and KI (0.981 g, 5.91 mmol) was dissolved in 20 mL water. To this stirred mixture, solution of 9-butyl carbazole **53** (2 g, 8.96 mmol) in methanol was added slowly. After the solution became clear concentrated HCl (1.1 mL) was added dropwise, and the reaction mixture was stirred rigorously. After addition of HCl oily mass was separated in the reaction mixture which was separated using separating funnel. It was washed with water and dissolved in ethyl acetate. The organic phase was washed with sodium thiosulfate and dried over sodium sulfate. Solvent was removed under vacuum and the crude product was purified through column chromatography on silica gel using petroleum ether as solvent. Pure product was isolated as brown oil (2.331 g, 74.52%). m.p.: 45ºC.

1H-NMR (CDCl3, 400 MHz): 8.42 (d, *J* = 1.2, 1H), 8.05 (d, *J* = 7.6Hz, 1H), 7.72 (dd, *J* = 8.4Hz and *J* = 1.6Hz, 1H), 7.53-7.49 (m, 1H), 7.42 (d, *J* = 8.0 Hz, 1H), 7.29-7.25(m, 1H), 7.21 (d, *J* = 8.0 Hz, 1H), 4.27 (t, *J* = 7.2 Hz, 2H), 1.88-1.81 (m, 2H), 1.42-1.37 (m, 2H), 0.97 (t, *J* = 7.2 Hz, 3H).

***(E)*-9-butyl-3-(4-methoxystyryl)-9*H*-carbazole compound (54)**

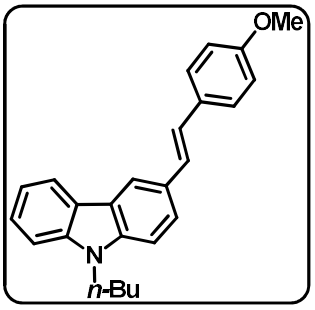

Molecular formula: $C_{25}H_{25}NO$
Molecular weight: 355.19
Physical state: white crystalline solid
M.p = 84-87℃

A two neck round bottom flask was charged with 9-butyl-3-iodo-9*H*-carbazole (2.00 g, 5.72 mmol), p-anisaldehyde (1.17 g, 8.60 mmol), methyl triphenyl phosphonium iodide (3.50 g,8.60 mmol), potassium carbonate (3.95 g, 28.6 mmol), palladium acetate (0.012 g,0.0572 mmol), dppp (0.047 g, 0.114 mmol), TBAB (0.369 g, 1.14 mmol) and *N*,*N*-dimethyl acetamide (20 mL) under the nitrogen atmosphere. This mixture was slowly heated to 140ºC and continued for 24 h. The reaction mixture was quenched with water and extracted with ethyl acetate (3 x 100 mL). The combined organic phase was washed with water and dried over anhydrous sodium sulphate. Solvent was removed in vacuum and the crude product was purified by column chromatography over silica gel using hexane-ethyl acetate (98:2) as eluent to obtain white crystalline solid. (1.50 g, 74 %).

IR (KBr): υ 3434, 3049, 2956, 2928, 2866, 1623, 1598, 1509, 1465, 1377, 1329, 1250, 1210, 1176, 1147, 1109, 1029, 964, 893, 856, 813, 743, 726, 609, 523, 423 cm^{-1}.

^{1}H NMR (400 MHz, $CDCl_3$): δ = 8.2 (d, *J* = 1.2 Hz, 1H), 8.1 (d, *J* = 7.6 Hz, 1H), 7.6 (dd, *J* = 1.6 & 8.4 Hz, 1H), 7.5 (m, 2H), 7.4 (d, *J* = 1.2 Hz, 1H), 7.2 (d, *J* = 16.4, 1H), 6.95-6.94 (m, 2H), 4.3 (t, *J* = 7.2 Hz, 2H), 3.86 (s, 3H), 1.9 (m, 2H), 1.4 (m, 2H), 0.9 (t, *J* = 7.2 Hz, 3H) ppm.

^{13}C NMR (100 MHz, $CDCl_3$): δ 158.86, 140.84, 140.05, 130.83, 128.81, 127.62, 127.36, 125.72, 125.57, 124.22, 123.16, 122.86, 120.42, 118.90, 114.12, 108.86, 55.36, 42.95, 31.17, 20.58, 13.92 ppm.

HRMS (ESI-TOF): m/z calcd. for $C_{25}H_{25}KNO$ is 394.1573; found, 394.1568

9-butyl-2-methoxy-9*H*-aza[5]helicene (55)

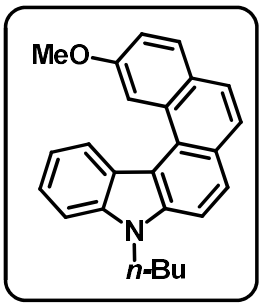

Molecular formula: $C_{25}H_{23}NO$
Molecular weight: 353.46
Physical state: pale yellow solid
M.p = 182-184 ℃

A solution of 9-butyl-3-(4-methoxystyryl)-9*H*-carbazole 6 (0.250 g, 0.71 mmol), Iodine (0.197 g, 0.77 mmol), dry THF (2.86 mL, 35.3 mmol), and toluene (610 mL) was irradiated using a 250W HPMV lamp (10 h monitored by TLC). After the completion of the reaction, the excess of Iodine was removed by washing the solution with aqueous $Na_2S_2O_3$ and water.

The organic layer was concentrated under reduced pressure to obtain the crude product. The crude product was purified by column chromatography over silica gel using hexane-ethyl acetate (98:2) as eluent to obtain a pale-yellow solid. (0.176 g, 71 %).

^{1}H NMR (400 MHz, $CDCl_3$): δ 8.8 (d, *J* = 8.4 Hz, 1H), 8.7 (d, *J* = 2.4 Hz, 1H), 7.9 (d, *J* = 8.4 Hz, 2H), 7.7 (m, 3H), 7.6 (d, *J* = 8.4 Hz, 1H), 7.5 (m, 1H), 7.3 (m, 2H), 4.5 (t, *J* = 7.2 Hz, 2H), 3.9 (s, 1H), 1.9 (m, 2H), 1.5(m, 2H), 1.0 (t, *J* = 7.2 Hz, 3H) ppm.

^{13}C NMR (100 MHz, $CDCl_3$): δ 156.70, 140.06, 140.03, 129.24, 127.88, 127.50, 127.23, 127.19, 125.15, 124.75, 123.91, 123.60, 123.53, 117.78, 117.75, 116.32, 110.16, 109.27, 108.59, 55.54, 43.04, 31.41, 20.63, 13.95 ppm.

HRMS (ESI-TOF): m/z calcd. for $[C_{25}H_{23}NO+H]^+$ is 354.1780; found, 354.1847.

9-butyl-2-hydroxy-9*H*-aza[5]helicene (56)

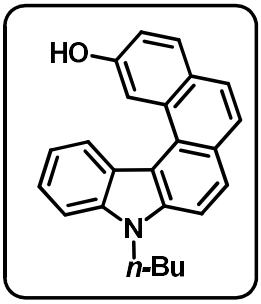

Molecular formula: $C_{24}H_{21}NO$
Molecular weight: 338.43
Physical state: buff coloured solid
M.p = 190-194 ℃

A solution of compound **55** (0.220 g, 0.62mmol) in dichloromethane solvent is stirred at 0ºC. To this solution, BBr_3 (1M in heptane, 0.62ml, 0.62mmol) is added dropwise and the reaction is continued at room temperature. After the completion of the reaction, the excess BBr_3 is quenched with the slow addition of water and extracted with dichloromethane. The product was purified using column chromatography over silica gel using hexane-ethyl acetate (80:20) as eluent to obtain a buff coloured solid. (0.110g, 52%)

^{1}H NMR (400 MHz, $CDCl_3$): δ 8.8 (m, 2H), 7.9 (dd, J_1= 8.4 J_2=2, 2H), 7.7 (m, 3H), 7.6 (d, *J*=8, 1H), 7.5 (m, 2H), 5.4 (s, 1H), 4.5 (t, *J*=7.2, 2H), 1.9 (m, 2H), 1.5 (m, 2H), 1.0 (t, *J*=7.2, 3H)

Mass spectra: m/z calcd. for $[C_{24}H_{21}NO]^+$ is 338.16; found, 338.43.

9-butyl-5,12-dibromo-2-methoxy-9*H*-aza[5]helicene (57)

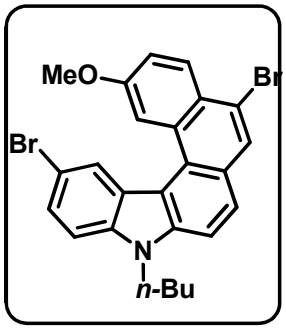

Molecular formula: $C_{25}H_{21}Br_2NO$
Molecular weight: 511.25
Physical state: brown solid
M.p = >215 ℃

To a minimum amount of water, KBr (0.05g, 0.47mmol) and $KBrO_3$ (0.04g, 0.23 mmol) is dissolved. In another flask, compound **55** (0.25g, 0.71 mmol) is dissolved in minimum amount of methanol. To this methanolic solution, the solution of KBr and $KBrO_3$ in water is slowly added. The resulting solution should be clear otherwise more amount of 50% solution of methanol and water is added. To this clear solution 30% HCl (0.08 ml, 0.71mmol) is added dropwise. The reaction was continued at room temperature and after work-up with ethyl acetate and water the resulting reaction mixture was purified using column chromatography to isolate the pure compound as brown solid. (0.11g, 31%)

^{1}H NMR (400 MHz, $CDCl_3$): δ 8.8 (d, *J*=8, 1H), 8.7 (d, *J*=2.4, 1H), 7.9 (m, 2H), 7.7 (m, 2H), 7.6 (d, *J*=8, 1H), 7.5 (m, 1H), 3.5 (m, 4H), 4.5 (t, *J*=7.2, 2H), 3.9 (s,3H), 1.9 (m, 2H), 1.5(m, 2H), 1.0 (t, *J*=7.2, 3H)

9-butyl-5,12-diiodo-2-methoxy-9*H*-aza[5]helicene (58)

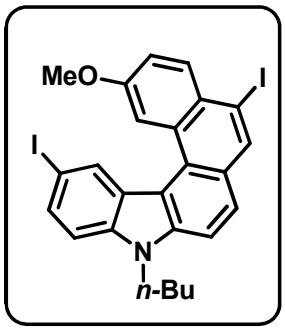

Molecular formula: $C_{25}H_{21}I_2NO$
Molecular weight: 605.25
Physical state: brown solid
M.p = >215ºC

To a minimum amount of water, KI (0.08g, 0.71mmol) and KIO_3 (0.11g, 0.52 mmol) is dissolved. In another flask, compound **55** (0.25g, 0.71 mmol) is dissolved in glacial acetic acid To this solution, the mixture of KI and KIO_3 in water is slowly added and the resulting solution is heated at 80 ºC. The reaction was continued overnight and after quenching the excess acid with $NaHCO_3$ the product was recrystallized with methanol and purified using column

chromatography to isolate the pure compound as brown solid. (0.10g, 24%)
^{1}H NMR (400 MHz, $CDCl_3$): δ 9.1 (d, *J*=1.6, 1H), 8.7 (d, *J*= 2.4, 1H), 7.9 (d, *J*=9.2, 1H), 7.8 (d, *J*=8.8, 1H), 7.7 (dd, J_1=8.8 J_2=1.6, 1H), 7.7 (d, *J*=8.8, 1H), 7.5 (s, 1H), 7.4 (m, 2H), 4.4 (t, *J*=7.2, 2H), 4.1 (s, 3H), 1.9 (m, 2H), 1.4 (m, 2H), 1.0 (t, *J*= 7.2, 3H)

3-Formyl *N*-butyl carbazole (70):

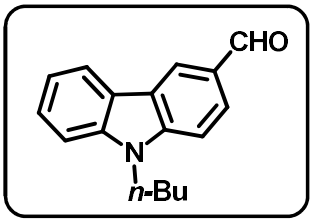

Molecular formula: $C_{17}H_{17}NO$
Molecular weight: 251.32
Physical state: brown solid
M.p = 60 ℃

In a dry two neck round bottom flask phosphoryl chloride (13.76 g, 8.36 mL, 89.0 mmol) was added slowly in DMF (16.36 g, 17.22 mL, 224 mmol) which was purged with nitrogen and cooled to 0 oC. The reactant was warmed to room temperature and stirred for 1 hour and cooled again to 0 oC. To this mixture was added *N*-butyl carbazole (10.0 g, 44.8 mmol) in 1, 2-dichloroethane (50 mL). In 1 hour, the reaction temperature was raised to 90 oC and then kept for 8 hours. The cooled solution was poured in to ice water and extracted with dichloromethane (3X100 mL). The organic layer was washed with water, dried over anhydrous sodium sulfate and concentrated at reduced pressure. The purification of compound was performed by column chromatography over silica gel using 10 % ethyl acetate pet ether as eluent to obtain 99 as viscous liquid which solidify as brown solid (10.g, 89%) on standing at low temperature. The analytical data were in complete agreement with the previously published data.
^{1}H-NMR (400 MHz, CDCl3): δ 10.11 (s, 1H), 8.62 (d, *J* = 1.2 Hz, 1H), 8.14 (d, *J* = 8.8 Hz, 1H), 8.03-8.01 (m, 1H), 7.57-7.55 (m, 1H), 7.53-7.47 (m, 1H), 7.46-7.32 (m, 2H), 4.35 (t, *J* = 7.2 Hz, 2H), 1.91-1.87 (m, 2H), 0.98 (t, *J* = 7.2 Hz, 3H).

6-bromo-9-butyl-9*H*-carbazole-3-carbaldehyde (75)

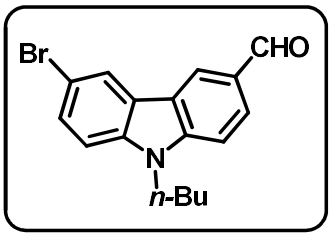

Molecular formula: $C_{17}H_{16}BrNO$
Molecular weight: 330.22
Physical state: brown solid
M.p = 100 ℃

In a dry round bottom flask, 9-butyl-3-formyl-9H-carbazole (2.08,8.20mmol) was dissolved in chloroform (15ml). To this solution NBS (1.46g,8.20 mmol) was added and the solution was allowed to stir at room temperature for one hour. After completion of reaction (which is monitored by TLC) the reaction mixture was extracted using dichloromethane (3 x 50) . The combined organic layer was washed with water, dried over anhydrous sodium sulphate and under reduced pressure. Crude product was purified by column chromatography over silica gel using petroleum ether: ethyl acetate (95:5) as eluent which resulted in pale yellow solid.

^{1}H NMR (400MHz, $CDCl_3$): δ 10.10 (s, 1H), 8.55 (d, *J* =1.2Hz, 1H) ,8.28 (d, *J*=8 Hz,1H), 8.04 (d, *J*=10 Hz, 1H), 7.63-7.60 (m, 1H), 7.50-7.46 (m, 1H), 7.35-7.28 (m, 1H) 4.33 (m, 2H), 1.89-1.85 (m, 2H), 1.43-1.38 (m, 2H), 0.99-0.95 (m, 3H).

(*E*)-9-butyl-3-(3,5-dimethylstyryl)-9*H*-carbazole (77)

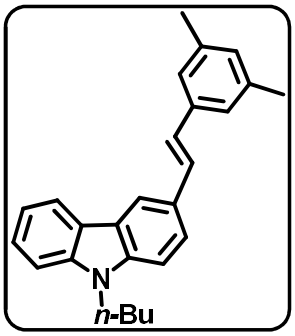

Molecular formula: $C_{26}H_{27}NO$
Molecular weight: 353.50
Physical state: white solid
M.p = 191-193 ℃

A solution of 3-formyl*N*-butylcarbazole **70** (2.0 g, 7.90 mmol) and bromo(3,5-dimethylbenzyl)triphenylphosphorane **76** (3.7 g, 7.90 mmol) in dry methanol (25 mL) was placed in a two neck flask fitted with septum which is degassed and purged with nitrogen. A solution of sodium dissolved in dry methanol was added dropwise under stirring, for 6 hours at room temperature. After completion of reaction the methanol was evaporated under reduced pressure, the mixture was poured into ice-cold water and extracted with ethyl acetate (3x50 mL). the combined organic phase was washed with water, brine and dried over anhydrous sodium sulphate. The solvent was removed under reduced pressure and the crude product was purified by column chromatography on silica gel using hexane-ethyl acetate (95:05) as eluent to afford white solid (2.25 g, 80%).

IR (KBr): υ 3423, 3016, 2978, 2928, 1823, 1594, 1498, 1385, 1339, 1304, 1242, 1178, 1114, 1036, 970, 860, 820, 751 cm^{-1}.

^{1}H NMR (400 MHz, $CDCl_3$): δ 8.2 (s, 1H), 8.1 (d, *J* = 7.6 Hz, 1H), 7.7 (dd, *J* = 1.6 & 8.4 Hz, 2H), 7.5 (m, 1H), 7.5 (m, 1H), 7.4 (d, *J* = 8.8 Hz, 1H), 7.4 (d, *J* = 8.8 Hz, 1H), 7.3 (d, *J* = 16

Hz, 1H), 7.2 (m, 1H), 7.1 (d, *J* = 16 Hz, 1H), 6.9 (s, 1H), 4.3 (t, *J* = 6.8 Hz, 2H), 2.4 (s, 6H), 1.9 (m, 2H), 1.5 (m, 2H), 1.0 (t, *J* = 7.2 Hz, 3H) ppm.

HRMS (ESI-TOF): m/z calcd. for $[C_{26}H_{27}N+H]^+$ is 354.2143; found, 354.2176.

(*E*)-6-bromo-9-butyl-3-(3,5-dimethylstyryl)-9*H*-carbazole (78)

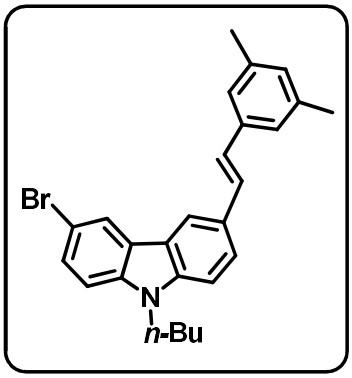

Molecular formula: $C_{26}H_{26}BrNO$
Molecular weight: 353.50
Physical state: white solid
M.p = 191-193 ℃

A solution of compound **75** (2.0 g, 7.90 mmol) and bromo(3,5-dimethylbenzyl)triphenylphosphorane **76** (3.7 g, 7.90 mmol) in dry methanol (25 mL) was placed in a two neck flask fitted with septum which is degassed and purged with nitrogen. A solution of sodium dissolved in dry methanol was added dropwise under stirring, for 6 hours at room temperature. After completion of reaction the methanol was evaporated under reduced pressure, the mixture was poured into ice-cold water and extracted with ethyl acetate (3x50 mL). the combined organic phase was washed with water, brine and dried over anhydrous sodium sulphate. The solvent was removed under reduced pressure and the crude product was purified by column chromatography on silica gel using hexane-ethyl acetate (95:05) as eluent to afford white solid (2.25 g, 80%).

IR (KBr): υ 3423, 3016, 2978, 2928, 1823, 1594, 1498, 1385, 1339, 1304, 1242, 1178, 1114, 1036, 970, 860, 820, 751 cm^{-1}.

^{1}H NMR (400 MHz, $CDCl_3$): δ 8.2 (s, 1H), 8.1 (d, *J* = 7.6 Hz, 1H), 7.7 (dd, *J* = 1.6 & 8.4 Hz, 2H), 7.5 (m, 1H), 7.5 (m, 1H), 7.4 (d, *J* = 8.8 Hz, 1H), 7.4 (d, *J* = 8.8 Hz, 1H), 7.3 (d, *J* = 16 Hz, 1H), 7.2 (m, 1H), 7.1 (d, *J* = 16 Hz, 1H), 6.9 (s, 1H), 4.3 (t, *J* = 6.8 Hz, 2H), 2.4 (s, 6H), 1.9 (m, 2H), 1.5 (m, 2H), 1.0 (t, *J* = 7.2 Hz, 3H) ppm.

HRMS (ESI-TOF): m/z calcd. for $[C_{26}H_{27}N+H]^+$ is 354.2143; found, 354.2176.

1,3-dimethyl-9-butyl-9H-aza[5]helicene (74)

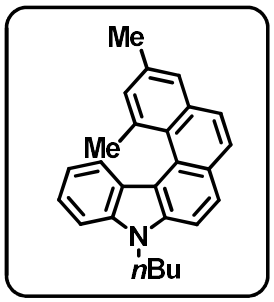

Molecular formula: $C_{26}H_{26}BrNO$
Molecular weight: 353.50
Physical state: brown fluffy solid
M.p = 191-193 ℃

A solution of compound **77** (0.250 g, 0.71 mmol), Iodine (0.197 g, 0.77 mmol), dry THF (2.86 mL, 35.3 mmol), and toluene (610 mL) was irradiated using a 250W HPMV lamp (10 h monitored by TLC). After the completion of the reaction, the excess of Iodine was removed by washing the solution with aqueous $Na_2S_2O_3$ and water.

^{1}H NMR (400 MHz, $CDCl_3$): δ 8.1 (d, *J* = 8.0 Hz, 1H), 7.9 (d, *J* = 8.8 Hz, 1H), 7.7 (d, *J* = 4.4 Hz, 2H), 7.5 (m, 4H), 7.3 (s, 1H), 7.1 (m, 1H), 4.4 (t, *J* = 4.0 Hz, 2H), 2.6 (s, 3H), 2.4 (s, 3H), 1.9 (m, 2H), 1.5 (m, 2H), 1.0 (t, *J* = 7.2 Hz, 3H) ppm.

^{13}C NMR (100 MHz, $CDCl_3$): δ 141.01, 140.33, 138.24, 138.05, 129.42, 129.00, 128.83, 126.33, 125.91, 124.51, 124.31, 123.32, 123.03, 120.58, 119.11, 118.76, 109.03, 77.51, 77.20, 76.88, 43.11, 31.33, 21.54, 20.74, 14.04 ppm.

12-bromo-1,3-dimethyl-9-butyl-9*H*-aza[5]helicene (79)

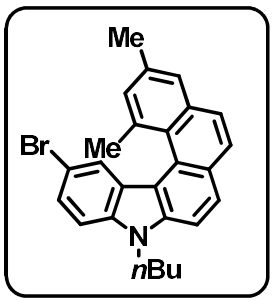

Molecular formula: $C_{26}H_{24}BrN$
Molecular weight: 430.38
Physical state: white solid
M.p = 191-193 ℃

A solution of compound **77** (0.250 g, 0.71 mmol), Iodine (0.197 g, 0.77 mmol), dry THF (2.86 mL, 35.3 mmol), and toluene (610 mL) was irradiated using a 250W HPMV lamp (10 h monitored by TLC). After the completion of the reaction, the excess of Iodine was removed by washing the solution with aqueous $Na_2S_2O_3$ and water.

^{1}H NMR (400 MHz, $CDCl_3$): δ 8.2 (d, *J* = 2.0 Hz, 1H), 7.9 (d, *J* = 8.8 Hz, 1H), 7.7 (d, *J* = 8.4 Hz, 2H), 7.6 (s, 1H), 7.6 (d, *J* = 8.8 Hz, 1H), 7.5 (dd, *J* =2.0 & 8.8 Hz, 1H), 7.3 (s, 1H), 7.3 (d, *J* = 8.8 Hz, 1H), 4.4 (t, *J* = 7.2 Hz, 2H), 2.6 (s, 3H), 2.4 (s, 3H), 1.9 (m, 2H), 1.5 (m, 2H), 1.0 (t, *J* = 7.2 Hz, 3H) ppm.

^{13}C NMR (100 MHz, $CDCl_3$): δ 140.39, 139.48, 138.18, 137.82, 129.09, 128.98, 128.41, 126.66, 125.12, 124.64, 123.20, 122.19, 118.71, 111.79, 110.36, 109.17 ppm.

HRMS (ESI-TOF): m/z calcd. for [$C_{26}H_{24}BrNNa$] is 450.3788; found, 450.3583

5,12-dibromo-1,3-dimethyl-9-butyl-9*H*-aza[5]helicene (82)

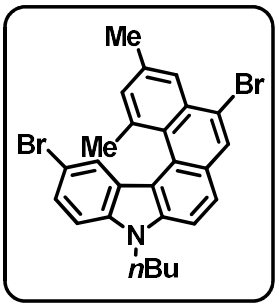

Molecular formula: $C_{26}H_{23}Br_2N$
Molecular weight: 509.28
Physical state: yellow crystalline solid
M.p = >200°C

To a stirred solution of 12-bromo-1,3-dimethyl-9-butyl-9*H*-aza[5]helicene **79** (0.10g, 0.23 mmol) in dichloromethane (10 mL), was added *N*-bromosuccinimide (0.03 g, 0.21 mmol) and stirred at room temperature (5 h). After completion of the reaction, the solvent was evaporated under reduced pressure and the compound was purified by column chromatography over silica gel using hexane-ethyl acetate (99:1) as eluent to obtain yellow crystalline solid (0.09 g, 82%).

IR (KBr): υ 3397, 3039, 2957, 2927, 2857, 1726, 1660, 1588, 1525, 1494, 1450, 1338, 1285, 1220, 798, 743, 641 cm^{-1}.

^{1}H NMR (400 MHz, $CDCl_3$): δ 8.1 (d, *J* = 2 Hz, 1H), 8.0 (d, *J* = 8.4 Hz, 1H), 8.0 (s, 1H), 7.8 (d, *J* = 8.8 Hz, 1H), 7.7 (d, *J* = 8.4 Hz, 1H), 7.5 (dd, *J* =2.0 & 8.8 Hz, 1H), 7.4 (s, 1H), 4.4 (t, *J* = 7.6 Hz, 2H), 2.6 (s, 3H), 2.4 (s, 3H), 1.9 (m, 2H), 1.5 (m, 2H), 1.0 (t, *J* = 7.6 Hz, 3H) ppm.

^{13}C NMR (100 MHz, $CDCl_3$): δ 141.13, 139.90, 136.38, 135.30, 133.67, 131.88, 131.78, 130.19, 129.50, 129.28, 127.00, 126.75, 124.06, 123.83, 121.79, 119.15, 118.97, 111.78, 110.10, 106.27, 77.52, 77.20, 76.88, 43.29, 30.99, 27.60, 21.52, 20.86, 14.09 ppm.

HRMS (ESI-TOF): m/z calcd. for $C_{26}H_{23}Br_2NNa$ is 530.0095; found, 530.0089

3-(9-butyl-9*H*-carbazol-3-yl)-3,5-dimethylphenylacetonitrile (83):

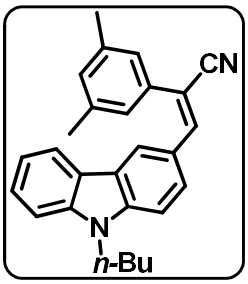

Molecular formula: $C_{27}H_{26}N_2$
Molecular weight: 378.51
Physical state: bright yellow solid
M.p = 191-193 ℃

. A solution of 3-formyl *N*-butyl carbazole **70** (2.0 g, 7.97 mmol) and 3,5-dimethylphenylacetonitrile (1.27 g, 8.76 mmol) in dry methanol (25 mL) was placed in a single neck R.B. flask fitted with a septum, which is degassed and purged with nitrogen. To this was added potassium hydroxide (0.89 g, 15.93 mmol) and the mixture was stirred vigorously for 5 hours at room temperature. After completion of reaction the methanol was evaporated under reduced pressure the mixture was poured into ice-cold water and extracted with ethyl acetate (3 x 50 mL). The combined organic phase was washed with water, brine, and dried over anhydrous sodium sulfate. The solvent was removed under reduced pressure and the crude product was purified by column chromatography on silica gel using petroleum ether–ethyl acetate (95:05) as eluent to afford **83** as bright yellow solid (2.65 g, 88%).

IR (KBr) : υ 3652, 3045, 3027, 2961, 2932, 2906, 2874, 2860, 2726, 2309, 2208, 1929, 1690, 1626, 1585, 1496, 1470, 1391, 1356, 1319, 1248, 1212, 1186, 1159, 1137, 1064, 1024, 915, 883, 839, 803, 769, 749, 730, 684, 641, 606, 552, 517, 482, 442, 423 cm^{-1}

^{1}H NMR (400 MHz, $CDCl_3$): δ 8.64 (d, J= 1.6Hz, 1H), 8.17 (m, 2H), 7.73 (s, 1H), 7.53 (m, 3H), 7.36 (s, 1H), 7.33 (d, J=0.8 Hz, 1H), 7.314 (s, 1H), 7.29 (d, J= 0.8Hz, 1H), 7.04 (s, 1H), 4.35 (t, *J*=6.8 Hz, 2H), 2.14 (s, 6H), 1.90 (m, 2H), 1.44 (m, 2H), 0.98 (t, *J*= 7.6 Hz, 3H) ppm

.

5-cyano-1,3-dimethyl-9-butyl-9*H*-aza[5]helicene (84)

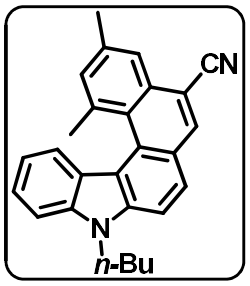

Molecular formula: $C_{27}H_{24}N_2$
Molecular weight: 376.19
Physical state: yellow crystalline solid
M.p = >200°C

Yield: 85%

IR (KBr) : υ 3643, 3045, 2955, 2934, 2869, 2212, 1933, 1886, 1776, 1732, 1688, 1580, 1517, 1465, 1382, 1358, 1331, 1265, 1245, 1232, 1218, 1170, 1153, 1116, 1067, 1035, 964, 938, 922, 890, 876, 849, 798, 773, 746, 654, 637, 615, 581, 562, 545, 496, 426 cm^{-1}

^{1}H NMR (400 MHz, $CDCl_3$): δ 8.25 (s, 1H), 8.01 (d, *J*= 8Hz, 2H), 7.92 (d, *J*=7.6Hz, 1H), 7.77 (d, *J*=8.8 Hz, 1H), 7.54 (m, 3H), 7.20 (m, 1H), 4.48 (t, *J*= 7.6 Hz, 2H), 2.68 (s, 3H), 2.43 (s, 3H), 1.96 (m, 2H), 1.52 (m, 2H), 1.02 (t, *J*= 7.2 Hz, 3H) ppm

^{13}C NMR (100 MHz, $CDCl_3$): δ 140.74, 139.76, 137.83, 137.68, 135.32, 131.45, 131.06, 128.21, 127.43, 126.42, 125.61, 125.13, 124.37, 122.83, 121.74, 119.08, 119.00, 118.94, 110.41, 109.16, 104.61, 43.22, 31.28, 23.15, 21.54, 20.61, 13.96 ppm.

2.5 Crystallographic Data

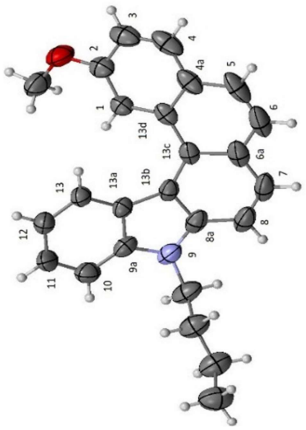

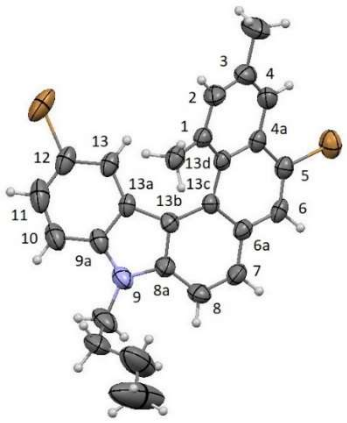

Identification code	CCDC 1062828	CCDC 1587287
Empirical formula	$C_{25}H_{23}NO$	$C_{19}H_{19}Br_2N_6$
Formula weight	353.47	509.25
Temperature/K	293(2)	293(2)
Crystal system	orthorhombic	orthorhombic
Space group	$Pna2_1$	$P2_12_12_1$
a/Å	19.6239(18)	8.9511(13)
b/Å	10.6269(10)	11.335(2)
c/Å	9.2416(8)	21.415(5)
α/°	90	90.00
β/°	90	90.00
γ/°	90	90.00
Volume/Å^3	1927.3(3)	2172.7(7)
Z	4	4
ρ_{calc}g/cm^3	1.2181	1.557
μ/mm^{-1}	0.073	3.743
F(000)	752.3	1024.0
Crystal size/mm^3	0.5 × 0.3 × 0.1	0.28 × 0.18 × 0.10
Source Radiation	MoKα (λ = 0.71073)	Mo Kα (λ = 0.71073)

2Θ range for data collection/°	6.2 to 58	6.74 to 57.54
Index ranges	$-26 \le h \le 24$, $-11 \le k \le 13$, $-11 \le l \le 6$	$-6 \le h \le 12$, $-15 \le k \le 6$, $-26 \le l \le 17$
Reflections collected	6134	6124
Independent reflections	5131 [R_{int} = 0.0305, R_{sigma} = 0.0536]	4180 [R_{int} = 0.0298, R_{sigma} = 0.0672]
Data/restraints/parameters	5131/0/253	4180/0/266
Goodness-of-fit on F^2	0.861	0.960
Final R indexes [I>=2σ (I)]	R_1 = 0.0529, wR_2 = 0.1451	R_1 = 0.0452, wR_2 = 0.0752
Final R indexes [all data]	R_1 = 0.0776, wR_2 = 0.1533	R_1 = 0.0848, wR_2 = 0.0880
Largest diff. peak/hole / e $Å^{-3}$	0.22/-0.25	0.31/-0.30
Flack parameter	-3(3)	0.357(15)

2.6 Computational Analysis

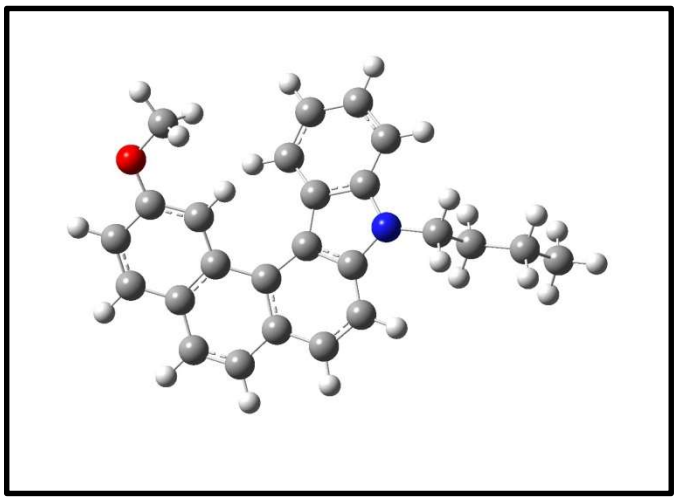

Optimized geometry of compound 55

Cartesian co-ordinates of compound **55**

C	-0.000007672	-0.000004295	0.000002077
N	-0.00000125	-0.000010418	0.000010072
C	0.000009182	0.00000417	-0.000000201
C	0.000003794	0.000003257	0.00000294
H	-0.000000026	0.000000282	-0.000001378
O	0.000010584	0.000002416	0.000004306
C	-0.000001624	0.000003675	-0.000007696
C	-0.000003551	0.000003258	-0.000003546
H	0.000004802	-0.000003331	0.000002802
C	-0.00000004	-0.000001145	-0.000004133
C	-0.000006543	-0.000003805	-0.000000466
C	0.000001664	0.000006259	0.00000362
C	-0.000000538	0.000000656	-0.000003044
C	0.000003869	0.000000008	0.000000439
C	-0.000005664	-0.00001111	0.000004119
H	-0.000001039	0.000000242	-0.000002657
C	0.00000021	0.000001155	-0.000004025
H	0.000002503	0.000001902	0.00000054
C	0.000000373	0.000008588	0.000005094
H	0.000003784	-0.00000151	0.000000123
C	-0.00000157	-0.000005319	-0.000006003
H	0.000001289	0.000004207	0.000002082
C	-0.000006323	0.00000661	-0.000013701
C	0.000006437	0.000005754	0.0000048
C	-0.000002085	-0.00000705	0.000003662
H	-0.000002447	0.000001645	-0.00000675

H	0.000002357	0.000004477	0.000001063
C	-0.000004739	-0.000003628	-0.000006051
H	0.000000723	0.000004736	0.000000807
C	-0.000004271	-0.000005752	0.000005052
H	0.000002365	0.000003707	-0.000002368
C	0.000005991	0.00000409	0.000001925
H	-0.000003031	-0.000002893	-0.00000011
C	-0.000002195	0.000006656	0.000001146
H	0.000002579	0.000003328	-0.000002745
C	0.000006568	-0.000000426	-0.000023388
H	0.00000424	-0.000000744	0.000008536
H	-0.000009245	-0.000005819	0.000005967
C	-0.000014392	0.000001261	0.000019798
H	0.000004402	-0.000000213	-0.000001206
H	-0.0000027	-0.000004523	-0.00000289
H	-0.000001099	-0.000000509	-0.000010405
C	0.000005361	0.00000059	0.000003229
H	-0.000001199	-0.000002185	0.000000902
C	-0.000000536	0.000001512	-0.000002791
H	0.000002145	-0.000000213	0.000000618
H	-0.00000014	-0.000002032	0.000000071
H	0.000001514	0.000000849	0.000003824
H	-0.000006738	-0.000006487	0.000001598
H	0.000003919	-0.000001884	0.000004344

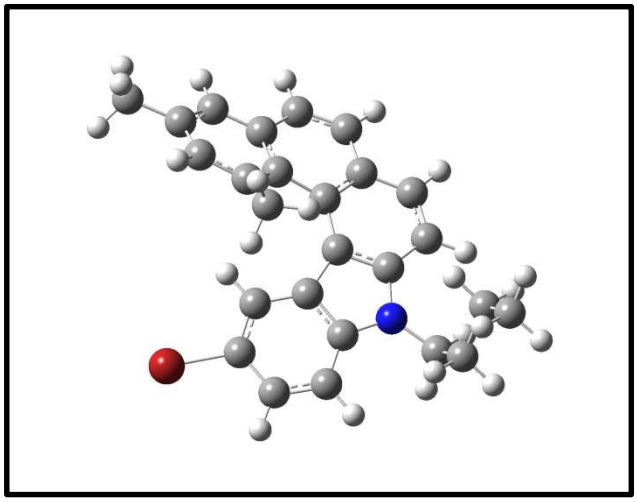

Optimized geometry of compound 79

Cartesian co-ordinates of compound **79**

Br	**1.239789**	**-4.327635**	**0.363559**
N	-2.755778	-0.240236	-0.661433
C	4.267636	-2.101223	-0.072138
C	-5.05471	-0.159034	0.370919
C	-3.540159	0.41808	1.468265
C	2.184737	-2.673818	-0.97764
C	-1.999642	0.920595	-0.504374
C	-0.221886	-3.14232	0.885849
C	-2.920032	-2.412376	0.368401
C	-2.195259	0.672479	1.198261
C	2.602455	-3.613542	-1.090863
C	-0.626741	0.560055	-0.3467
C	0.336392	-1.584167	0.321571
C	-2.41821	2.255913	-0.557942
C	-4.198538	-0.268002	-0.90643
C	-0.094882	2.901	-0.398225
C	-0.5626	-0.8963	-0.375327
C	1.173679	-0.106387	2.17052
C	-1.888847	-1.33816	-0.646948
C	1.307139	-4.011294	-1.244179
C	1.858874	-1.592506	0.148841
C	0.50613	-1.846945	-0.339792
C	6.03531	-0.707864	1.091338
C	-1.119766	-3.537076	-1.146297

C	-1.446476	3.255173	-0.499569
C	4.598226	-1.072662	0.798849
C	-4.905987	-1.349922	1.333753
C	-5.778779	-1.206402	2.590901
H	3.782844	0.276787	2.269129
H	5.050641	-2.712556	-0.513429
H	1.392557	1.359597	-0.260835
H	-1.729892	4.299247	-0.544791
H	-3.46485	2.519274	-0.659307
H	-4.798693	0.771007	0.8975
H	-6.106762	-0.065312	0.062857
H	-3.200234	-3.003043	-1.162997
H	-4.440486	0.55558	-1.589314
H	-4.432738	-1.195622	-1.438521
H	1.567627	-0.194345	3.189376
H	0.952272	0.951695	1.999454
H	0.226964	-0.647707	2.128237
H	1.070148	-4.968708	-1.69934
H	6.726795	-1.458889	0.696198
H	6.299456	0.256767	0.6375
H	6.215027	-0.615379	2.169351
H	-1.297105	-4.548896	-1.498735
H	-5.172998	-2.27805	0.806437
H	-3.852966	-1.451813	1.626634
H	-5.656992	-2.066387	3.258927
H	-5.511543	-0.304492	3.155638
H	-6.842013	-1.132965	2.329563
H	-3.421456	-4.234489	1.441347

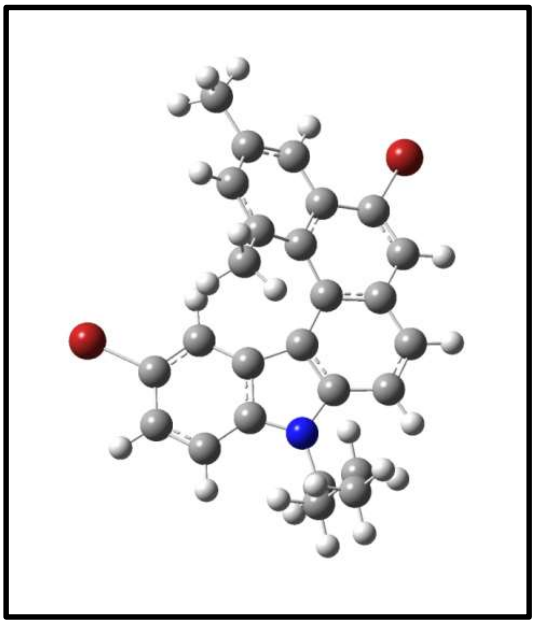

Optimized geometry of compound 82

Cartesian Coordinates of compound **82**

Br	0.000002455	-0.000001724	-0.000001016
N	-0.000010027	0.000006983	0.000010118
C	0.000003151	0.000001652	-0.000002486
C	-0.000000988	-0.000003089	0.000002792
C	0.000007681	0.000000084	-0.00000077
C	-0.000005402	0.000002545	-0.000000263
C	-0.000001112	-0.000000115	0.000001269
C	-0.000000111	0.000002412	-0.000001346
C	0.000003065	-0.000002693	0.000002292
C	-0.000004538	-0.000005152	-0.000000827
C	-0.000000776	0.00000341	-0.000002107
C	0.000002774	0.00000253	0.000001096
C	0.000001005	-0.000001056	-0.000003082
C	-0.000001979	-0.000001176	0.000000139
C	0.000002673	0.000000318	-0.000005213
C	0.00000268	-0.000001602	0.000002567
C	-0.000001759	-0.000001697	-0.000004331
C	0.000004343	-0.000006237	-0.000001082
C	0.000007694	-0.000002378	-0.000002314
C	0.000003351	0.000001893	0.000000429
C	0.000004064	0.000004358	-0.000003477
C	-0.000000943	0.000000416	0.000003625

C	0.000008113	0.000000445	-0.000002696
C	0.0000009	0.000001431	0.000002368
C	-0.000000069	0.000001087	-0.000003443
C	0.000002069	-0.000001594	-0.000001393
C	-0.000024482	0.00002381	-0.000004024
C	0.000011563	-0.000025344	-0.000006852
H	-0.000000295	-0.000002747	-0.000000628
H	0.000004775	-0.000001126	0.000000607
H	0.000001774	-0.000001145	0.000000561
H	0.000001087	-0.000001095	0.000000748
H	-0.000000051	0.00000111	-0.000000436
H	-0.000006142	0.000001139	-0.000000402
H	-0.000002765	0.000002392	-0.000000187
H	-0.000001159	0.000002857	0.000000798
H	-0.000001117	-0.000000432	-0.000001632
H	-0.000004745	0.000003947	0.000001943
H	-0.000002547	-0.000002995	0.00000202
H	-0.000000187	-0.000001399	-0.000001852
H	0.000002106	0.000002671	0.000000319
H	0.000000227	0.000002657	0.00000049
H	0.000006323	-0.00000274	0.000000184
H	0.000004058	-0.000003401	-0.000003418
H	0.000000354	-0.000002506	0.000001194
H	-0.000001324	0.000002701	0.000000183
H	-0.000000763	-0.00000025	0.000004846
H	-0.000002105	-0.000004273	0.000004241
H	-0.000005592	0.000002409	0.000005103
H	-0.000004427	-0.000000024	0.000002564
H	-0.000005519	0.000001574	0.00000265
Br	0.000002639	0.000001157	0.000000137

2.7 Spectral Data

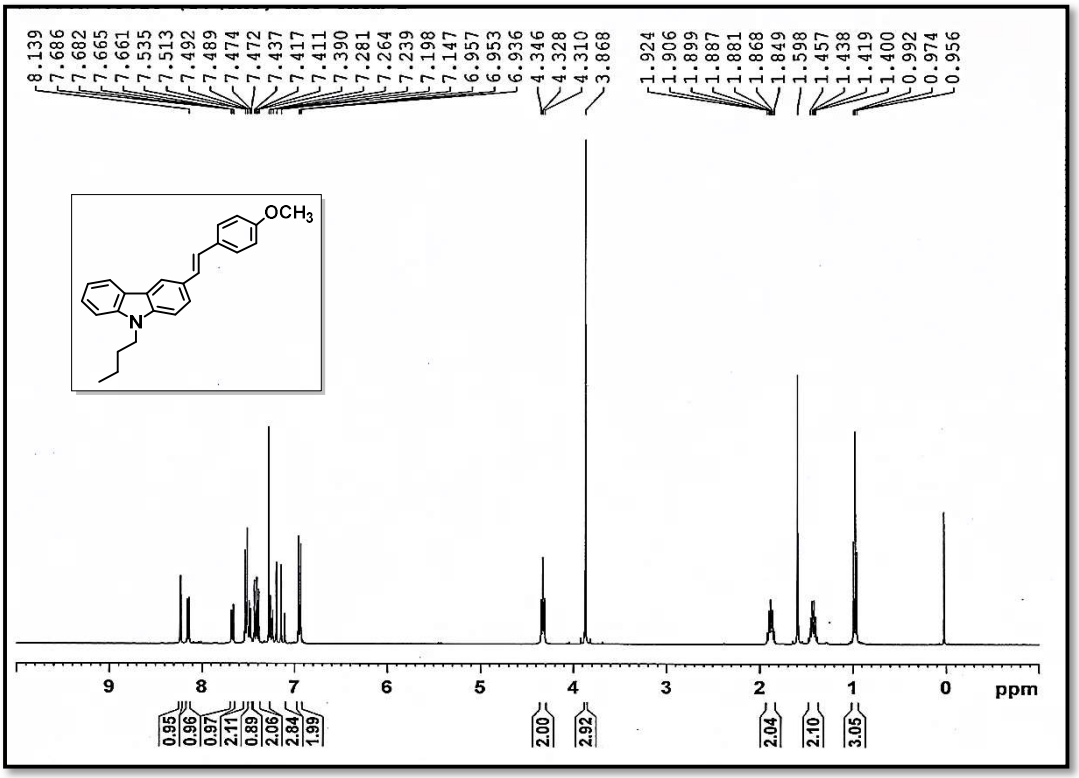

^{1}H-NMR Spectra of compound 54

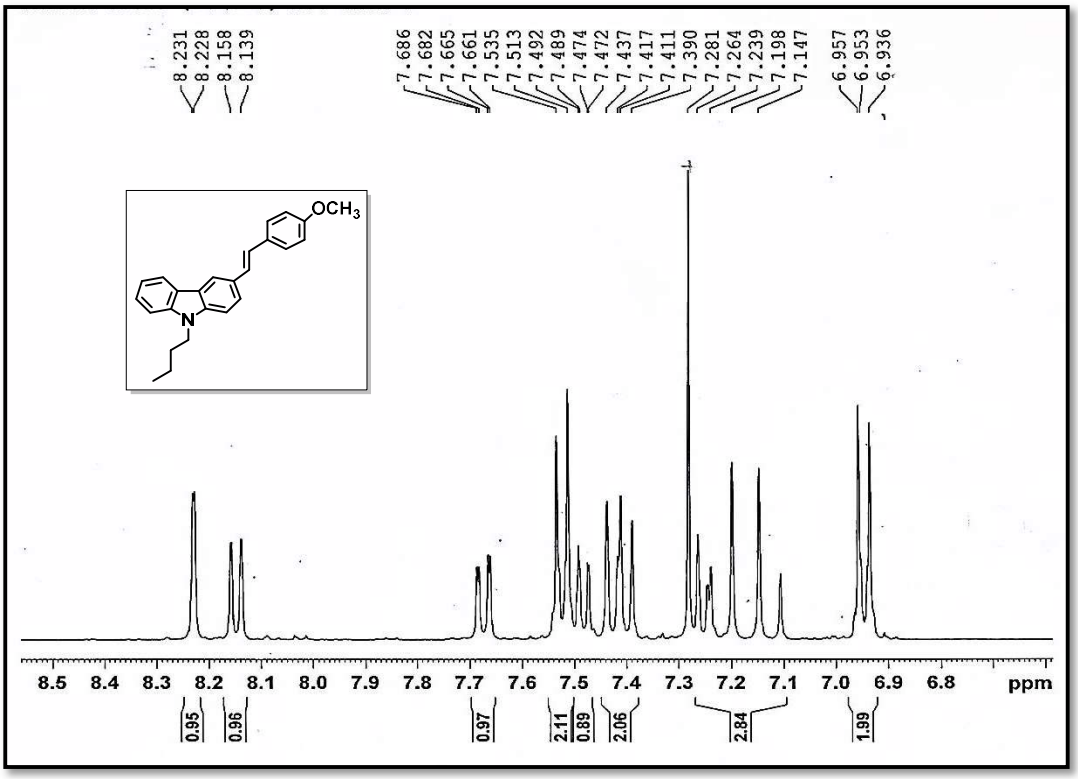

Enlarged aromatic region of the ^{1}H-NMR Spectra of compound 54

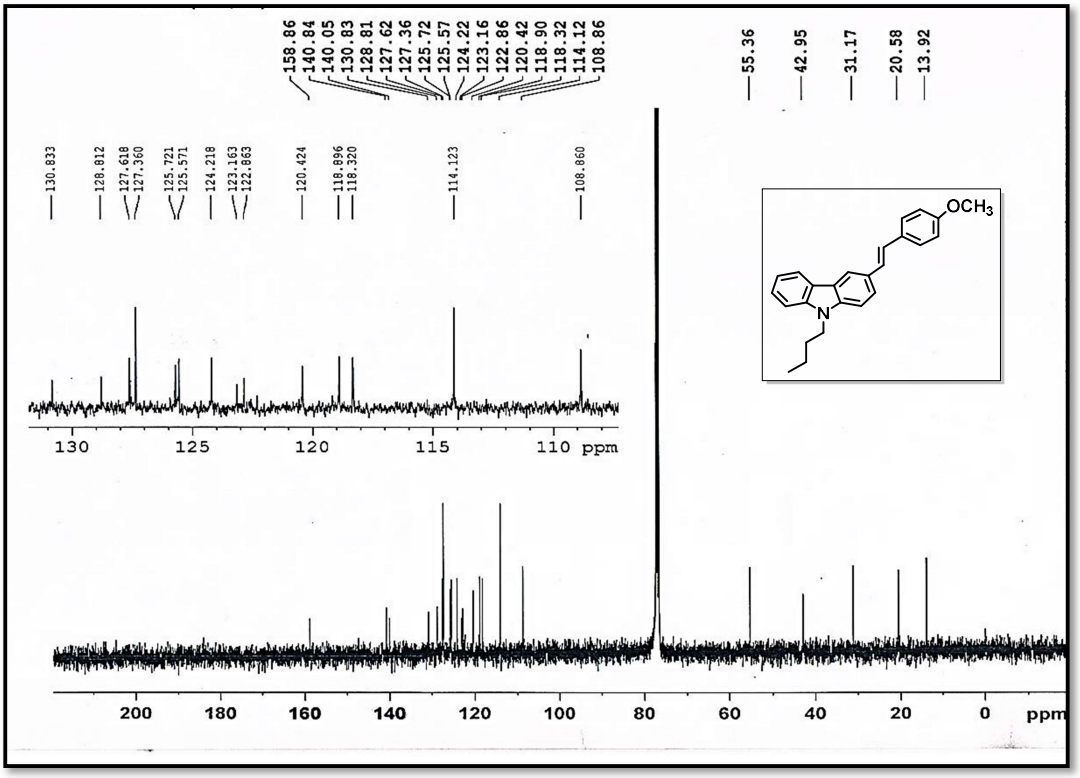

^{13}C-NMR Spectra of compound 54

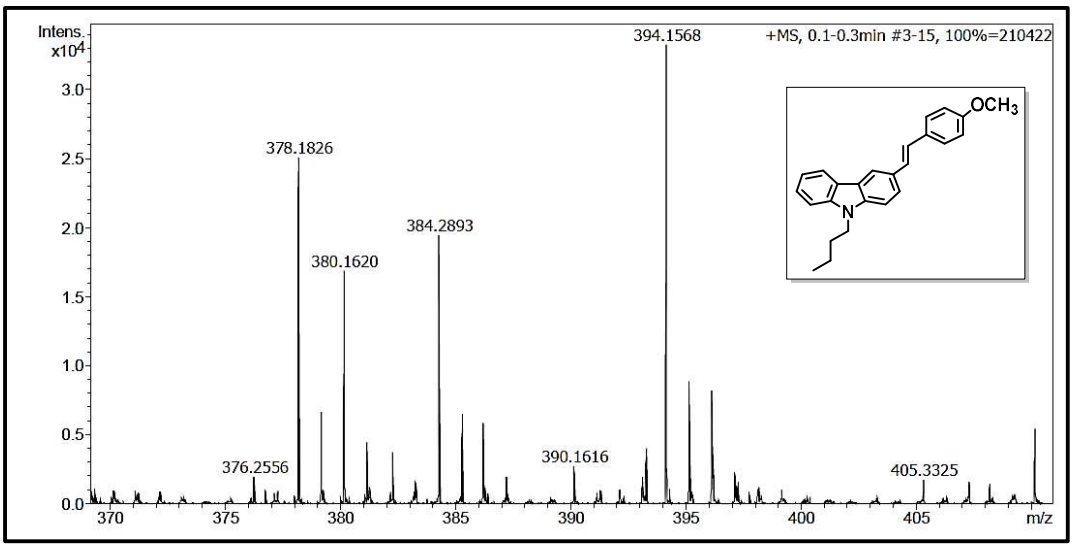

HRMS Spectra of compound 54: m/z calcd. for $C_{25}H_{25}KNO$ is 394.1573; found, 394.1568.

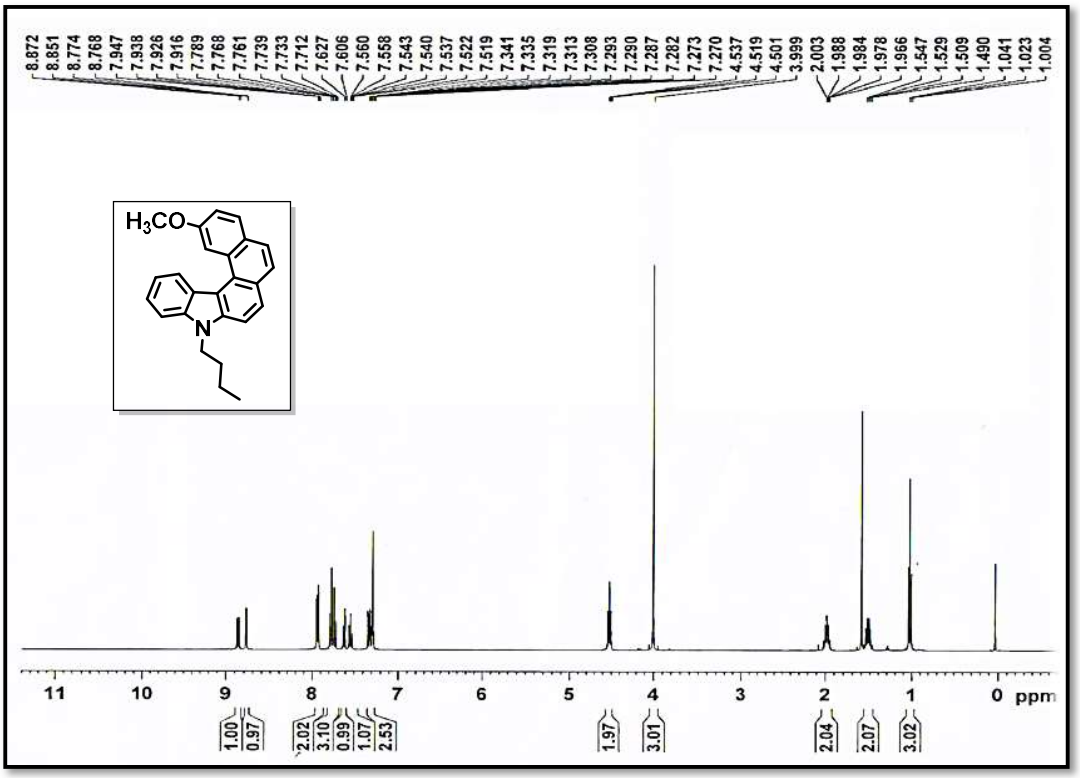

^{1}H-NMR Spectra of compound 55

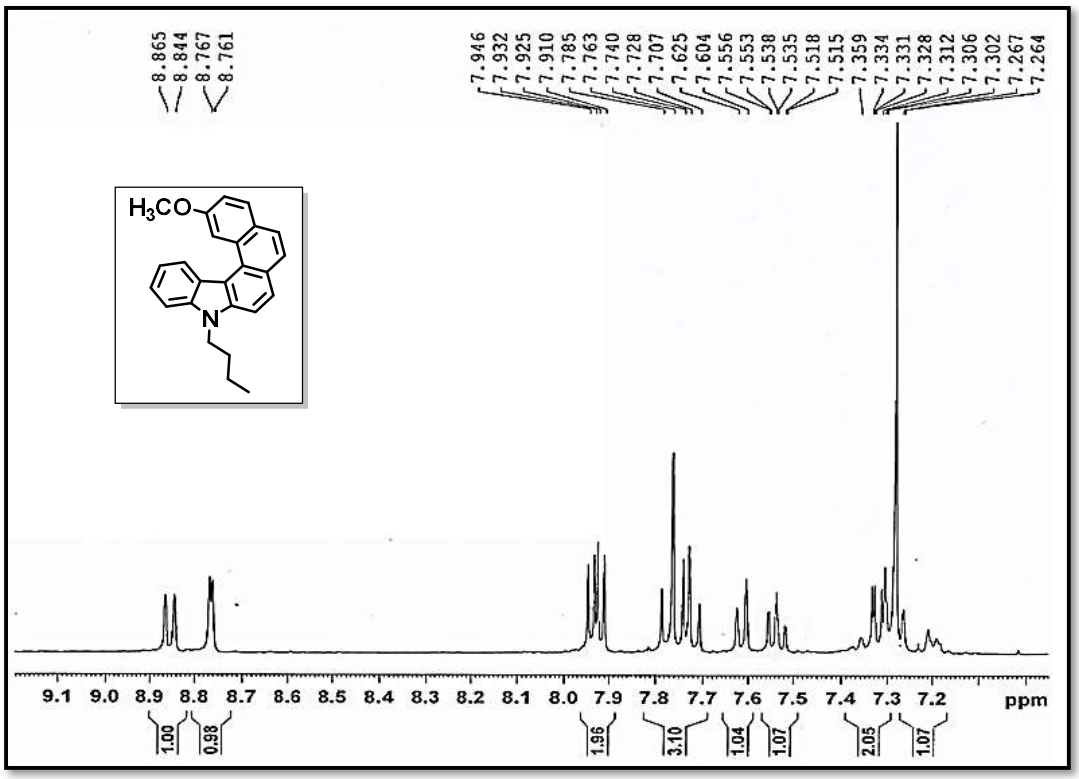

Enlarged aromatic region of the ^{1}H-NMR Spectra of compound 55

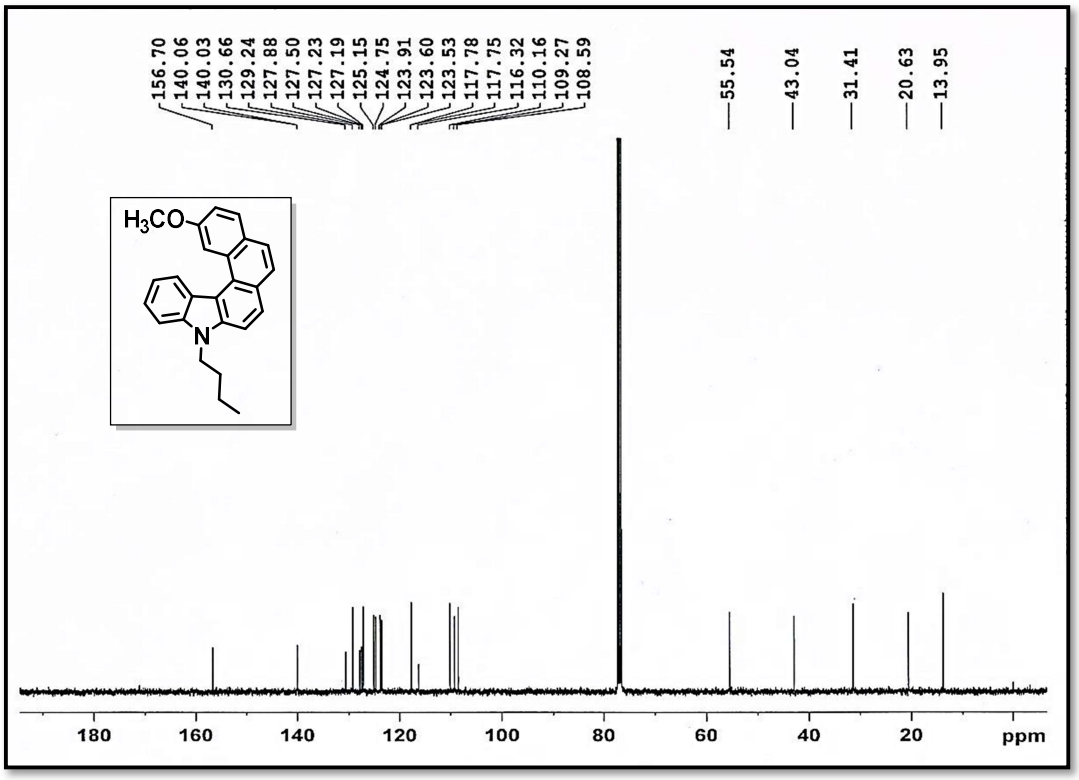

^{13}C-NMR Spectra of compound 55

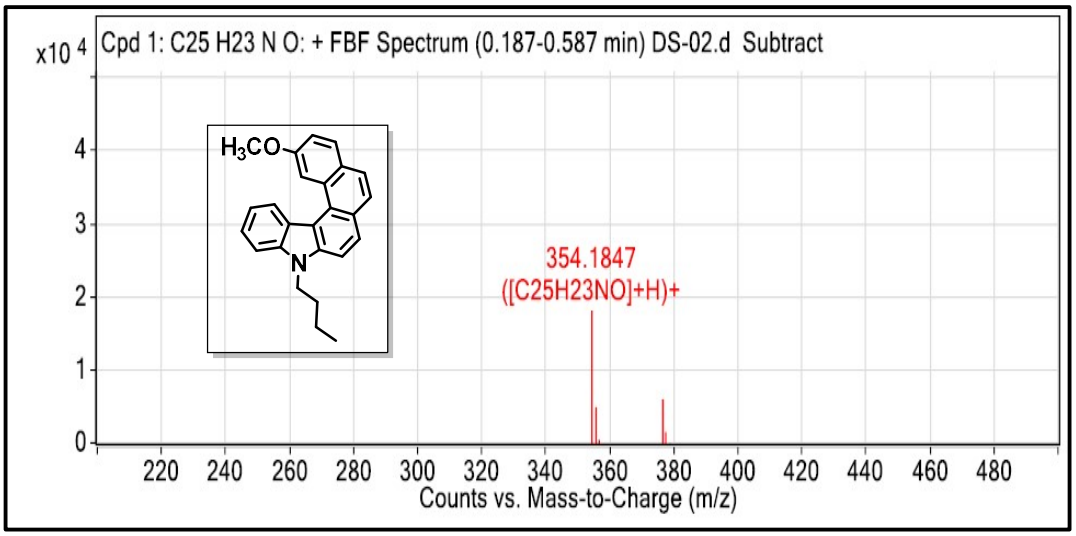

HRMS Spectra of compound 55: m/z calcd. for [$C_{25}H_{23}NO$+H] is 354.1780; found, 354.1847.

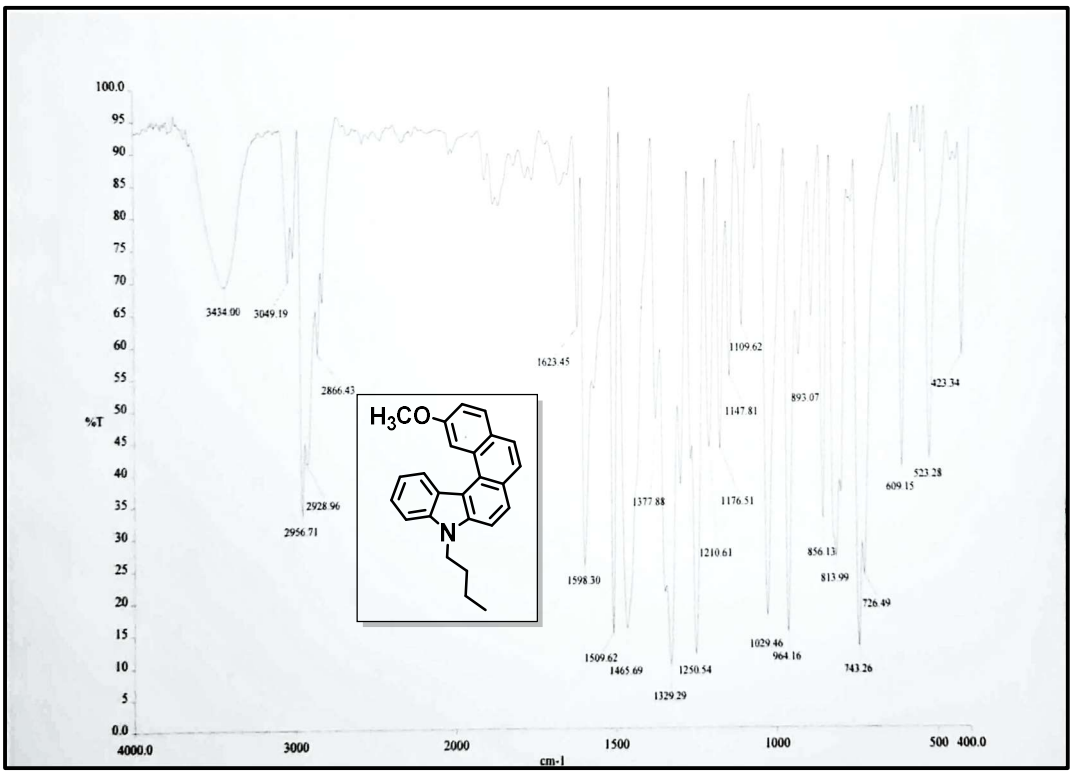

IR Spectra of compound 55

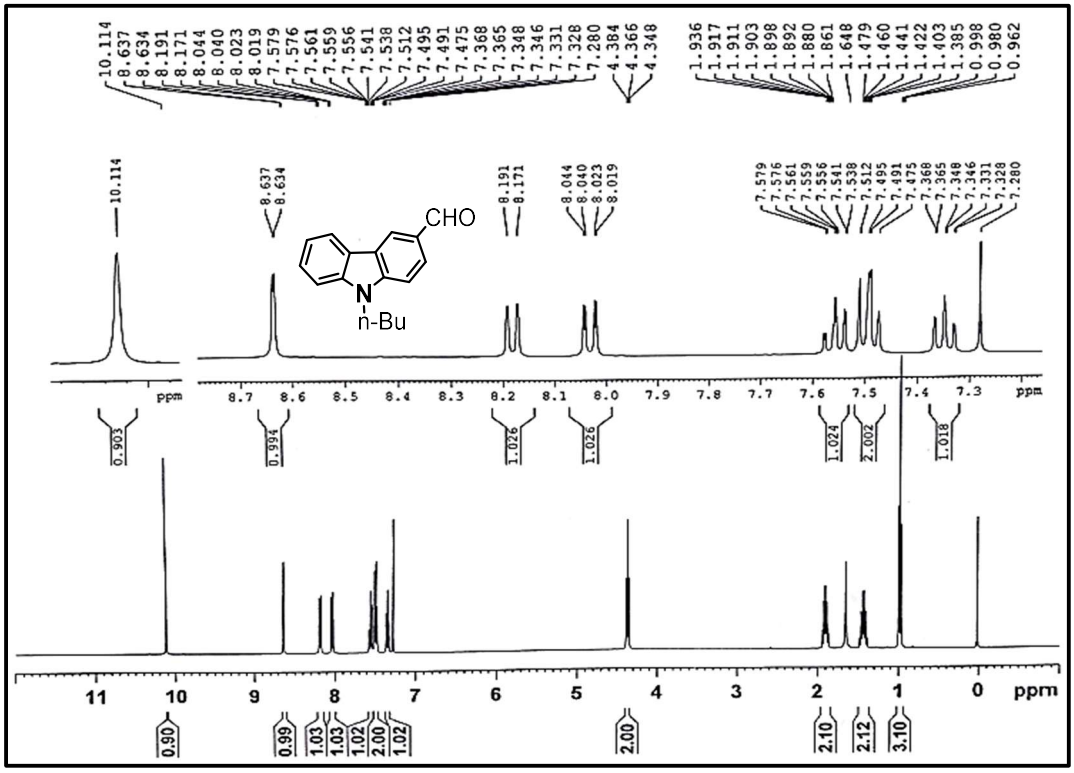

^{1}H-NMR Spectra of compound 70

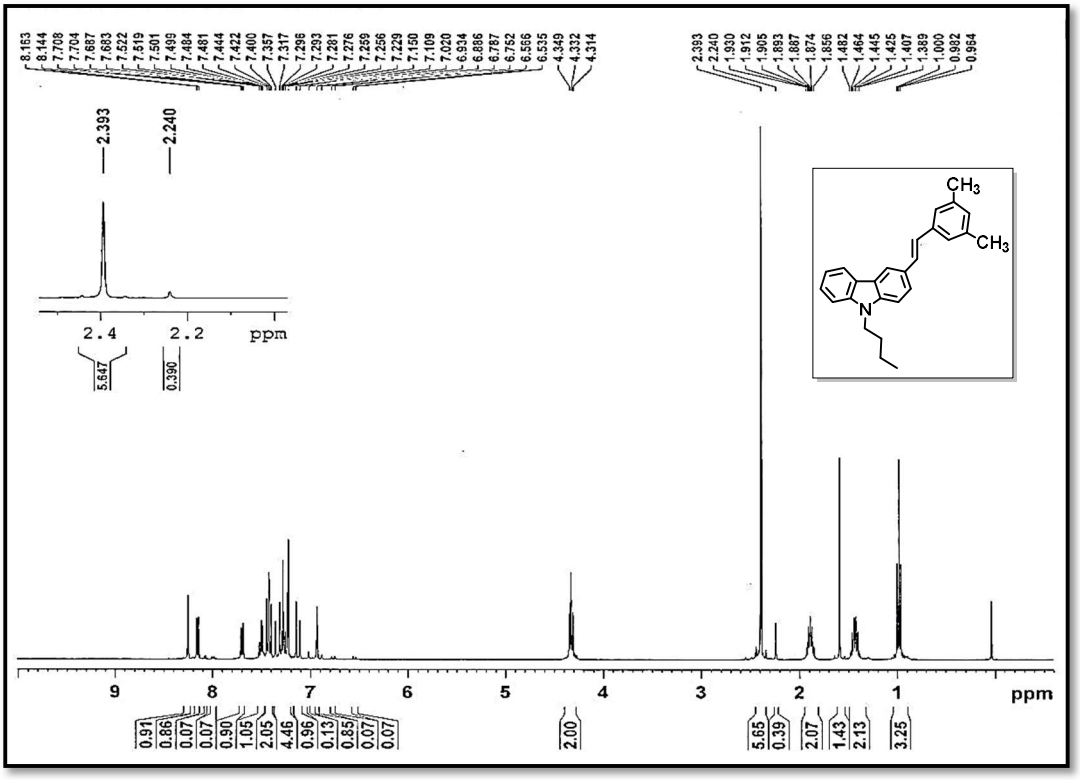

[1]H-NMR Spectra of compound 77

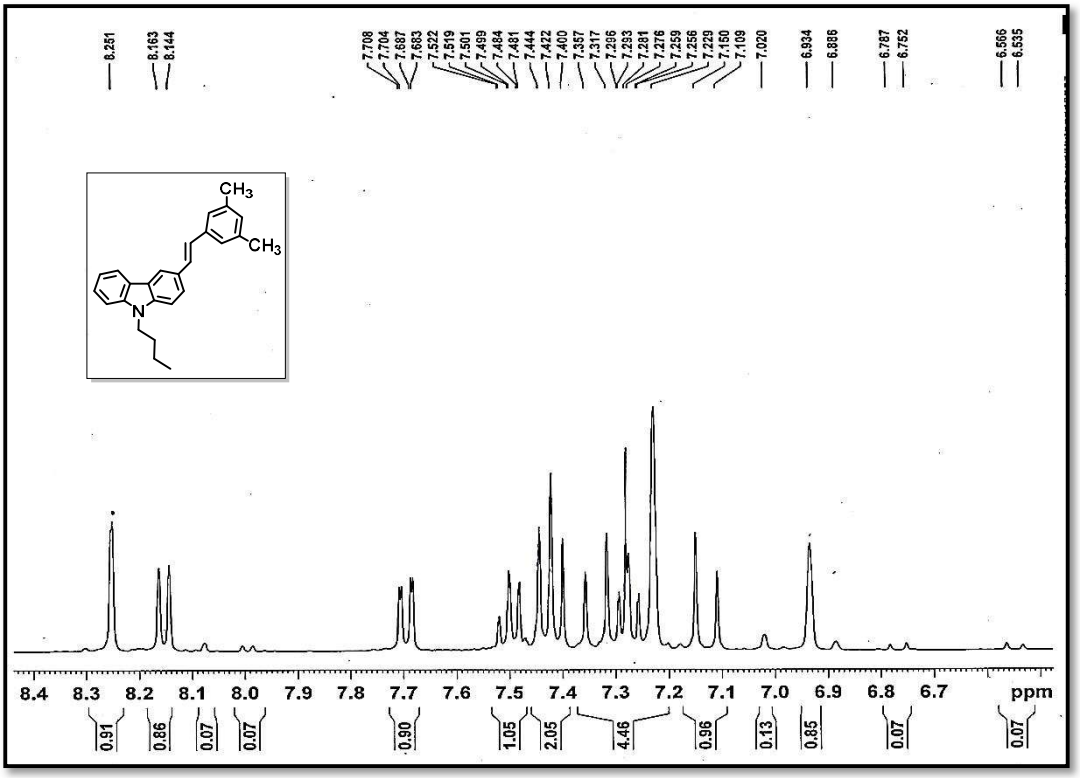

Aromatic region of the [1]H-NMR spectra of compound 77

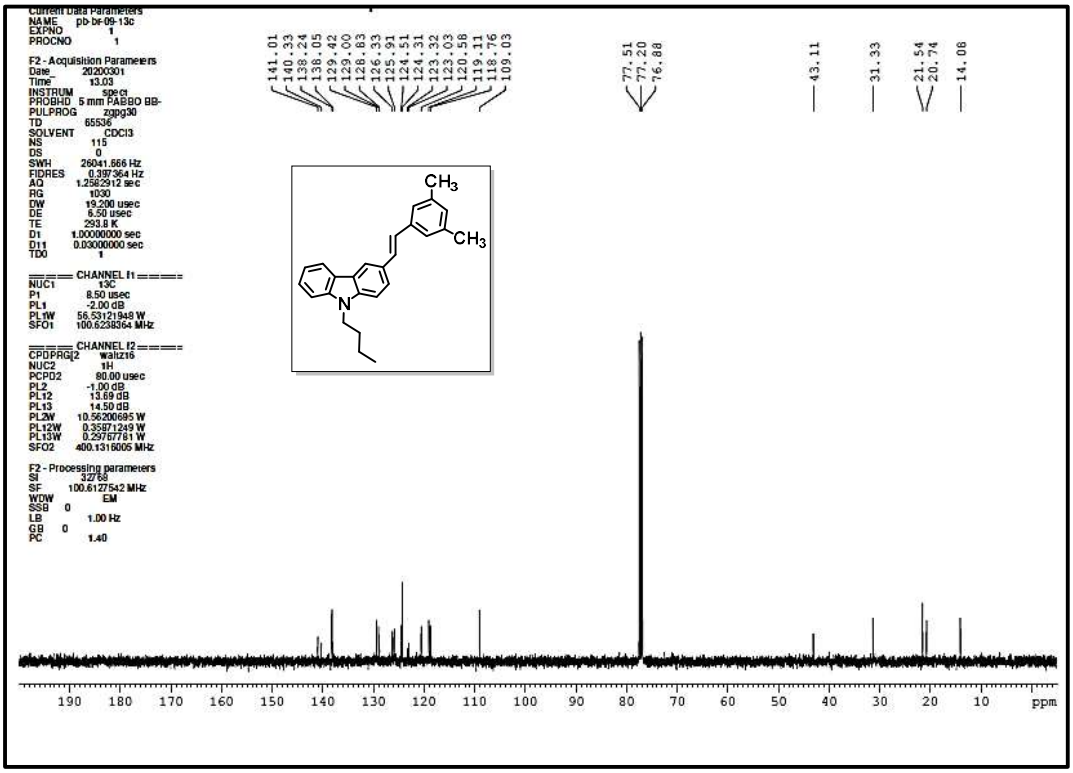

^{13}C-NMR Spectra of compound 77

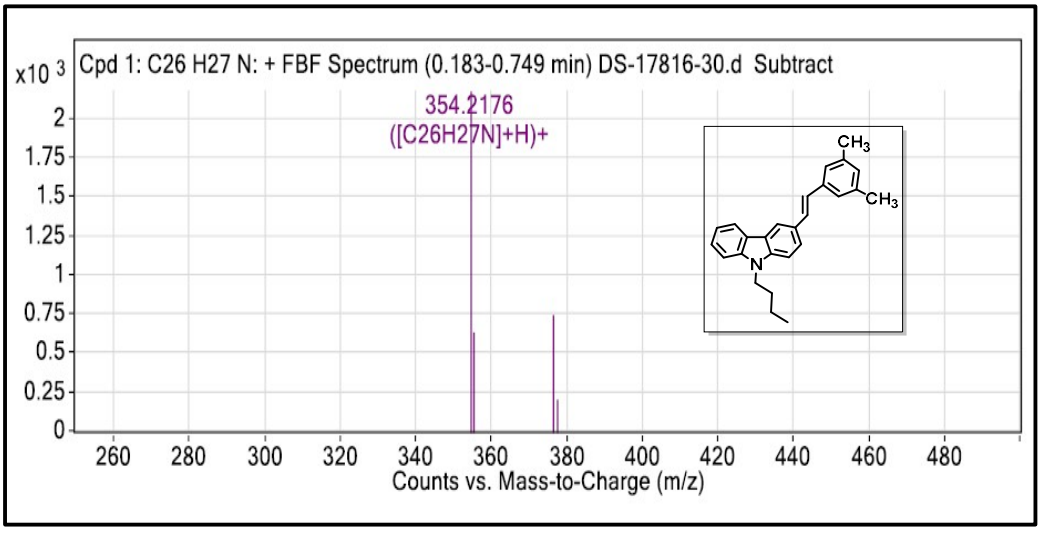

HRMS Spectra of 77: m/z calcd. [$C_{26}H_{27}N$+H]$^+$ is 354.2143; found, 354.2176.

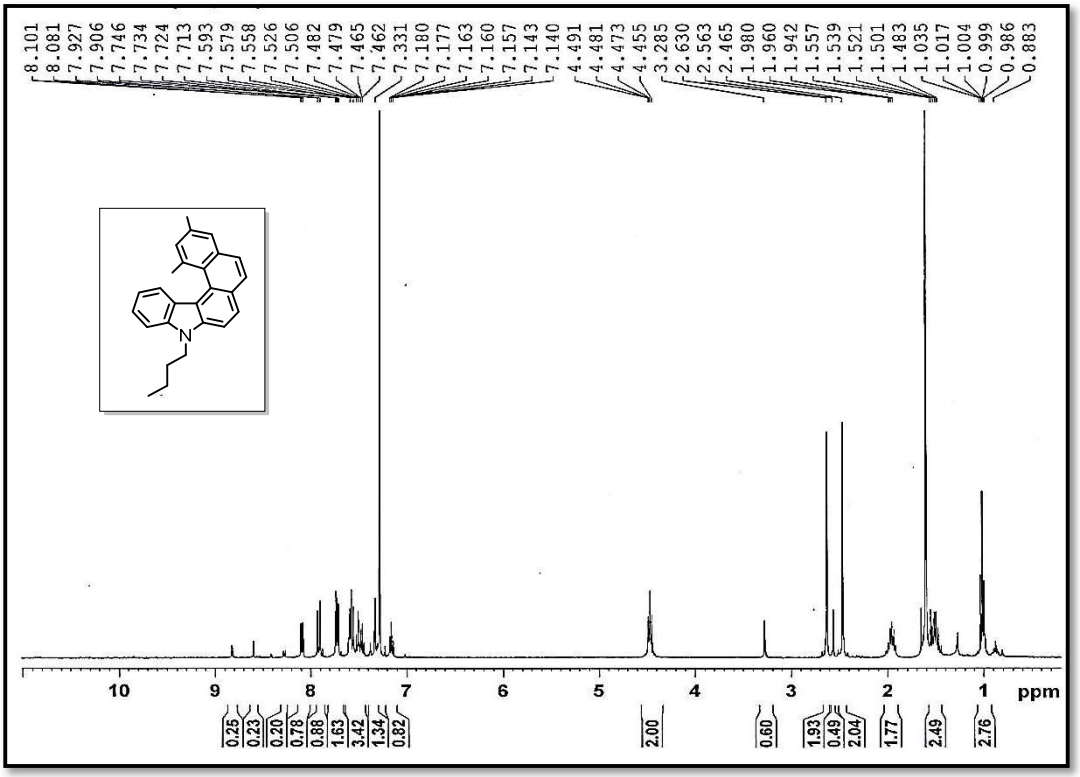

^{1}H-NMR Spectra of compound 74

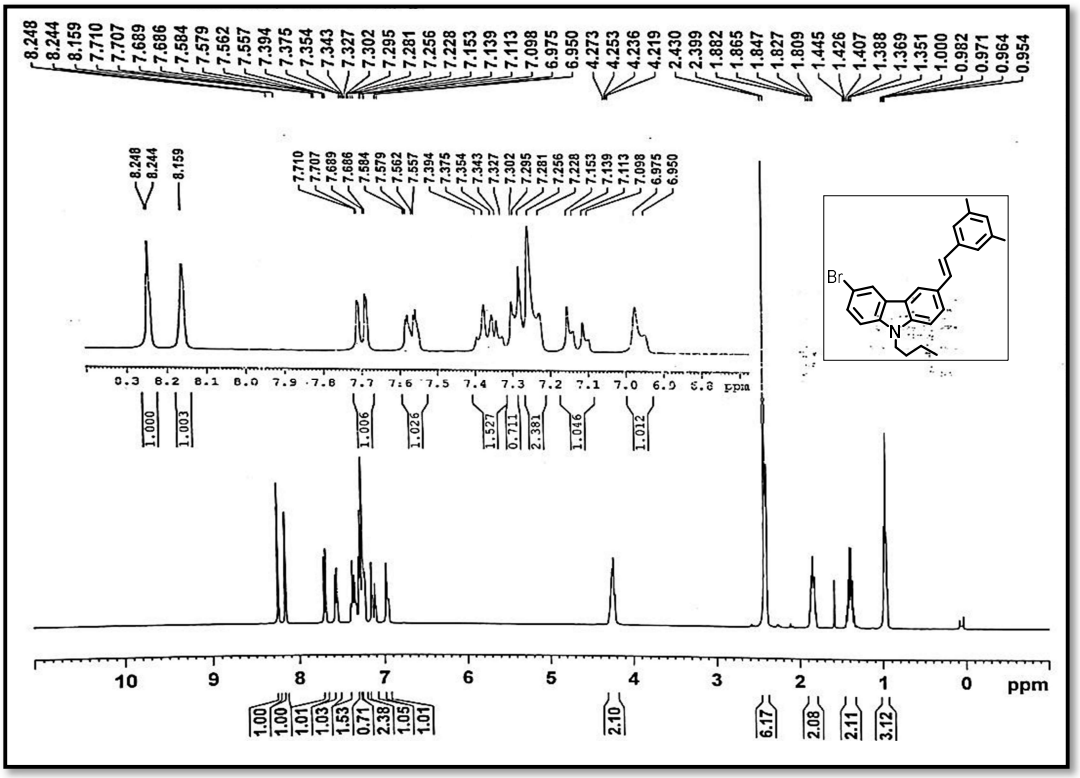

^{1}H-NMR Spectra of compound 78

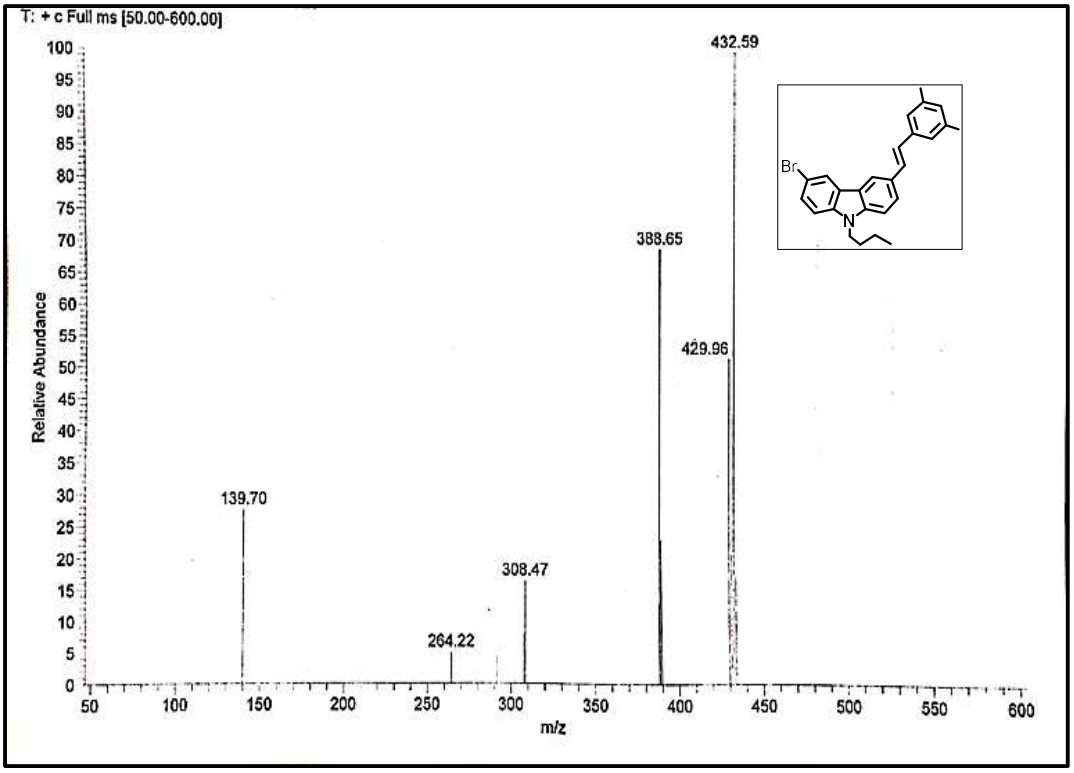

Mass Spectra of 78: m/z found $[C_{26}H_{26}BrN]^+$ is 432.59.

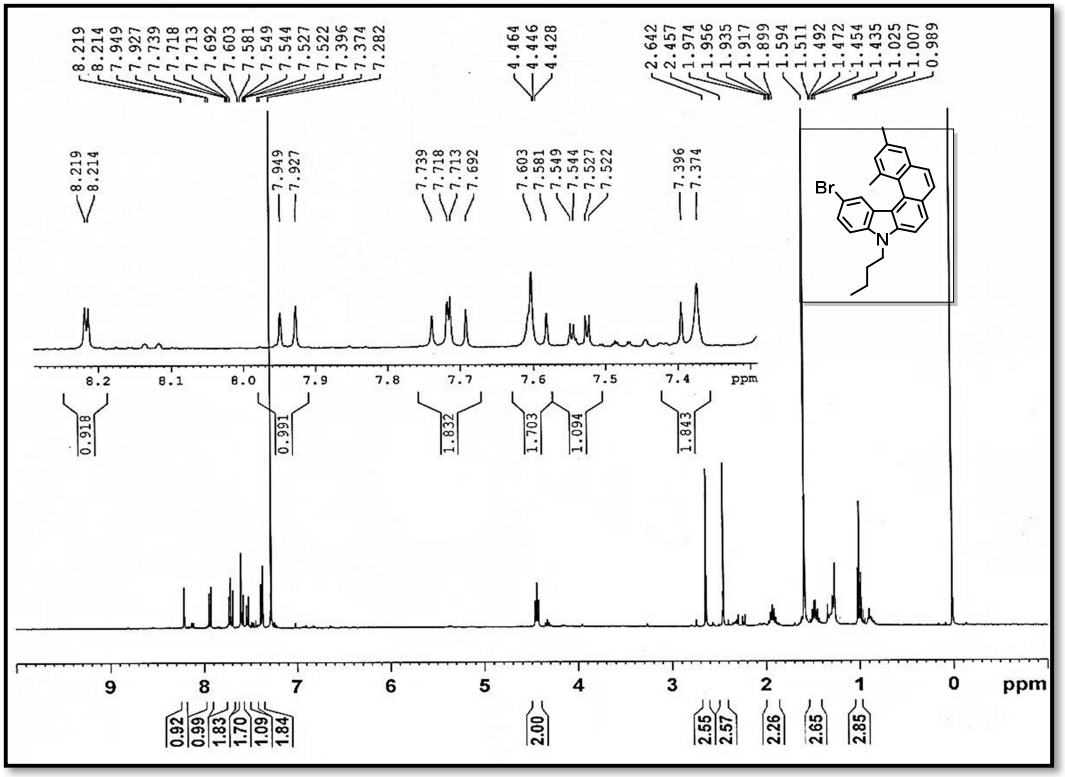

^{1}H-NMR Spectra of compound 79

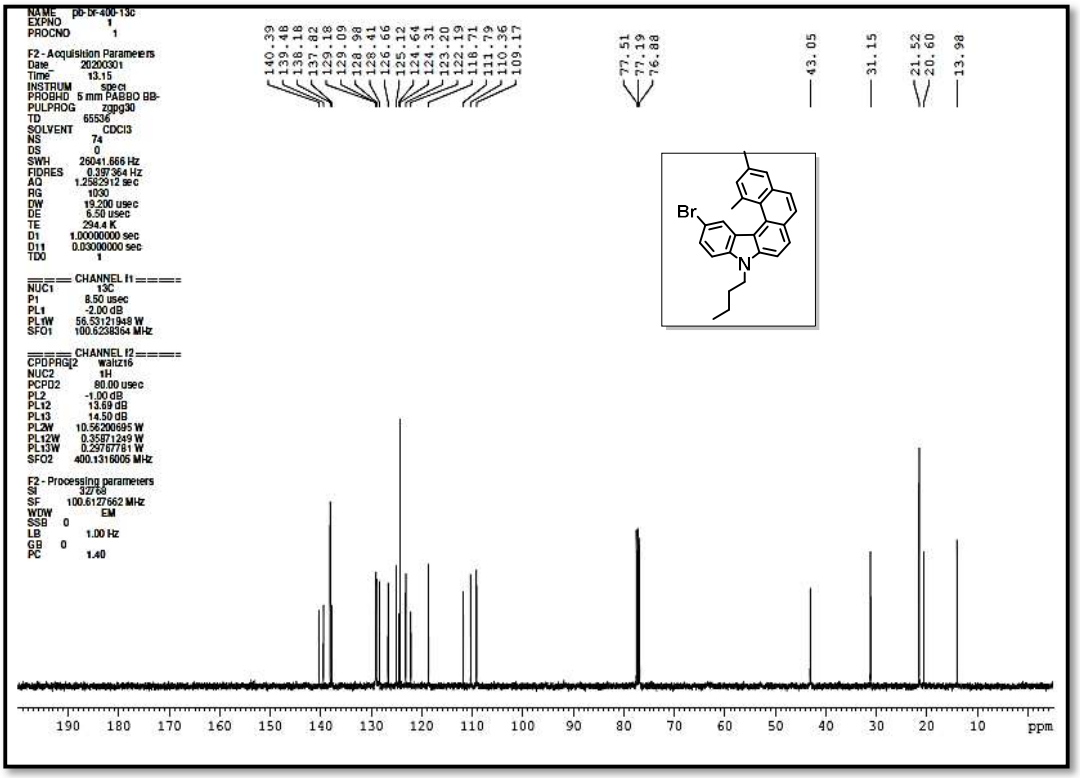

^{13}C-NMR Spectra of compound 79

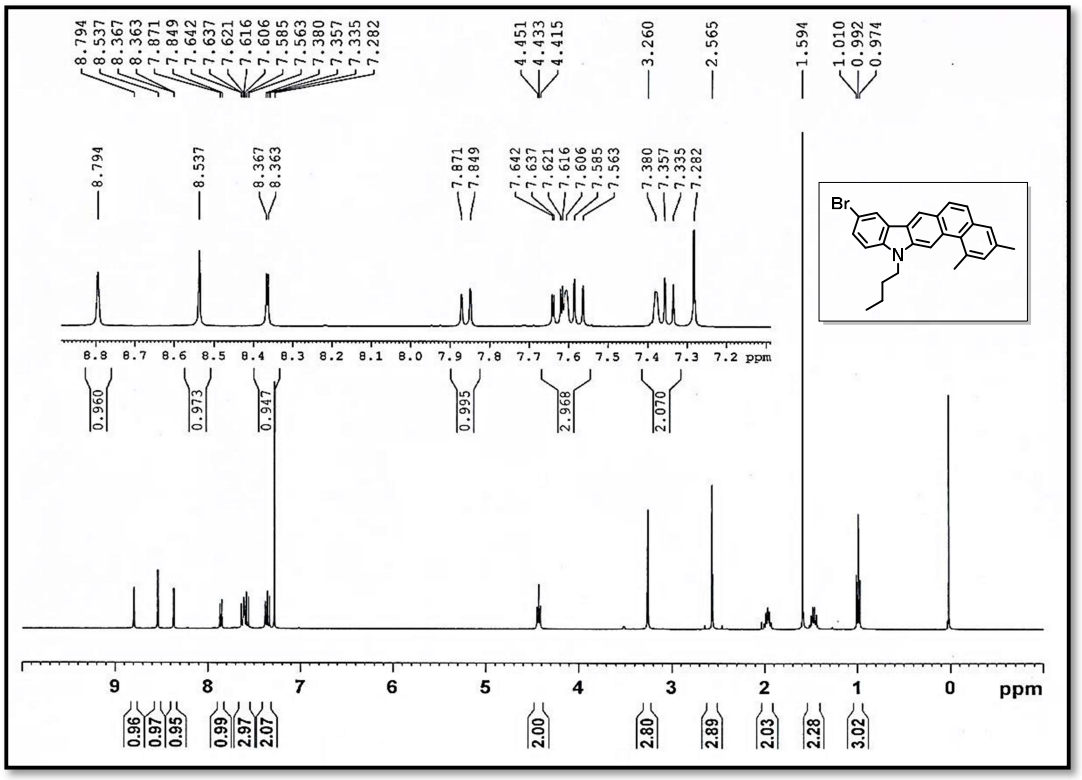

^{1}H-NMR Spectra of compound 81

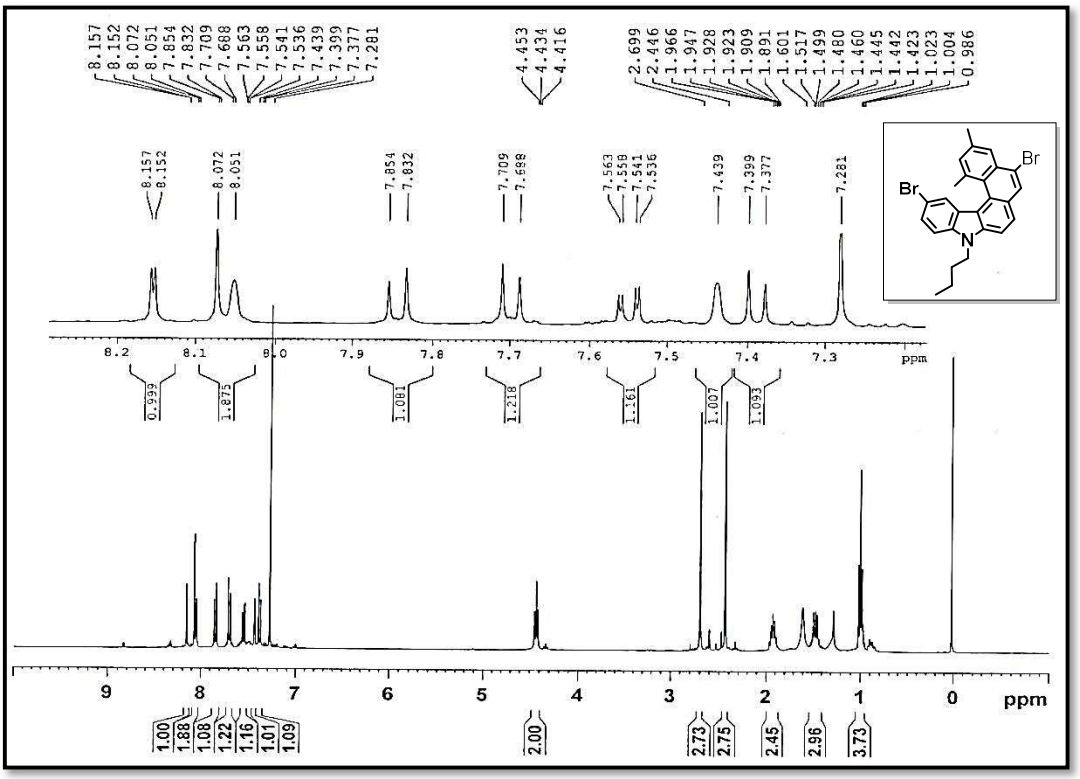

^{1}H-NMR Spectra of compound 82

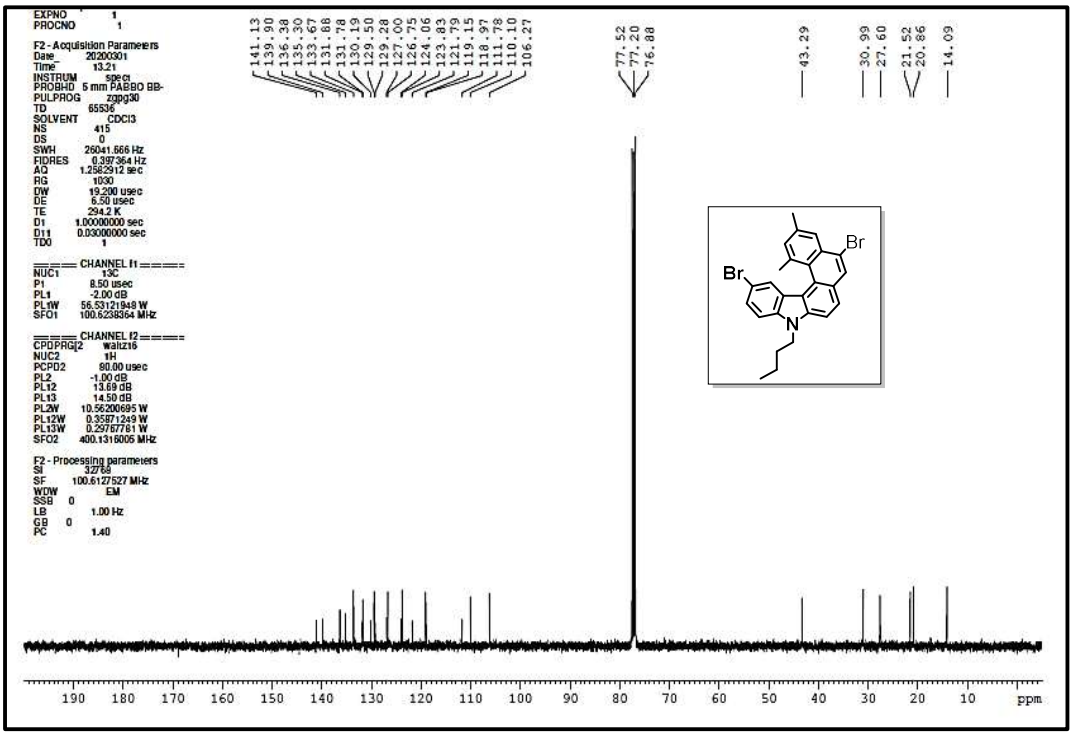

^{13}C-NMR Spectra of compound 82

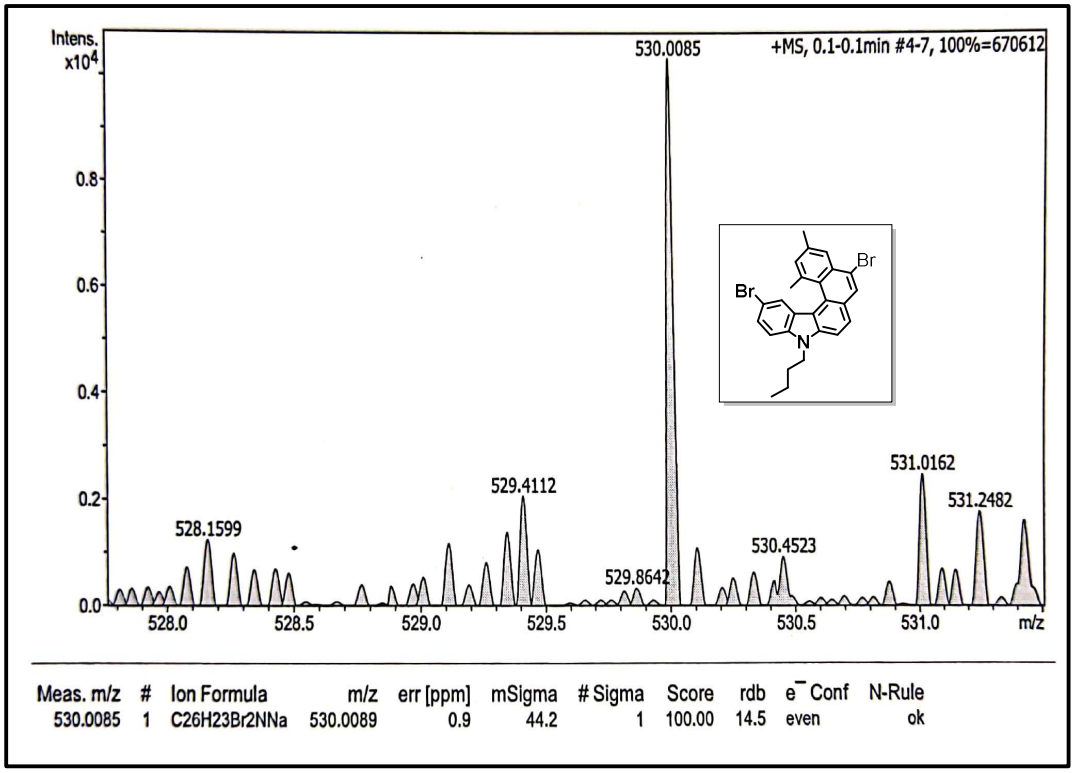

HRMS spectra of compound 82: m/z calcd. for $C_{26}H_{23}Br_2NNa$ is 530.0095; found, 530.0089

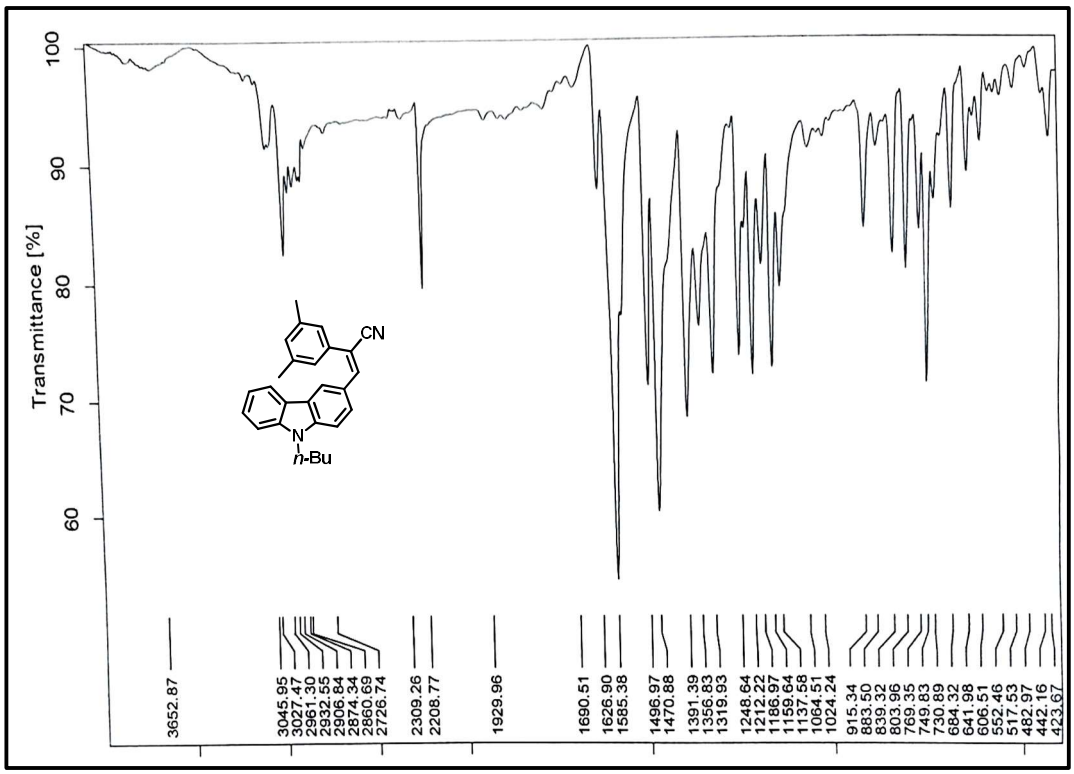

IR Spectra of compound 83

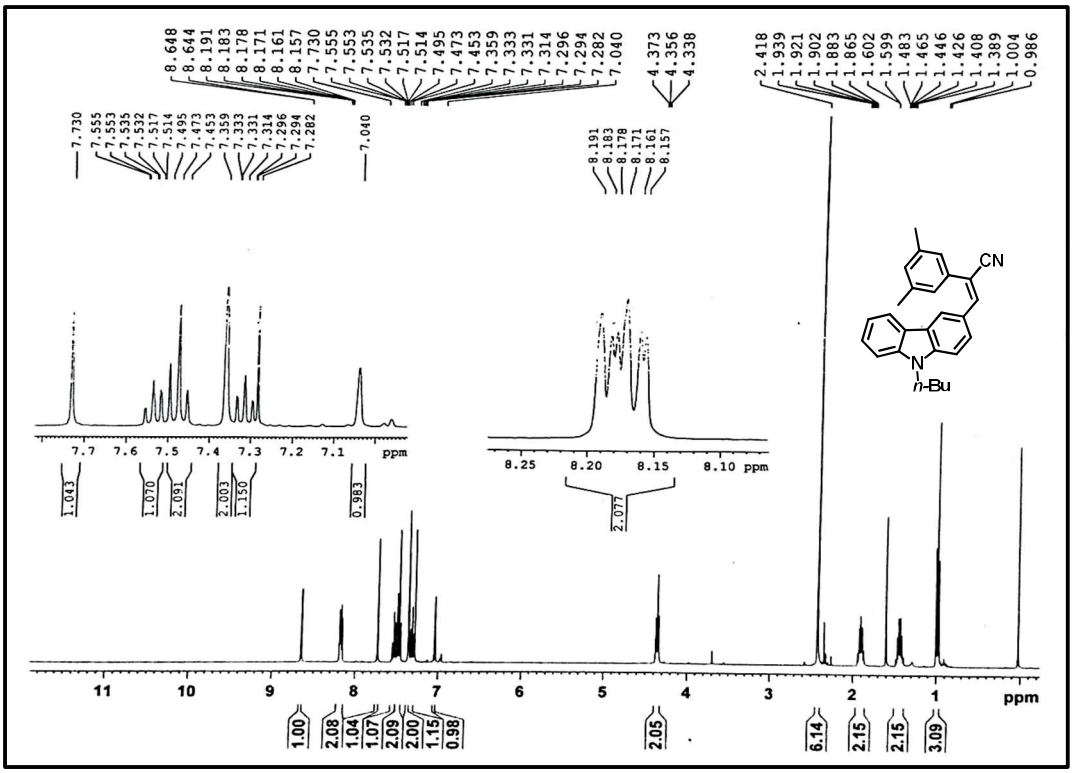

^{1}H-NMR Spectra of compound 83

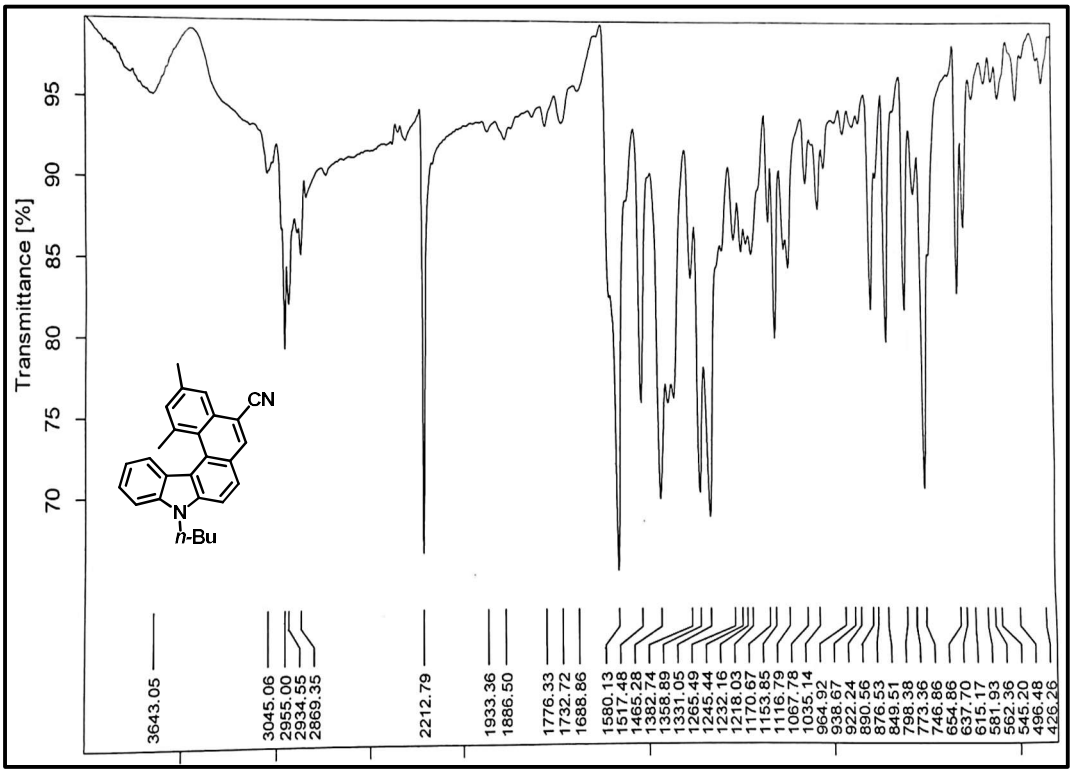

IR Spectra of compound 84

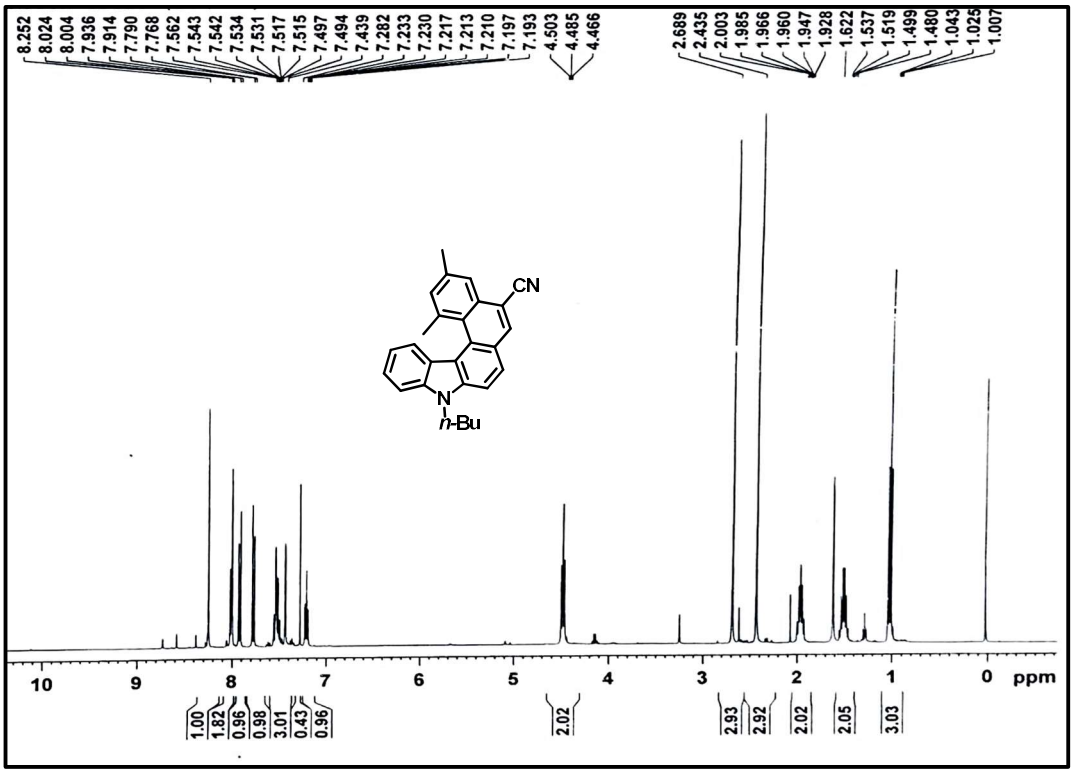

^{1}H-NMR Spectra of compound 84

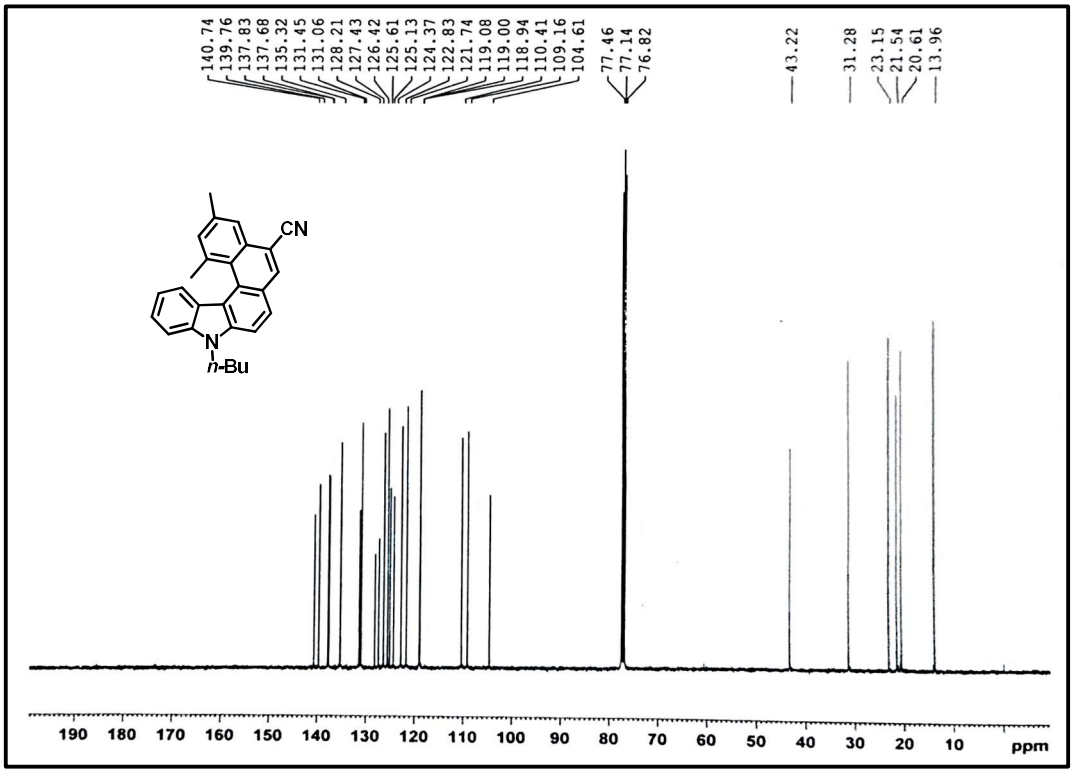

^{13}C-NMR Spectra of compound 84

2.8 References

1. Meisenheimer, J. & Witte, K. Reduction von 2-Nitronaphtalin. *Berichte der deutschen chemischen Gesellschaft* **36**, (1903).
2. R Weitzenbock & A Klingler. Synthesis of the isomeric hydrocarbons 1, 2, 5, 6-dibenzanthracene and 3, 4, 5, 6-dibenzophenanthrene. *J. Chem. Soc* **114**, 494 (1918).
3. Scholz M, , Mühlstädt M & Dietz F. Chemie angeregter zustände. I. Mitt. Die richtung der photocyclisierung naphthalinsubstituierter äthylene. *Tetrahedron Lett* **8**, 665–668 (1967).
4. Mallory, F. B. & Mallory, C. W. Photocyclization of stilbenes. VII. Unusual fluorine atom rearrangement in the photocyclization of 1-fluoro[5]helicenes. *The Journal of Organic Chemistry* **48**, (1983).
5. Usui, K. *et al.* Synthesis and Resolution of Substituted [5]Carbohelicenes. *Journal of Organic Chemistry* **80**, 6502–6508 (2015).
6. Raouafi, S., Aloui, F. & Hafedh, N. Synthesis, characterization, and photophysical properties of a new pentacyclic helicene. *Comptes Rendus Chimie* **20**, 1047–1052 (2017).
7. Bazzini, C. *et al.* Synthesis and Characterization of Some Aza[5]helicenes. . *Eur. J. Org. Chem.* **2005**, 1247–1257 (2005).
8. ben Braiek, M. *et al.* Synthesis, X-ray analysis and photophysical properties of a new N-containing pentacyclic helicene. *Tetrahedron Letters* **54**, 5421–5425 (2013).
9. Dreher, S. D., Paruch, K. & Katz, T. J. Acidified alcohols as agents to introduce and exchange alkoxyls on the periphery of helicenes. *Journal of Organic Chemistry* **65**, 806–814 (2000).
10. Yamamoto, K. *et al.* Rational Design and Synthesis of [5]Helicene-Derived Phosphine Ligands and Their Application in Pd-Catalyzed Asymmetric Reactions. *Scientific Reports* **6**, (2016).
11. Nakazaki M, Yamamoto K, Ikeda T, Kitsuki T & Okamoto Y. Synthesis and chiral recognition of novel crown ethers incorporating helicene chiral centres. *Chem Commun* **14**, 787–788 (1983).
12. Li, M. *et al.* Tetrahydro[5]helicene-based imide dyes with intense fluorescence in both solution and solid state. *Chemical Communications* **50**, 2993–2995 (2014).
13. Virk, T. S. *et al.* Sultam-Based Hetero[5]helicene: Synthesis, Structure, and Crystallization-Induced Emission Enhancement. *ACS Omega* **1**, (2016).
14. (a) Talele, H. R., Sahoo, S., Bedekar, A.V. Synthesis of chiral helical 1,3-oxazines. *Organic Letters* **14**, 3166-3169 (2012). (b) Newman, M. S. & Lednicer, D. The Synthesis and Resolution of Hexahelicene [1]. *Journal of the American Chemical Society* **78**, (1956). (c) Waghray, D.; Zhang, J.; Jacobs, J.; Nulens, W.; Basarić, N.;Meervelt, L. V.; Dehaen, W. The *Journal of Organic Chemistry* **77**, 10176-10182 (2012).

15. Martin RH, Marchant M-J & Baes M. Rapid syntheses of hexa and heptahelicene. *Helv Chim Acta* **54**, 358–360 (1971).
16. Grimme, S. *et al. MICROREVIEW Structure/Chiroptics Relationships of Planar Chiral and Helical Molecules*. *Eur. J. Org. Chem* (1998).
17. Abbate, S. *et al.* Monoaza[5]helicenes. Part 2: Synthesis, Characterisation and Theoretical Calculations. *Tetrahedron* **62**, 139–148 (2006).
18. Yamamoto, K., Okazumi, M., Suemune, H. & Usui, K. Synthesis of [5]helicenes with a substituent exclusively on the interior side of the helix by metal-catalyzed cycloisomerization. *Organic Letters* **15**, 1806–1809 (2013).
19. Daniels, M. *et al.* Bay-Substituted Thiaza[5]helicenes: Synthesis and Implications on Structural and Spectroscopic Properties. *Journal of Organic Chemistry* **84**, 13528–13539 (2019).
20. Ravat, P. *et al.* Configurational Stability of [5]Helicenes. *Organic Letters* **19**, 3707–3710 (2017).
21. Upadhyay, G.M., Talele, H.R., Bedekar, A.V. Synthesis and photophysical proper- ties of aza[n]helicenes, *The Journal of Organic Chemistry* **81** 7751–7759 (2016).
22. Liu LB & Katz TJ. Bromine auxiliaries in photosyntheses of [5]helicenes. *Tetrahedron Lett* **32**, 6831–6834 (1991).
23. Upadhyay, G.M., Mande, H. M., Pithadia, D. K., Maradiya, R. H. Bedekar, A.V. Effect of the position of the cyano group on molecular recognition, supramolecular superhelix architecture, and spontaneous resolution of aza[7]helicene. *Crystal growth and design* **19,** 5354-5358 (2019).